Characterisation and Behavioural Consequences of α-Synucleinopathy in Transgenic Mice

Dissertation

der Mathematisch-Naturwissenschaftlichen Fakultät

der Eberhard Karls Universität Tübingen

zur Erlangung des Grades eines

Doktors der Naturwissenschaften

(Dr. rer. nat.)

vorgelegt von

Heinrich Schell

aus Zernen

Tübingen

2012

Tag der mündlichen Qualifikation:	17.04.2012
Dekan:	Prof. Dr. Wolfgang Rosenstiel
1. Berichterstatter:	Prof. Dr. Philipp J. Kahle
2. Berichterstatter:	Prof. Dr. Olaf Rieß

I. Table of Contents

II. Table of Figures

III. Abbreviations

°C	degree celcius
µM	micro meter
aa	amino acid
AD	Alzheimer's disease
BA	basal amygdala
BCA	bicinchoninic acid assay
BDNF	brain derived nervel growth factor
BLA	basolateral amygdala
BS	brainstem
BSA	bovine serum albumine
CA	cornu amonis
Ce	cerebellum
CeL	central nucleus (lateral part)
CeM	central nucleus (medial part)
CNP	2',3'-cyclic nucleotide 3'-phosphodiesterase promoter
CS	conditioned stimulus
Cx	cortex
DA	dopaminergic
DG	dentate gyrus
DLB	dementia with lewy bodies
DMEM	dulbecco's minimal essential medium
E. coli	escherichia coli
EntCx	entorhinal cortex
ER	endoplasmatic reticulum
FC	fear conditioninig
g	gram
h	hour
HEK	human embryonal kidney cells
HEPES	4-(2-hydroxyethyl)-1-piperazineethanesulfonic acid
Hip	hippocampus
HRP	horseradish-peroxidase
HSP	heat shock protein
kD	kilodalton
l	liter
LA	lateral amygdala
LB	Lewy body
LBs	Lewy bodies
LC	locus coeruleus
L-Dopa	L-3, 4-dihydroxyphenylalanine
LN	Lewy neurite
LNs	Lewy neurites
LRRK2	leucine-rich repeat kinase 2
m	milli
M	molar
MB	midbrain
min	minute
MPTP	1-methyl-4-phenyl, 1, 2, 3, 6-tetrahydropyridine
mRNA	messenger ribonucleic acid
MSA	multiple system atrophy
n	nano
NAc	nucleus accumbens
NAC domaine	non-Ab component
OB	olfactorial bulb

PAC	large P1 artificial chromosome
PAGE	polyacrylamide gelelectrophoresis
Paraquat	N,N'-dimethyl-4,4'-bipyridinium dichlorid
PBS	phosphate buffered saline
PCR	polymerase chain reaction
PD	Parkinson´s disease
PINK1	phosphatase and tensin [PTEN] homolog-induced putative kinase 1
PLP	proteolipid protein promoter
PrP	prion protein promoter
PrP	prion protein promoter
rpm	rotations per minute
RT	room temperature
SDS	sodium dodecyl sulfate
SN	substantia nigra
SNpc	substantia nigra pars compacta
ßSyn	beta-synuclein
Sub	subiculum
TH	tyrosin hydroxylase
ThS	thioflavine S
U	units
US	unconditioned stimulus
xg	gravitation constant
αSyn	alpha-synuclein
γSyn	gamma-synuclein
µ	micro

Amino acids:
Ala, A: Alanin; Arg, R: Arginin; Asn, N: Asparagin; Asp, D: Aspartat; Cys, C: Cystein; Gln, Q: Glutamin; Glu, E: Glutamat; Gly, G: Glycin; His, H: Histidin; Ile, I: Isoleucin; Leu, L: Leucin; Lys, K: Lysin; Met, M: Methionin; Phe, F: Phenylalanin; Pro, P: Prolin; Ser, S: Serin; Thr, T: Threonin; Trp, W: Tryptophan; Tyr, Y: Tyrosin; Val, V: Valin

IV. Publications

Parts of this work have been published in:

Manuscripts

Schell H, Hasegawa T, Neumann M, Kahle PJ.
Nuclear and neuritic distribution of serine-129 phosphorylated α-synuclein in transgenic mice. *Neuroscience*. 2009 Jun 2;160(4):796-804.

Waak J, Weber SS, Waldenmaier A, Görner K, Alunni-Fabbroni M, Schell H, Vogt-Weisenhorn D, Pham TT, Reumers V, Baekelandt V, Wurst W, Kahle PJ.
Regulation of astrocyte inflammatory responses by the Parkinson's disease-associated gene DJ-1. *FASEB J.* 2009 Aug;23(8):2478-89.

Mbefo MK, Paleologou KE, Boucharaba A, Oueslati A, Schell H, Fournier M, Olschewski D, Yin G, Zweckstetter M, Masliah E, Kahle PJ, Hirling H, Lashuel HA.
Phosphorylation of synucleins by members of the polo-like-kinase family. *J Biol Chem*. 2010 Jan 22;285(4):2807-22

Rieker C, Dev KK, Lehnhoff K, Barbieri S, Ksiazek I, Kauffmann S, Danner S, Schell H, Boden C, Ruegg MA, Kahle PJ, van der Putten H, Shimshek DR**.**
Neuropathology in mice expressing mouse alpha-synuclein. *PLoS One.* 2011;6(9):e24834.

Manuscript in preparation

Schell H, Boden C, Chagas AM, Kahle PJ.
Impaired c-FOS and PLK2 induction after fear-conditioning in aged alpha-synuclein transgenic mice.

Poster presentation

Alpha-Synuclein symposium EFSB-Lausanne (2009):
S129-phosphorylated α-synuclein pathology in transgenic mice: Implications for age-dependent cognitive decline

Oral Presentation

Neuromodel/NEURASYN, PhD Training Course, Lund, Sweden 2010
Mouse behaviour phenotyping demonstrations.

Collaborations

ADPD poster 2009
Exogenous induction of protein aggregation in mouse models of different neurodegenerative diseases.

ICAD abstract 2010
Seeding of cross linked alpha-synuclein oligomers *in vitro* and *in vivo.*

SFN abstract 2010
Alpha-synuclein protofibrils can seed fibril formation *in vitro.*

PDDK-FSE 2010
Diffusion kurtosis as a pre-symptomatic marker in an α-synucleinopathy mouse model.

SFN abstract 2011
Alpha-synuclein oligomer selective antibodies recognize intracellular pathology in human and transgenic mouse brain.

V. Zusammenfassung

Die Parkinson'sche Erkrankung (PD: Parkinson´s disease) ist eine chronisch fortschreitende Erkrankung, welche durch die Degeneration von dopaminergen Neuronen charakterisiert ist. Das neuronale Protein alpha-Synuklein (αSyn), welches in synaptischen Enden angereichert ist und die synaptische Vesikel-Aktivität reguliert, wird mit PD in Verbindung gebracht. Die drei Punktmutationen A30P, A53T and E46K, sowie eine Erhöhung der αSyn Proteinkonzentration durch Gen-Duplikation oder -Triplikation, werden mit autosomal dominantem PD und Lewy Body Demenz (DLB) in Verbindung gebracht. Sowohl in PD, als auch in DLB bildet αSyn Fibrillen, die den Hauptbestandteil von Lewy Bodies (LB), Lewy Neuriten (LN) und cytoplasmatischen Einschlüssen in Gliazellen in der multiplen System Atrophy (MSA) ausmachen. Die zellulären Mechanismen, die zu neuronalen Dysfunktionen bei diesen Erkrankungen führen, werden *in vitro* und in dieversen Tiermodellen intensiv untersucht. Dadurch wird ein besseres Verständnis der bei diesen Erkrankungen ablaufenden zellbiologischen Vorgänge erzielt. Zusammen mit MSA, bei der αSyn in Gliazellen akkumuliert, werden die αSyn verwandten neuronalen Erkrankungen DLB und PD als α-Synukleinopathien zusammengefasst.

In dieser Arbeit wurde ein [A30P]αSyn überexprimierendes Mausmodell verwendet, um eine Gehirnregion-spezifische Charakterisierung von αSynukleinopathie im Hirnstamm (HS), dem Mittelhirn (MH), dem Cortex (Cx), dem Bulbus Ofactorius (BO), dem Hippocampus (Hip) und der Amygdala durchzuführen; Regionen in denen bereits die Überexpression des [A30P]αSyn Transgens nachgewiesen worden ist. Besonders in der Amygdala, der zentralen Region des emotionalen Lernens, welche auch in dementen Patienten betroffen ist, wurden die Konsequenzen einer vorhandenen α-Synukleinopathie auf die neuronale Funktionalität nach Aktivierung durch Angstkonditionierung detailliert untersucht. Histologische Untersuchungen von Gehirnen gealterter transgener Tieren zeigten eine

altersabhängige Akkumulation von neuropathologischem, am Ser129 phosphoryliertem αSyn (pSer129 αSyn). Dieses war hauptsächlich in LB und LN ähnlichen Strukturen im HS und MH auffindbar und korrelierte mit Thioflavine-S (ThS) positiver Amyloidose und neuropathologischer Gallyas Silberfärbung. Die glomeruläre Region des BO zeigte eine ähnliche altersabhängige Pathologie, obwohl LB/LN ähnliche pSer129 αSyn positive Strukturen im BO nicht beobachtet werden konnten. pSer129 αSyn wurde außerdem im Zytoplasma des Cx und auch in Nuclei des Hippocampus CA1, CA3 (CA: hippocampaler Cornus Amonis) und in der subicularen Region von jungen und alten transgenen Mäusen detektiert. Im Gegensatz dazu war keine dieser Gehirnregionen positiv für Amyloidose oder eine durch Silberfärbung nachweisbaren Neuropathologie. Interessanterweise zeigten proteinbiochemische Analysen eine αSyn Form, die nur in der unlöslichen Fraktion von kortikalen Lysaten zu finden war. Eine weitere Beobachtung war die altersabhängige Akkumulation von transgenem nicht-phosphoryliertem αSyn in synaptischen Regionen des CA1 und CA3, in welchen Langzeit-Potenzierung (LTP) statt findet. Damit einhergehend zeigten alte transgene Tiere ein vermindertes Kontext-Lernvermögen. In der basolateralen Amygdala (BLA) wurde vor allem in alten transgenen Mäusen nukleäres pSer129 αSyn detektiert. Außerdem wurden nur in alten transgenen Mäusen im amygdaloiden medialen Centralen Nucleus (CeM) LN-artige pSer129 αSyn positive Strukturen detektiert. Beide Regionen der Amygdala, sowohl die BLA als auch der CeM, sind Bereiche in denen LTP stattfindet. Korrelierend mit dieser Pathologie bestätigte sich das beeinträchtigte emotionale Lernen alter transgener Tiere. Diese Beeinträchtigung korrelierte außerdem mit einem reduzierten Level des immediate early Gens c-FOS in der BLA und dem CeM der Tiere direkt nach Angstkonditionierung (AK). Auch die Ser129 αSyn Phosphotransferase Polo-Kinase-2 (PLK2), welche die neuronale Plastizität im Hippocampus beeinflußt, wurde in alten transgenen Tieren nicht durch AK hochreguliert.

Nur junge transgene und alte Wildtyp-Tiere zeigten eine PLK2 Hochregulation in der BLA und in dem CeM nach der AK.

Um die pathologische pSer129 αSyn Situation *in vitro* zu reproduzieren, wurden humane embryonale Nierenzellen (HEK293E) mit αSyn und seiner Kinase G-Protein-Rezeptor-Kinase-5 (GRK5) transfiziert. Tatsächlich konnte die gleiche nukleäre pSer129 αSyn Färbung wie in den transgenen Tieren nachgewiesen werden. Noch wichtiger aber ist, dass die pSer129 αSyn postitive Färbung in den transgenen Mäusen im Neutropil mit PLK3, im Zytoplasma und in den nukleären Regionen mit PLK2 kolokalisiert, was darauf hindeutet, dass PLK2 und PLK3 wichtige Kinasen representieren, die αSyn am Ser129 phosphorylieren und demnach bei der Entstehung von α-Synukleinopathien eine wichtige Rolle spielen.

Zusammengefasst zeigt diese Arbeit unterschiedliche Qualitäten von α-Synukleinopathie in verschiedenen Gehirnregionen von transgenen (Thy1)h[A30P]αSyn Mäusen, die αSyn überexprimieren. Des weiteren konnte nach emotionalen Lerntests eine direkte Korrelation zwischen α-Synukleinopathie und einer verminderten neuronalen Aktivierung in der Amygdala gezeigt werden.

VI. Summary

Parkinson's disease (PD) is a chronic progressive neurodegenerative disorder, which is characterized by the degeneration of dopaminergic neurons. The neuronal protein alpha-Synuclein (αSyn), which is enriched in synaptic terminals and regulates synaptic vesicle activity, is linked to PD. The three known point mutations leading to an amino acid exchange in αSyn, A30P, A53T and E46K as well as duplications or triplications of the αSyn coding gene are linked with autosomal dominant PD and dementia with Lewy bodies (DLB). In PD and DLB αSyn forms fibrils, which are the major component of Lewy bodies (LB), Lewy neurites (LN) and of glial cytoplasmic inclusions in multiple system atrophy (MSA). The cellular mechanisms regulating neuronal dysfunction during these diseases are intensively examined *in vitro* and in diverse animal models. Together with MSA, where αSyn accumulates in glial cells, the αSyn related neuronal disorders DLB and PD are together referred as α-Synucleinopathies.

In this work an [A30P]αSyn overexpressing mouse model was used to perform brain region specific characterisation of α-Synucleinopathy in the brainstem (BS), midbrain (MB), cortex (Cx), olfactorial bulb (OB), hippocampus (Hip) and the amygdala, all regions which were shown to overexpress the αSyn transgene. Especially the amygdala, the key region of the emotional learning circuitry, which is affected in demented patients, was closer investigated for the effect of α-Synucleinopathy on neuronal function. Histological investigation of brains of aged transgenic animals showed age-dependent accumulation of neuropathological αSyn phosphorylated at the Ser129 residue (pSer129 αSyn) mostly in LB and LN like structures in the BS and MB. This staining pattern was colocalised with Thioflavine-S (ThS) positive amyloidosis as well as with Gallyas silver staining showing neuropathology. The glomerular region of the OB displayed similar age-dependant pathology although genuine LB/LN like pSer129 αSyn positive structures could not be observed in the OB. PSer129 αSyn was detected also

throughout the Cx in the cytoplasm as well as in a nuclear staining pattern of young and old transgenic mice, likewise in hippocampal cornus amonis 1 (CA1), CA3 and subicular region. In contrast, none of these brain regions were positive for amyloidosis or silver staining positive neuropathology. Interestingly proteinbiochemical investigation revealed an αSyn form only present in the insoluble fraction of cortical lysates. Another striking observation was the age-dependent accumulation of transgenic non-phosphorylated αSyn in the synaptic regions of CA1 and CA3, which are known to be important for neuronal plasticity. Concomitantly old transgenic mice displayed reduced context learning. The emotional learning circuit of the basolateral amygdala (BLA) was found to be highly positive in cells displaying nuclear pSer129 αSyn staining, which was prominent in aged mice. Furthermore only aged transgenic mice displayed pSer129 αSyn positive, LN-like staining pattern most prominent in the medial part of the central nucleus (CeM). Both regions, the BLA as well as the CeM are known to be involved in long term potentiation (LTP) and again, old transgenic mice performed worst in the fear conditioning (FC) related emotional learning test. The poor performance of old transgenic mice coincided with reduced levels of the immediate early gene c-FOS measured in the BLA and CeM of the same animals directly after FC. Moreover levels of a Ser129 phosphotransferase Polo-Like-Kinase-2 (PLK2), which has been shown to be involved in neuronal plasticity in the hippocampus, were not upregulated after FC in old transgenic animals. Only young transgenic and old wild type animals displayed PLK2 upregulation in the BLA and in the CeM after FC.

As for the pathologic pSer129 αSyn, cell culture experiments with human embryonic kidney (HEK293E) cells transfected with αSyn and its candidate kinase G-protein-reseptor-kinase-5 (GRK5) reproduced the nuclear pSer129 αSyn-staining pattern observed in transgenic mice. More importantly, in the transgenic mice pSer129 αSyn positive stainings were observed to colocalise in the neuropil with PLK3 and in the cytoplasm and in nuclear regions with

PLK2, pointing to PLK2 and PLK3 as relevant kinases for the phosphorylation of the Ser129 residue of αSyn in α-Synucleinopathies.

Taken together, this work could show the different qualities of α-Synucleinopathy in all brainregions overexpressing αSyn in transgenic (Thy1)h[A30P]αSyn mice. Furthermore a direct correlation between α-Synucleinopathy and a lower neuronal activation could be demonstrated in the emotional learning circuitry.

1 Introduction

In 1817, James Parkinson published "An essay of the shaking palsy" and described the disease of six patients with tremor, impaired motor skills and speech difficulties (Parkinson, 1817). 60 years later the disease received the name of the discoverer: Parkinson's disease (PD). In the 1950's a new finding raised the hope of researchers, physicians and patients. The deficiency of dopamine in the brains of PD patients was discovered and a compensation of this deficiency with the dopamine precursor L-3, 4-dihydroxyphenylalanine (L-Dopa) was in the process of investigation. In 1967 the use of L-Dopa became a clinical treatment (Yahr et al., 1969, Hornykiewicz, 2002) that is still used today. L-Dopa is a precursor of dopamine and is able to cross the blood brain barrier. In the brain it can be metabolised to dopamine. Unfortunately this treatment does not provide a cure for PD, as L-Dopa treatment is only able to compensate the low levels of dopamine in the brain, but the neuronal degeneration continues in the affected brains. L-Dopa treatment can at best only slow down the initiated avalanche of neurodegeneration. Unfortunately this stage of drug treatment has not been crossed until today. An additional treatment option used today is the „deep brain stimulation" in which a brain pulse generator is used to stimulate fireing of neurons in the subthalamic nucleus (STN). This therapy is used for advanced PD patients with motor complications (Weaver et al., 2009) and improves motor disability, motor fluctuation, levodopa-induced dyskinesias and make the reduction of dosage of parkinsonian medication possible (Houeto et al., 2002). However the dopamine disregulation syndrome (DDS) may appear as a comlication of this treatment (Houeto et al., 2002, Lim et al., 2009, De la Casa-Fages and Grandas, 2012). A cure which is able to stop the degeneration of neurons is still not known and it's finding represents a challenge for all scientists working on the field of neurodegeneration. The magnitude of the challenge becomes clear when it is taken into account that aged individuals represent a huge part of western

populations and the fact that PD ist the second most common neurodegenerative disease after Alzheimers disease (AD). Although an enormous advance has been achieved in the diagnosis and the understanding of neurological disorders, numerous questions remain to be answered and numerous findings wait for their discovery, until the biological processes involved in neuronal death are completely understood and an appropriate cure can be developed.

In this work neuropathology induced by the PD associated protein alpha-synuclein (αSyn) was investigated in a transgenic animal model with age dependent deveolpment of failure in function of different neuronal systems.

1.1 Parkinson's disease

Parkinson's disease (PD) is a chronic progressive neurodegenerative disorder, which is characterised by the degeneration of dopaminergic neurons. Clinical symptoms are hypokinesia, resting tremor and a variety of degrees of rigidity (Jankovic, 2008). Very often patients report a disturbance of olfaction as a first symptom (Kranick et al., 2008). 70% of affected individuals realise a tremor in one of the hands, which is a cardinal sign of PD (Findley et al., 1981, Calne et al., 1986). Furthermore altered cognition is also often observed, moreover some patients develop dementia in late stages of the disease (Buter et al., 2008, Hely et al., 2008). Only 5% of all cases known represent genetical dominant or recessive disease forms resulting from mutations in PD associated genes (Lesage et al., 2009) and (Table 1-1). Most of the PD cases are idiopathic (Lesage et al., 2009). Suggested risk factors are pesticides (Franco et al., 2010), heavy metals (de Lau et al., 2006), or traumatic injuries of the brain (Critchley, 1957), furthermore the role of nutrition factors are also under investigation (Kalmijn et al., 1997, Shie et al., 2002).

As PD is a disease of the elderly and sometimes starts with intermittent symptoms, which are similar to signs of normal aging (Jenkyn et al., 1985,

Galasko et al., 1990), an accurate diagnosis is complicated. Moreover Parkinsonism is related also to other neurological disorders like multiple system atrophy (MSA), cortical-basal ganglionic degeneration or progressive supranuclear palsy (Kurata et al., 2011, Payan et al., 2011). Therefore a careful differential diagnosis has to be stated. This very often leads to a delayed start of the appropriate therapy, which unfortunately supports the neurodegenerative progression of PD.

Table 1-1 Known genes and loci related to recessive and dominant forms of PD.

Loci	Gene	Position	Inheritance	Currently known Functions
PARK 1/4	*SNCA*	4q22	dominant	Localized in nucleus and synapse, higly concentrated in Lewy bodies; regulation of synaptic vesicle activity
PARK 2	*parkin*	6q25-q27	recessive	E3 ubiquitin ligase
PARK 3	???	2p13	dominant	???
PARK 5	*UCHL1*	4p14	dominant	Ubiquitin C-terminal hydrolase
PARK 6	*PINK1*	1p35-p36	recessive	Mitochondrial kinase
PARK 7	*DJ-1*	1p-36	recessive	Chaperone, antioxidant
PARK 8	*LRRK2*	12q12	dominant	Mixed lineage kinase
PARK 9	*ATP13A2*	1p36	recessive	Lysosomal p-type ATPase
PARK 10	???	1p32	?(dominant)	???
PARK 11	*GIGYF2*	2q36-q37	dominant	Signal transduction
PARK 12	???	Xq	X-linked	???
PARK 13	*HtrA2/Omi*	2p13	dominant	Mitochondrial serine protease
PARK 14	*PLA2G6*	22q13.1	recessive	Phospholipase A2
PARK 15	*FBXO7*	22q12-q13	recessive	E3 ubiquitin ligase
PARK 16	*NUKS1/ RAB7L1*	1q32	dominant	Risk factor for sporadic PD
-	*EIF4G1*	3q27	dominant	???
-	*VPS35*	16q12	dominant	???

1.2 Neuropathology

The neuropathological hallmarks of PD are the selective loss of dopaminergic neurons in the substantia nigra pars compacta (SNpc), the locus coeruleus (LC) and the formation of proteinacious inclusions in the cytoplasm or in

extensions of affected neurons. These neuropathological protein aggregates are called Lewy bodies (LBs) and Lewy neurites (LNs) respectively. Friedrich Lewy originally identified these lesions in 1912. The cell loss in the SNpc leads to a depleation of dopamine in the putamen (Figure 1.1) and causes the motor symptoms observed in PD patients (Poirier et al., 1965). At the onset of the disease about 60% of dopaminergic neurons are already dead. This leads in the putamen to a depletion of dopamine of about 80% (Dauer et al., 2003). The only available therapies are the compensation of low dopamine levels with levodopa (L-Dopa), which is able to cross the blood-brain barrier, or the deep brain stimulation, which stimulates the remainig dopaminergic neurons to a higher dopamine excitation (see above).

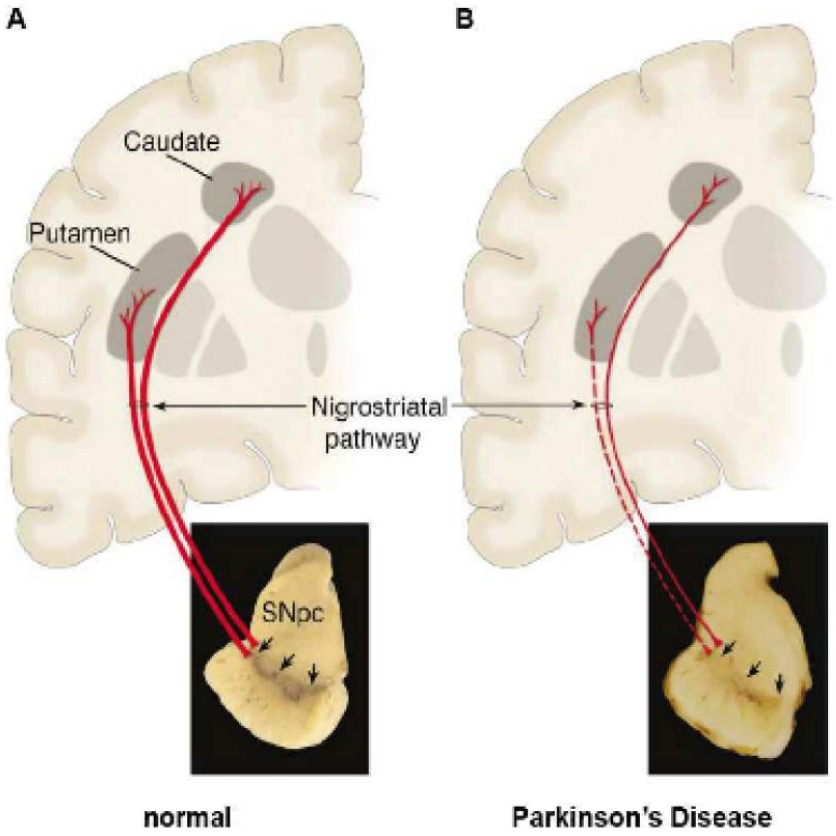

Figure 1.1 Nigrostriatal pathway in healthy and PD patients (with modifications from (Dauer et al., 2003).

A, sceme of the nigrostriatal pathway in a healthy individual. The substantia nigra pars compacta (SNpc) contains numerous neuromelanin positive neurons (arrows pointing to the pigmentation in the photograph) projecting to the putamen and the caudate nuclei of the striatum. B, the same pathway in an individual affected by PD. Loss of pigmentation in the SNpc points to the loss of neuromelanin containing dopaminergic neurons. This loss leads to a weakening of the projection to the caudate nuclei and to a stronger weakening of the projection to the putamen.

The described Lewy bodies and Lewy neurites interestingly are not specific for PD and can also be detected in other brain disorders, e.g. dementia with Lewy bodies (DLB) and Alzheimer's disease (AD) in which 50%-60% of patients display LB pathology. DLB is characterised by the loss of different neuronal populations including not only dopamine producing cells, but also acetylcholine producing cells (Hanson et al., 2009). This neuronal loss leads to parkinsonian symptoms, dementia, fluctuating cognition or visual hallucinations (Hanson et al., 2009). In PD, LB and LN are detectable in the substantia nigra and in the midbrain. With progression of the disease deposits appear also in other areas of the brain like the limbic system or the neocortex (Braak et al., 2003, Braak et al., 2004) and Figure 1.2. Therefore with progression of the disease an extension of the pathology on other brain regions is observed. This correlates with the onset of physiological deficiencies and induces heterogenous symptoms in LB associated disorders. As PD patients not only display the motoric symptoms, but also abnormalities in visual perception and olfaction (Chung et al. 2003), depression, dementia, cognitive dysfunctions and anxiety (Lang and Lonzano 1998a; Lang and Lonzano 1998b). Taken together, the topological distribution of LBs determines the affected brain regions and therefore the nature of the symptoms and the respective LB associated disease. Moreover, aggregates of the normally neuronal protein αSyn can be found as characteristic (oligodendro)-glial cytoplasmatic inclusions in multiple system atrophy (MSA) patient brains. MSA neuropathologically features neuronal loss in the cerebellum, pons, basal ganglia and the inferior olivary nuclei. Furthermore filamentous inclusions are detectable also in the cytoplasm of glia cells. Patients suffering from MSA display autonomic disfunctions and parkinsonism and/or cerebellar ataxia (Graham et al., 1969).

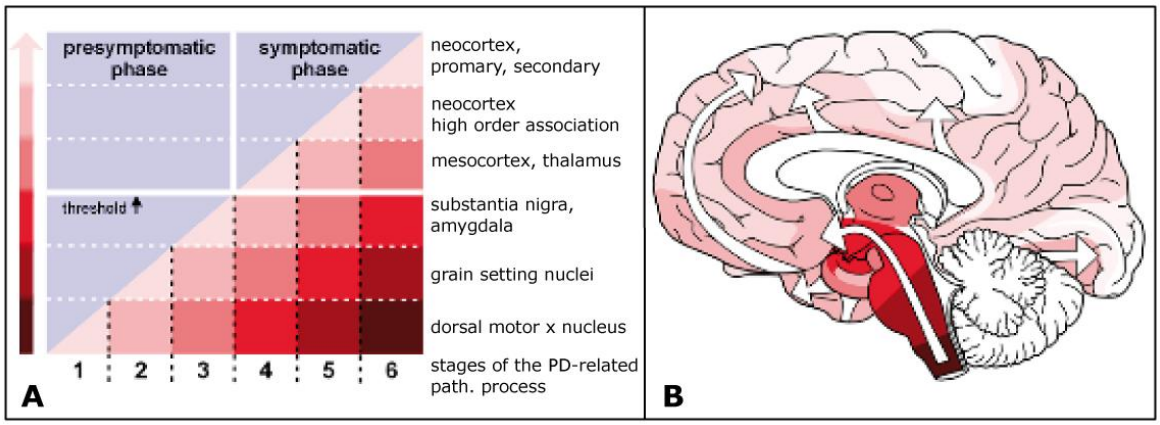

Figure 1.2 Stages in the PD related pathology (from (Braak et al., 2004)).

A, PD related pathology in affected brain regions is displayed in relation to the stage of the disease. B, the ascending pathological process (white arrows). The intensitiy of the colored areas corresponds to the intensity in A. (from Braak et al., 2004)

LBs are eosinophilic, round inclusions located in the cytoplasm of affected neurons. They have a size of 5-25 µm and are composed of a halo of radiating fibrils surrounding a less defined core (Spillantini et al., 1997) and Figure 1.3. LBs were first found to be positive for ubiquitin (Lowe et al., 1988) and αSyn was found to be the main component of LBs (Spillantini et al., 1997). Today it is known that αSyn involved in aggregation processes underlies also biochemical changes like nitrosylation (Giasson et al 2000, Duda et al 2000) and phosphorylation of the Ser129 residue (pSer129 αSyn) (Fujiwara et al 2002, Anderson et al 2006). Also cleavage and truncation of αSyn has been suggested to play a role in the pathogenenesis of LB diseases (Liu et al., 2005). It is not clear whether Lewy pathology is protective or toxic. The pioneer study of Tompkins and Hill (Tompkins and Hill 1997) showed that LB-positive neurons looked healthier than LB-negative ones. It has been observed that e.g. in PD 3-4% of the neurons in the SN contain LBs. This proportion remains constant, regardless of the stage of the disease (Greffard et al., 2010). Similar observations were noted in DLB patients, where amount of LBs do not correlate with severity or duration of dementia (Harding et al., 2001). Therefore the biological function and the pathological significance of LBs for synucleinopathies still remain to be shown. Today

more and more evidence is indicating that affected neurons try to get rid of misfolded and fibrillar toxic proteins by forming LB. It is suggested that the formation of LB is a cellular defense mechanism against unfolded protein stress, and a mechanism that facilitates and increases the degradation of unwanted and possibly cytotoxic proteins (Garcia et al 2002; Kopito 200; Sherman and Goldberg, 2001). With respect to structural organisation, protein content and intracellular localisation LBs show similarities to aggresomes. Therefore it was suggested, that these inclusions are related and may be formed in a similar way (Olanow et al 2004). This mechanism may protect cellular survival but the price could be a LB-growing related increase of misfunction of intracellular processes like e.g. transport and degradation of proteins (McNaught et al 2003; McNaught and Olanow 2003). This may contribute to the growing of the intracellular LB and to neuronal disfunction, which must not directly kill the affected cell, but significantly impair its functions e.g. neurotransmission and synaptic plasticity. Cell populations affected in this way may contribute to the misfunction of whole areas in affected brain regions and therefore lead to the misregulations of whole neuronal systems, as observed in PD, DLB and MSA.

Figure 1.3 Lewy bodies positive for alpha-synuclein (αSyn) and ubiquitin (modified from (Dauer et al., 2003)).

Lewy bodies are positive for ubiqutin and the synaptic and nuclear protein alpha-synuclein (αSyn).

1.3 Alpha-synuclein (αSyn)

Synuclein was originally discovered 1988 by Maroteaux at al. (Maroteaux et al., 1988) as a protein expressed in the nervous system of the electric eel, *Torpedo Californica*. Three major molecular weight classes could be identified in this species, 17.5, 18.5, and 20.0 kD, furthermore immunostaining of tissue displayed predominant staining of the 17.5 kD species in synapses and a partial localisation in the nuclear envelope (Maroteaux et al., 1988). The mammalian synuclein family consists of three proteins: αSyn, βSyn and γSyn (Ueda et al., 1993, George, 2002). These have been only described in vertebrates. γSyn is highly expressed in different brain regions, especially in the substantia nigra (Lavedan, 1998) and bSyn is expressed like αSyn at presynaptic terminals particularly in the hippocampus, neocortex, striatum, thalamus and cerebellum (Iwai et al., 1995). However only αSyn is aggregated in LB diseases (George, 2002). Spillantini at al. could demonstrate that αSyn is the main component of LBs (Spillantini et al., 1997). The sequence of αSyn can be subdivided into three different domains (Figure 1.4). The α-helical domain (residues 1-65) is important for the binding to phospholipids (Davidson et al., 1998, Eliezer et al., 2001, Li et al., 2001) and contains the three independent point mutations A53T (Polymeropoulos et al., 1997), A30P (Kruger et al., 1998) and E46K (Zarranz et al., 2004), which have been shown to cause autosomal dominant early-onset PD (Comellas et al., 2011). The central hydrophobic domain (residues 66-95) carries a phosphorylation site at Ser87 (Okochi et al., 2000) and is historically termed as the non-Aβ component (NAC) of AD plaques (Ueda et al., 1993). The NAC domaine enables αSyn to form β-sheet structure (el-Agnaf et al., 2002) and furthermore to form amyloid-like protofibrils and fibrils (Giasson et al., 2001, el-Agnaf et al., 2002). This feature distinguishes αSyn from βSyn and γSyn (Giasson et al., 2001). The acidic carboxy terminal domain (residues 96-140) is composed mainly of acidic amino acids and therefore has a strong negative charge (George, 2002). Furthermore it contains the acidic domain 125-140, which

seems to be important for the chaperone like activity of αSyn (Souza et al., 2000). Moreover the carboxy-terminal domain hosts several phosphorylation sites (Negro et al., 2002) of which the Ser129 residue was shown to be phosphorylated in synucleinopathy lesions (Fujiwara et al., 2002) and represents the most important biochemical change in synucleinopathies (Anderson et al., 2006).

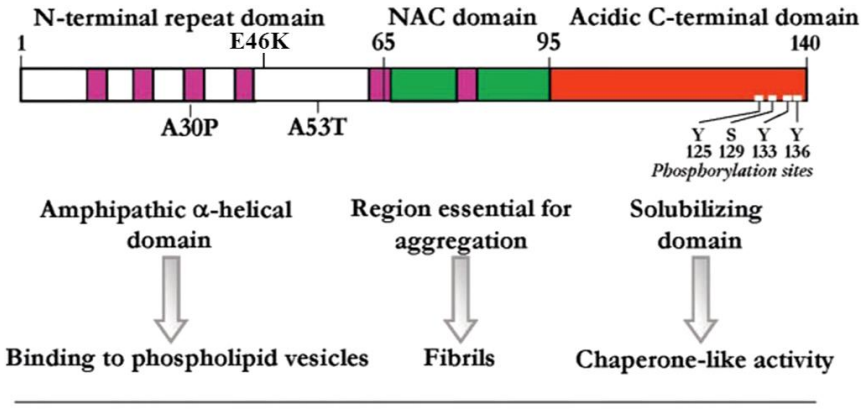

Figure 1.4 Human αSyn sequence and domains (modified from (Recchia et al., 2004)).

αSyn consits of 3 domains: the α-helical domain in which the 3 missense mutations A53T, A30P and E46K are localised, the NAC region which is essential for aggregation and the C-termianl part with chaperon-like activity which contains the Ser129 phosphorylation site.

Nitration of different tyrosines within αSyn c-terminus may also influence aggregation (Takahashi et al., 2002). Nevertheless as the importance of the Ser129 phosphorylation for synucleinopathies was assessed, extensive research was done to identify the kinases involved in the Ser129 phosphorlytion of αSyn. It could be shown that the Casein Kinase I (CK I) and CK II are phosphorylating αSyn at the Ser129 residue (Okochi et al., 2000). Furthermore this side is also a target for the G-protein-coupled receptor kinases (Pronin et al., 2000). Moreover studies could show that kinases from the Polo-like-kinase (PLK) family, which normally are involved in the regulation of cell-cycle (Barr et al., 2004, van de Weerdt et al., 2006), are also phosphorylating αSyn at the Ser129 residue *in vitro* and *in vivo* (Inglis et al., 2009, Mbefo et al., 2010). *In vitro* studies have suggested that phosphorylation at Ser129 promotes formation of αSyn filaments and

oligomers (Fujiwara et al., 2002) as a consequence of change in charge distribution and hydrophobicity of αSyn in the carboxy-terminal region (McLean et al., 2002). Phosphomimic Ser129 mutants were shown to enhance aggregation as well as cytotoxicity in cell culture and in flies (Smith et al 2005, Chen and Feany 2005). However, phosphorylation of the Ser129 αSyn residue was shown to not increase ubiquitination *in vitro* (Nonaka et al 2005) and a recent *in vitro* work showed decreased fibrillisation of pSer129 αSyn (Paleologou et al 2008). Moreover the mutant, non-phosphorylatable [S129A] αSyn was reported to be more toxic than wild-type αSyn *in vivo* (Gorbatyuk et al 2008, Azeredo da Silveira et al 2009). This observation increases the possibility that the phosphorylation of the Ser129 αSyn residue is a cellular defense mechanism and not disease causing in patients. αSyn aggregation has been suggested to be cytoprotective (Tanaka et al., 2004) by sequestering potentially toxic soluble αSyn (Xu et al., 2002). On the other hand αSyn aggregates have been shown to impair proteasomal activity (Snyder et al., 2003, Lindersson et al., 2004), therefore it is not clear which exact conformational state of αSyn may confer toxic abilities (Dev et al., 2003). Therefore the mode of αSyn action remains to be clarified (Di Rosa et al., 2003, Sidhu et al., 2004). In addition to the three mentioned autosomal dominant point mutations, A53T, A30P and E46K also genomic multiplication of the αSyn locus was described to cause PD (Singleton et al., 2003, Chartier-Harlin et al., 2004, Ibanez et al., 2004). Thus, evidence became clear that even elevated levels of wild-type αSyn are able to cause synucleinopathy related diseases. Furthermore, recently performed genome-wide association studies identified *PARK16* as a new susceptibility locus for PD, moreover *PARK16, SNCA* and *LRRK2* were identified as shared risk loci for PD (Satake et al 2009, Simon-Sanchez et al 2009). Animal models including flies, nematode, rodents and primates confirmed the evidence that elevated levels of wild-type αSyn are enough to cause synucleinopathy related diseases (Feany et al., 2000, Masliah et al., 2000, Giasson et al., 2002, Lee et al., 2002, Neumann et al., 2002, Lakso et al., 2003, Yamada et

al., 2004, Freichel et al., 2007). Gene knock-out mice for αSyn displayed functional deficits of the dopaminergic system (Abeliovich et al., 2000) and resistance to 1-methyl-4-phenyl-1,2,3,6-tetrahydropyridine (MPTP) induced toxicity (Dauer et al., 2002). To gain more insights in synucleinopathy related action of neurotoxicity and of pathogenesis, different αSyn overexpressing animal models, that drive transgene overexpression under the control of different promoters, have been generated (see following chapter).

1.4 Animal models for α-Synucleinopathy

To date mouse models that overexpress full-length human wild type αSyn, the human A53T or A30P mutant αSyn, highly aggregation prone truncated human αSyn or full-length wild type mouse αSyn have been generated. With the choice of the promoter regulating the transgene overexpression, special cell types have been targeted for αSyn overexpression. Crossbreeding experiments were used to generate double transgenic animals in order to test possible modifier genes in αSyn overexpressing mice. Animals expressing wt and mutant αSyn under control of different tyrosin hydroxylase (TH) promoters are used to investigate the effect of overexpression in catecholaminergic neurons. These (TH)-αSyn mice displayed a great variability of phenotypes (Kahle, 2008). However, a common phenotype is the specific accumulation of overexpressed αSyn within dopaminergic cell bodies (Matsuoka et al., 2001, Rathke-Hartlieb et al., 2001, Maskri et al., 2004) and an αSyn transport to striatal terminals. Nevertheless, no obvious phenotype (Matsuoka et al., 2001, Rathke-Hartlieb et al., 2001, Maskri et al., 2004) and also no sensitisation to MPTP toxicity has been observed (Rathke-Hartlieb et al., 2001). The generation of a TH-αSyn overexpressing mouse model harbouring both point mutations, A30P and A53T resulted in a model that display neuropathology and symptoms related to it (Richfield et al., 2002). The (TH)-[A30P/A53T]αSyn mice display a similar distribution of the transgene as the single mutant models, however

in contrast they develop a marked loss of locomotor activity after MPTP intoxication (Richfield et al., 2002). Moreover the animals display reduced activity upon aging combined with an age dependant reduction of dopamine and its metabolites in the striatum. Furthermore it could be shown that these animals are strongly sensitive to the dopamine neurotoxic effects of the pesticides paraquat and maneb (Thiruchelvam et al., 2004). The observation that the C-terminally truncated αSyn has a very high tendency to aggregate *in vitro* (Murray et al., 2003, Hoyer et al., 2004), induced further investigations in *in vivo* models. Therefore two (TH)-αSyn mouse models were generated, one that overexpress an αSyn lacking the last 10 amino acides (αSyn (1-130)) (Wakamatsu et al., 2008) and one that overexpress an αSyn that lacks the last 20 amino acids (αSyn (1-120)) (Tofaris et al., 2006). The (TH)-αSyn (1-120) mice, as observed in the other (TH)-αSyn mice, develop somatodendritic accumulations in the SN and axonal pathology in the striatum and the olfactory bulb (OB) at an age of 6 months. Furthermore, the olfactory bulb is positive for granulofilamentous material and for stainings with the amyloid dye thioflavine S (ThS). Biochemical investigation revealed insoluble αSyn aggregates in urea extracts from the OB and SN (Tofaris et al., 2006). Striatal dopamine levels have been shown to be reduced between 1 and 3 months old mice. 18 months old mice displayed locomotor impairment both in beam walking (a motoric test) and after increased amphetamine-induced ambulance. As no fulllength αSyn mouse was generated in parallel unfortunately the disease-initiating potential of the C-terminal truncation can not be estimated in this model (Kahle, 2008). A (TH)-[A53T]αSyn (1-130) mouse model was generated in parallel with an additional line overexpressing the full lenght [A53T]αSyn (Wakamatsu et al., 2008). With these two lines the neurotoxic effect of the C-terminally truncated αSyn on dopaminergic neurons could be assesed (Wakamatsu et al., 2008). Only the [A53T]αSyn (1-130) mice displayed an impressive loss of dopamine neurons and a significantly reduced spontaneus locomotion, which can be treated with L-Dopa

(Wakamatsu et al., 2008). However the dopamine neuron loss occurs during the embryogenesis and LB pathology is not present in these mice. Therefore the toxic effect of C-terminally truncated mutant αSyn could be confirmed, but the reproduction of the age dependant progressive nature of PD is missing in these models (Kahle, 2008). Due to the missing LB pathology this model does not permit closer investigation of synucleinopathy and neuropathology related to it.

Another mouse model generated by Masliah et al. is expressing wt αSyn under the control of the platelet-derived growth factor-b (PDGFb) (Masliah et al., 2000). This model develops granular inclusions of overexpressed αSyn in neuronal neurites and cell bodies and has a reduction of TH positive terminals in the striatum. Furthermore, locomotor performance on the rotarod is reduced (Masliah et al., 2000) and lysosomal pathology (Rockenstein et al., 2005) and reduced neurogenesis in the OB of this animal model can be observed (Winner et al., 2004, Winner et al., 2008).

Several groups employed the prion protein (PrP) promoter to overexpress wt αSyn, [A30P]αSyn or [A53T]αSyn in neurons. In conclusion, these mice recapitulate neuronal α-Synucleinopathy and demonstrate the neurotoxicity of αSyn fibrillisation (Kahle, 2008).

Other groups used the large P1 artificial chromosome (PAC) containing the entire human αSyn including 34kB of upstream sequence to overexpress αSyn in a rodent model (Touchman et al., 2001, Gispert et al., 2003). Groups investigating the α-Synucleinopathy in MSA use a myelin proteolipid protein (PLP) promoter (Kahle et al 2002b, Stefanova et al 2005, Stefanova et al 2007), a 2',3'-cyclic nucleotide 3'-phosphodiesterase (CNP) promoter (Giasson et al., 2003, Yazawa et al., 2005), or a myelin basic protein (MBP) (Shults et al., 2005) to achieve overexpression of αSyn in oligodendrocytes. Such animal models offer the possibility to investigate MSA related synucleinopathies in oligodendroglial cells. A summary of the most important features of the described models is presented in Table 1-2.

Table 1-2 Genotypes and phenotypes of transgenic αSyn mouse models (modified from Kahle, 2008).
(*Rieker et al, 2011)

Promoter	Transgene	Histology	Biochemistry	Neurochemistry	Behaviour	MPTP toxicity
Strictly neuronal						
9 kb rat TH	[wt]αSYN	Somatodendritic accumulation of transgenic αSYN No Fibrillar inclusions	–	Normal	Normal	Enhanced reduction of locomotor activity
4.5 kb rat TH	[A30P]αSYN	Somatodendritic accumulation of transgenic αSYN	Normal	Normal	–	Unchanged
4.8 kb rat TH	[A53T] αSYN	Somatodendritic accumulation of transgenic αSYN	-	–	–	Unchanged
9 kb rat TH	[A30P,A53T] αSYN	Somatodendritic accumulation of transgenic αSYN No fibrillar inclusions	-	Reduced TH+ neurons and DA levels upon aging	Mildly reduced locomotor activity upon aging	Enhanced reduction of locomotor activity
9 kb rat TH	αSYN(1–120)	Somatodendritic accumulation of truncated αSYN Thioflavin S-positive fibrillar inclusions	Detergent-insoluble truncated αSYN	Very young-onset, non-progressive DA reduction	Progressive locomotor decline	–
9 kb rat TH	[A53T] αSYN(1–130)	Somatodendritic accumulation of truncated αSYN		Embryonal, non-progressive DA reduction	Reduced locomotion	–
Mouse Thy1	[wt] αSYN	Somatodendritic accumulation of transgenic αSYN	–	–	Very young-onset sensorimotor impairments	–
Mouse Thy1	[A30P] αSYN	Somatodendritic accumulation of transgenic αSYN Argyrophilic, thioflavin S-positive fibrillar inclusions	Detergent-insoluble phosphorylated transgenic αSYN aggregates Progressive proteinase K-resistance	Normal	Progressive cognitive and locomotor decline	Unchanged
Mouse Thy1	[A53T] αSYN	Marked somal and neuritic accumulation of transgenic αSYN; Amorphous inclusions	–	–	Fulminant progressive neuromuscular junction loss	–
Mouse Thy1	mouse-αSYN*	Ubiquitine immunopathology in spinal cord and brainstem.	Multiple αSyn isoforms including phosporylated αSyn	Neuronal phosphorylated αSyn or ubiquitin in granular and small fibrillar aggregates, accumulaton of aSyn and phosphorylated aSyn in hippocampal neurons without ubiquitin immunopathology	Axonal degeneration in long white matter tracts, breakdown of myelin sheets, degeneration of neuromuscular junctions, mild impairment of motor performance with late onset	–
Hamster PrP	[A30P] αSYN	Somatodendritic accumulation of transgenic αSYN gliosis	αSYN aggregates	Normal	Progressive locomotor decline	Increased DA neuron loss
Mouse PrP	[A53T] αSYN	Somatodendritic accumulation of transgenic αSYN Argyrophilic, thioflavin S-positive fibrillar inclusions Gliosis; Neurodegeneration	Detergent-insoluble transgenic αSYN aggregates	Normal	Progressive locomotor decline	–
Predominantly neuronal						
PDGF-ß	[wt] αSYN	Marked somal and neuritic accumulation of transgenic αSYN; Amorphous inclusions	Detergent-insoluble transgenic αSYN	Non-progressive reduction of TH+ neurons and terminals	Mildly reduced locomotor activity	–
Oligodendroglial						
PLP	[wt] αSYN	(Oligodendro)glial cytoplasmic inclusions; Gliosis	Detergent-insoluble, phosphorylated transgenic αSYN	Non-progressive reduction of TH+ neurons and terminals	Mildly reduced locomotor activity	3-NP sensiti-zation
CNP	[wt] αSYN	(Oligodendro)glial cytoplasmic inclusions; Gliosis	Detergent-insoluble transgenic αSYN	–	Progressive locomotor decline	–
MBP	[wt] αSYN	(Oligodendro)glial cytoplasmic inclusions; Gliosis	Detergent-insoluble transgenic αSYN	–	Mildly reduced locomotor activity	–

The animal model used in this work is overexpressing the [A30P]αSyn under control of the CNS neuron specific Thy1 promoter and is a well established

modell for α-Synucleinopathy (Kahle et al., 2000, Kahle et al., 2001, Neumann et al., 2002, Freichel et al., 2007, Schell et al., 2009). The Thy1 promoter was used by several groups to overexpress human wt, A30P and A53T αSyn in transgenic mice. A shared feature of all these models is the formation of somatodendritic accumulations of granular and detergent insoluble αSyn throughout the brain and the spinal cord (Kahle et al., 2000, van der Putten et al., 2000, Kahle et al., 2001, Rockenstein et al., 2002, Maskri et al., 2004). Furthermore, the development of severe motor phenotypes is common (Table 1-2). Another group used the Thy1 promoter to overexpress mous αSyn in a transgenic mouse model (Rieker et al., 2011). Indeed this model has shown that increased levels of mouse αSyn do not induce early-onset behavioural changes, but induce end-stage pathophysiological changes in murine neurons. These changes are strikingly similar to those evoked by the expression of human wild type or mutant αSyn (Rieker et al., 2011). The (Thy1)h[A30P]αSyn mice used in this study stand out as a useful model to investigate the relationship between the behavioural impairments, the neurodegeneration and the complex αSyn fibrillisation process (Kahle, 2008). These mice display already at young age somatodendritic accumulation of detergent insoluble human αSyn, although without displaying any obvious phenotype. Furthermore, young (Thy1)h[A30P]αSyn mice display pSer129 αSyn stainings in neuronal nuclei in several cortical areas, hippocampal CA1, CA2 and CA3 regions as well as in the basolateral amygdala (BLA) without showing any region related deficits. Only upon aging transgenic overexpressed αSyn acquires a fibrillar amyloid conformation, that is observed by electron microscopy, thioflavine S staining and proteinase K resistance (Neumann et al., 2002). This age dependent pathology correlates with phenotypic motoric symptoms which are the beginning of the motoric endstage of these mice (Freichel et al., 2007) and partially also with emotional learning deficiencies, which interestingly already are apparent at an age of 12 months (Freichel et al., 2007).

1.5 Learning and memory

As already mentioned, emotional and contextual learning deficites of old (Thy1)h[A30P]αSyn mice could be correlated with different stages of synucleinopathy observed in amygdala and hippocampus only of old transgenic animals. The amygdala is known as the key region for emotional learning (LeDoux et al., 1988, Killcross et al., 1997, LeDoux, 2000, Goosens et al., 2001, Holahan et al., 2004) and is shown to be also higly affected in patients suffering from neurodegenerative diseases like LBD diseases or PD (Braak et al., 1994, Harding et al., 2002, Iseki et al., 2005). Hippocampal function again is shown to be crucial for contextual learning and memory (McNish et al., 1997, Mizumori et al., 1999). But also the amygdala is modulating this type of memory (Goosens et al., 2001, Scicli et al., 2004). Memory in general is allowing an organism to store information and to gain access to it in the case of need. The memory system is mainly devided into two parts, the declarative and the non-declarative part (Figure 1.5). According to the type of information, different brain regions are involved in the processing and storage. The declarative memory involves information, which the individual is aware of, i.e. memory involving knowledge e.g. mathematics. The non-declarative memory systems, to which the emotional learning belongs, is involving processed i.e. learned information, which is recalled automatically, e.g. reflexes and learned fear (Figure 1.5).

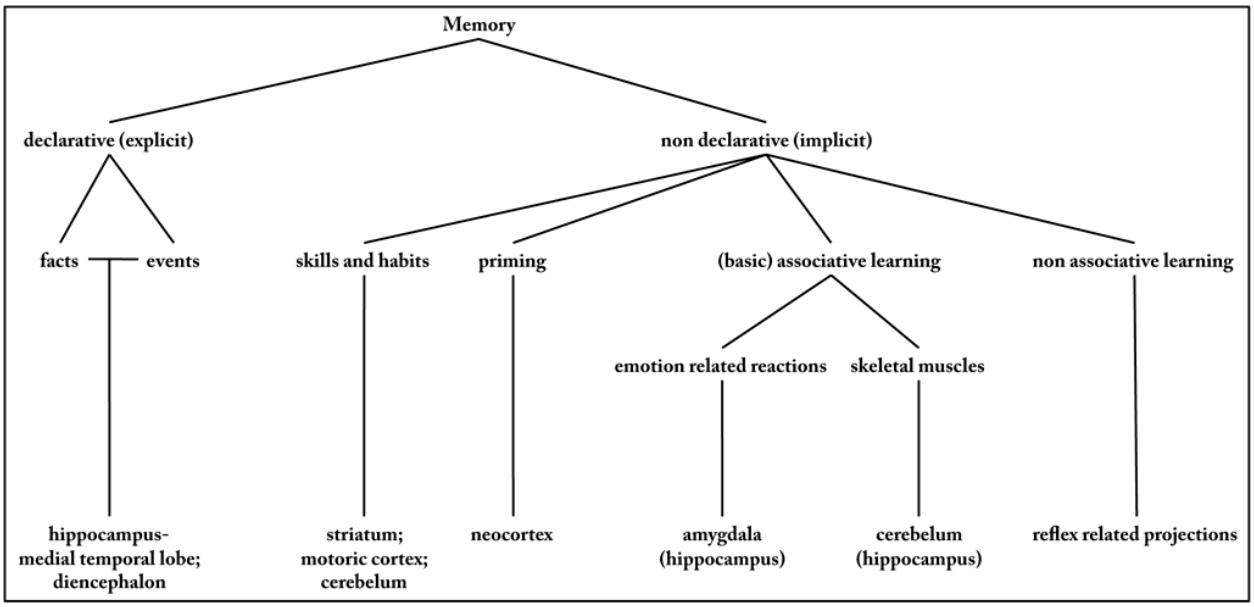

Figure 1.5 Overview over the different types of memory.

The memory system is mainly devided into declarative and non declarative memory. This division bases on the different types of informations (modified from Thompson, 2001).

The process of learning is one of the most important processes the organism uses for the adaption to different environments, and it increases the probability of the individual to survive under extreme conditions. Learning is subdivided in two main forms, the non-associative and the associative learning (Figure 1.6). Non-associative learning involves the learning of the relevance of one stimulus. Depending on the stimulus type -aversive or not aversive- sensitisation or habituation, respectively, takes place. Associative learning involves the classical conditioning and the instrumental conditioning. In the classical conditioning the coherence between one or two neutral stimuli (CS) and an unconditioned stimulus (US) is learned. Thereby a neutral stimulus, without biologicl relevance (CS), receives a biological relevance and is able to induce a response (CR). Learning in the instrumental conditioning involves the ability to associate an aktive action to the expected result of the action. Thereby a causal determined sequence of happenings arises. For this work the learning system involved in classical conditioning was relevant.

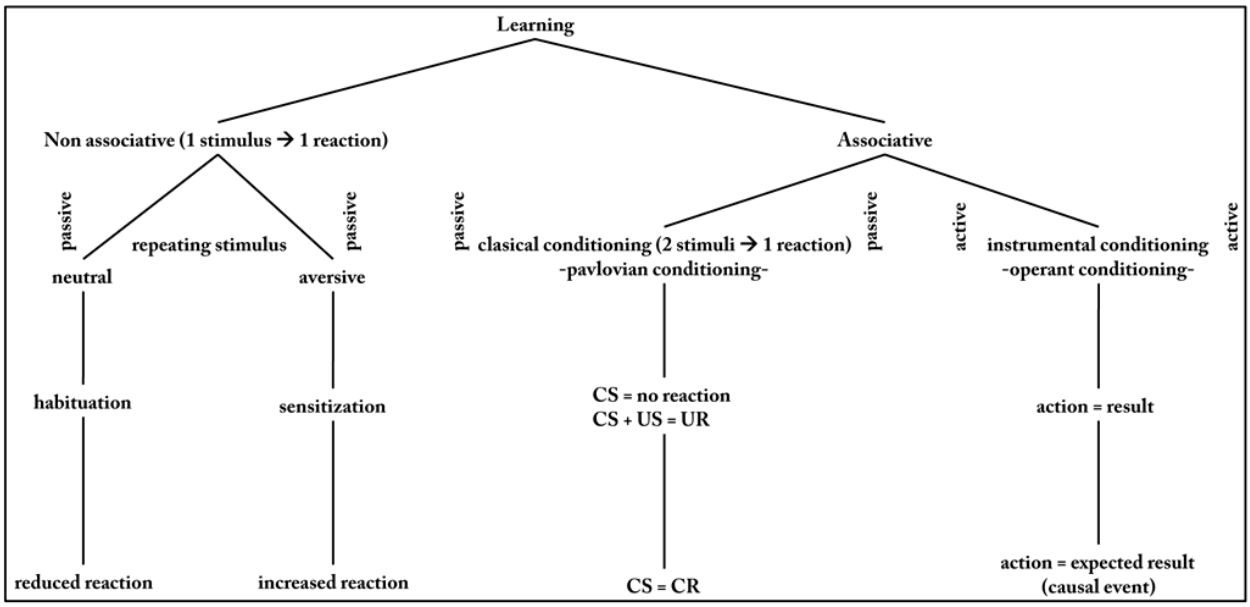

Figure 1.6 Subdivision of learning.

Learning is subdivided in 2 main forms: The non-associative and the associative learning. The classical conditioning related learning performed in this work belongs to the associative learning.

The classical conditioning, also called Pavlovian conditioning, was discovered by the Russian physiologist Ivan Pavlov in 1927 and is one of the most important forms of associative learning. Thereby the association between one or two stimuli, called the condition stimuli (CS) without a biological relevance, e.g light or tone cue, is connected to an other stimulus, called the unconditioned stimulus (US), which has a biological relevance and can be either positive, e.g. food, or negative e.g. footshocks. In the learning phase the answer to this stimuli represents the unconditioned respond (UR) (Figure 1.6 and Figure 1.7). Due to the paired, i.e. either together or shortly after each other, and repetitive presentation of both CS and US during a longer period of time (the duration of conditioning phase) the CS receives a biological relevance for the organismus trained. After conditioning, only an exposure to the CS is enough to elicite a respond, which is called conditioned response (CR). Thus in training phase a UR was transformed to a CR (Figure 1.6 and Figure 1.7).

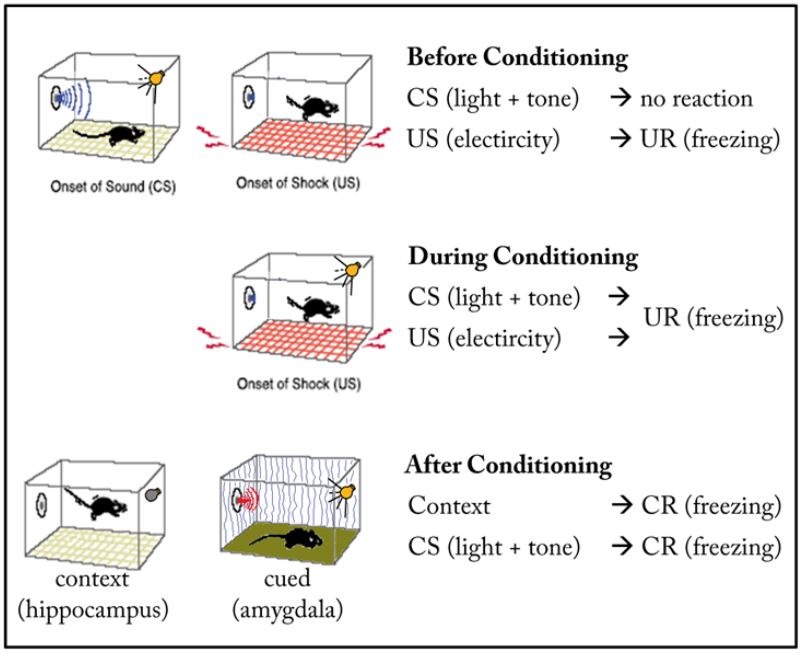

Figure 1.7 The classical fear conditioning performed in this work belongs to the associative learning.

Before the training, exposure to the neutral condition stimuli (CS: light and tone cue) does not elicit any reaction from the animals. An exposure to an unconditioned stimulis (US: electric foot shocks) would elicit sturtle and freezing behaviour. During the training CS and US are presented together and repeatedly. In this phase association between CS and US is consolidated. The animals display an unconditioned respond (UR).
After training the presentation of the CS in a different context is enough to elicit the respective conditioned response (CR). This learning is amygdala related emotional learning. Presentation of only the conditioning context to the animals is also enough to elicit a CR. This is hippocampus related context learning.

It is obvious that this mechanism is crucial for an organism to adapt to its environment, so that it has the possibility to connect special stimuli to positive happenings, e.g. food or mating partners, and other stimuli to danger, e.g. predators, alien territiory or bad food). This very basic amygdala and hippocampus related learning mechanism protects and assures survival. Figure 1.7 shows how the classical conditioning was performed with the [A30P]αSyn transgenic animals used in this work. As mentioned before the amygdala and the hippocampus are affected by synucleinopathy in an age-dependant manner in this mouse model (Freichel et al., 2007, Schell et al., 2009). This correlates with the emotional and contextual impairment of the learning in affected old transgenic mice. The amygdala is located in the temporal lobe and consists of several nuclei (LeDoux, 2000). Fear conditioning relevant is the basolateral amygdala

(BLA) that consist of the lateral (LA), basal (BA) and basomedial (BM) part and the central nucleus CeA (CeM, medial and lateral, Cel) (Goosens et al., 2001) and (Figure 1.8). As visible in Figure 1.8 B, the BLA receives and integrates information from a variety of sources; the thalamic medial geniculate nucleus (MGN, auditory), the perirhinal cortex (PERI, visual), the insular cortex (INS, somatosensory and gustatory), the thalamic posterior intralaminar nucleus (PIL, somatosensory), the hippocampus (Hip, spatial and contextual) and the piriform cortex (PIR, olfactory) (Maren, 1999, LeDoux, 2000, Maren, 2001). Therefore the BLA is a place for sensory convergence where the association between conditioned stimulus-unconditioned stimulus (CS-US) is registered and stored. The emotional learning related information leaves the amygdala via the central nucelus, which mediates appropriate fear responses via projections to the hypothalamus and the brainstem.

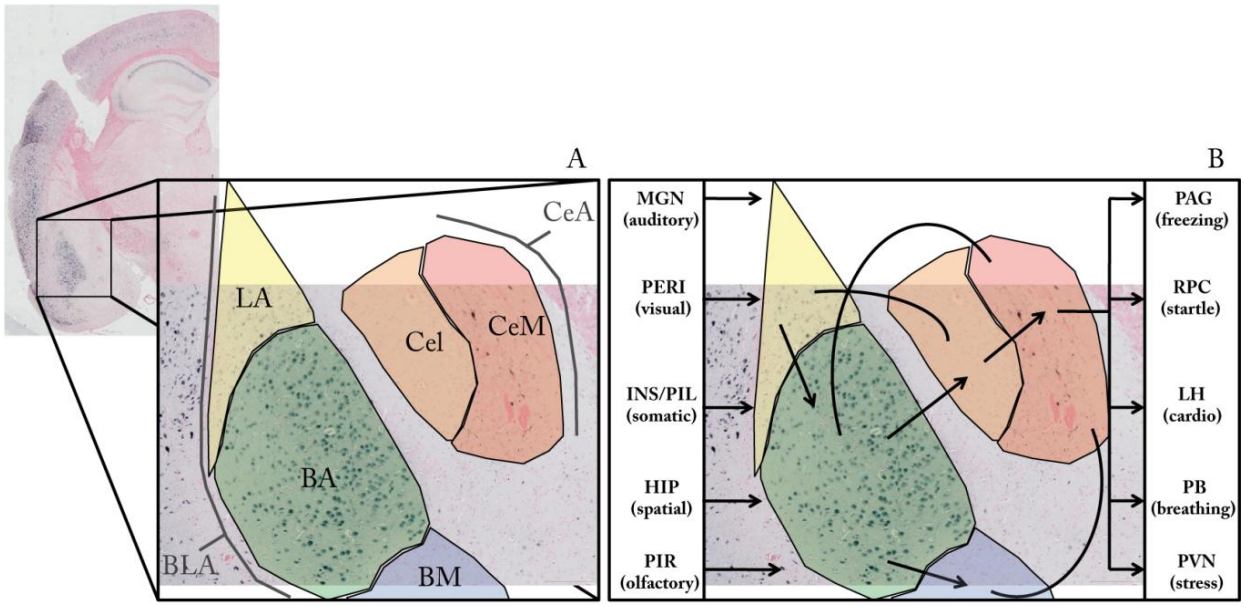

Figure 1.8 Anatomy and connections of the fear conditioning circuit in the amygdala.

Pictures in A and B display pathologic pSer129αSyn amygdala regions of old [A30P]αSyn transgenic mice suffering from synucleinopathy. The nuclei known to be important for fear conditioning are the lateral (LA), basal (BA) the basomedial (BM) nuclei and the central nucleus, CeA (CeM, medial and Cel, lateral). The BA and the Ce are the regions most heavily affected by synucleinopathy in the animal model used in this work.

These stress related responses are freezing (periaqueductal gray, PAG), potentiated acoustic startle (nucleus reticularis pontis caudatis, RPC), increased heart rate and blood pressure (lateral hypothalamus, LH), increased respiration (parabrachial nucleus, PB) and glucocorticoide release (paraventricular nucleus of the hypothalamus, PVN) (Maren, 1999).

The mammalian hippocampal formation is a brain structure, which comprises of the dentate gyrus (DG), the cornu ammonis (CA) fields, the subicular (sub) complex and the entorhinal cortex (EntCx). It is shown that the hippocampal contribution to memory is manifold. The hippocampus is involved in the cognitive mapping and the scene menory, in the declarative and the relational memory, the rapid acquisition of configural or conjunctive associations and to context-specific encoding and retrieval of specific events (Morris, 2006). This work focus in particular on the context related memory of the hippocampal formation, as neuropathological α-Synucleinopathy was detected in all hippocampus related regions into different extents.

1.6 Influence of polo-like-kinases on synucleinopathies and their involvement in neuronal plasticity

Recently Polo-Like-Kinases (PLKs) were found to phosphorylate αSyn at the pathologic Ser129 residue (Inglis et al., 2009). Furthermore PLKs are shown to be regulated by neuronal activation and to have an influence on neuroplasticity (Kauselmann et al., 1999, Pak et al., 2003, Seeburg et al., 2008a). PLKs are known as key regulators of the cell cycle (Barr et al., 2004, Xie et al., 2005, van de Weerdt et al., 2006). In mammals, 4 PLKs have been identified (Dai, 2005) and Figure 1.9. The structure of the PLKs consists of two domains, the amino terminal kinase domain and the carboxy terminal polo box domain (PBD), which contains two polo boxes. The only exception is PLK4, as it contains only one PBD (Figure 1.9).

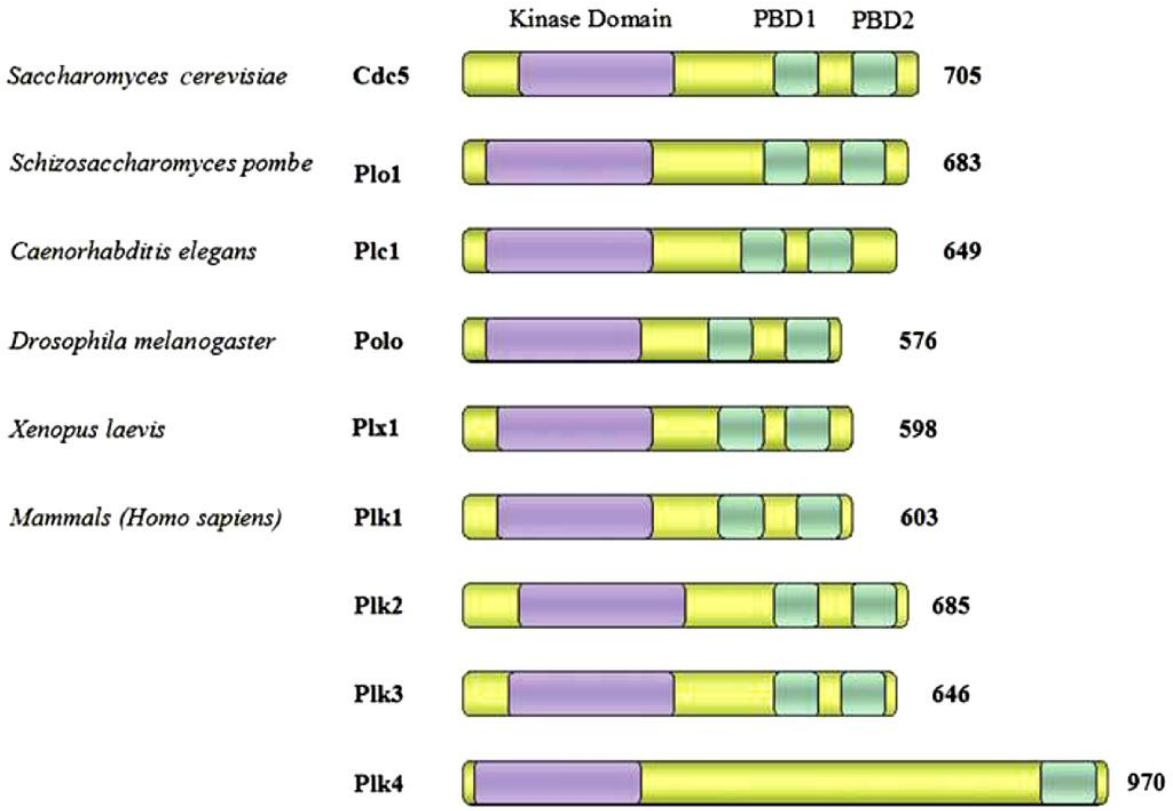

Figure 1.9 The family of the Polo-Like-Kinases (PLKs) (modified from (Dai, 2005)).

PLKs are the only category of proteins bearing PBDs (Dai, 2005). These domains permit the PLKs to execute unique regulatory functions during several phases of the cell cycle (Figure 1.10). Due to the observations that PLKs play important roles in the control of cell proliferation and furthermore genomic stability and oncogenesis (Barr et al., 2004, Dai, 2005, Winkles et al., 2005, Xie et al., 2005, Archambault et al., 2009), different additional functions are suggested, e.g. regulation of gene expression, regulation in cell cycle checkpoint or involvement in cancer related cellular processes. PLKs are not only involved in the regulation of cell cycle related processes but also have important functions in postmitotic neurons (Seeburg et al., 2005). PLK2 and PLK3 were observed to be dynamically regulated by synaptic activity at the mRNA and protein level in activated neurons. Therefore especially these two PLKs have a relevant function in the nervous system.

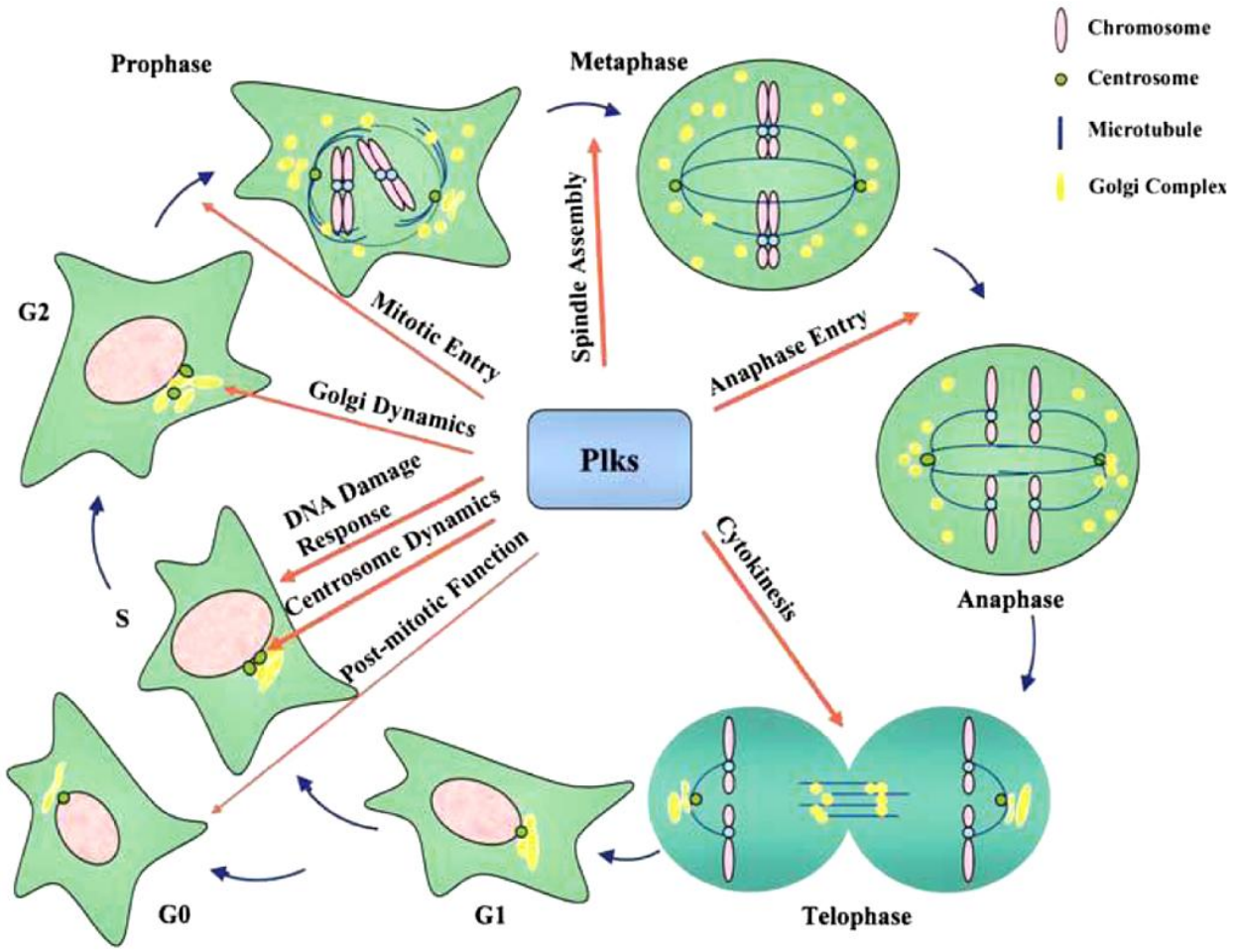

Figure 1.10 Sceme of the regulatory function of PLKs in the control of mammalian cell cycle (from (Dai, 2005).

Brown arrows indicate the specification of the PLKs regulatory function in the respective phase of the cell cycle. As depicted PLKs are involved in the regulation of nearly all phases of the cell cycle.

In cell culture it was observed, that both PLK2 and PLK3 bind to spine-associated Rap guanosine triphosphatase-activating protein (SPAR) and lead to its degradation (Kauselmann et al., 1999, Seeburg et al., 2008a) and Figure 1.11. The result is a loss of stability of synaptic and dendritic integrity. This finding was also confirmed in hippocampal neurons (Seeburg et al., 2008b). Taken together PLKs might mediate the neuronal plasticity and therefore the neuronal activity by influencing synaptic strenght. Furthermore recent publikations demonstrate the involvement of PLK2 and PLK3 in the pathologic phosphorylation of the Ser129 residue of αSyn (Inglis et al., 2009).

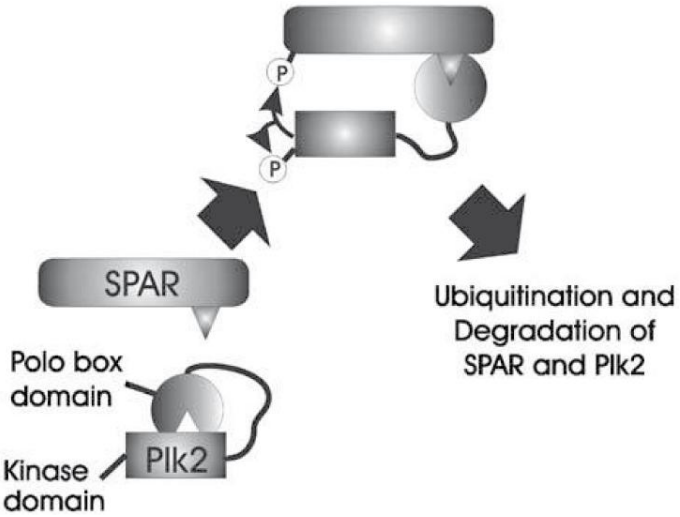

Figure 1.11 PLK2 leads to the degradation of the spine associated protein SPAR (spine-associated RapGAP) and influences the remodeling of synapses (from (Seeburg et al., 2005)).

As this protein modification represents a hallmark of the synucleinopathy mouse model used in this work, and also for all syucleinopathies in human diseases, investigation of PLK distribution in relation to neuropathology was monitored. Furthermore the relation of PLKs to a possibly reduced neuroplasticity in emotional learning impaired αSyn transgenic mice was analysed.

1.7 Objectives

Parkinson's disease is a common neurodegenerative disorder, which is characterised by the loss of neuromelanin containing dopaminergic neurons in the substantia nigra pars compacta (Dauer et al., 2003). Interestingly, the disease is not limited to only this area, moreover a spreading of neurodegeneration through a variaty of brain regions is observed in the course of the disease (Braak et al., 2004). Research in the past decade has revealed that the synaptic and nuclear protein alpha-synuclein (αSyn) is the main component of pathologic inclusions called Lewy bodies and Lewy neurites (Spillantini et al., 1997). These pathologic inclusions are a hallmark of all diseases inwhich the protein αSyn is involved. All these diseases are together referred as α-Synucleinopathies.

In this work an animal model for α-Synucleinopathy (Kahle et al 2000, Kahle et al 2001, Neumann et al 2002), which is shown to develop age dependent motoric impairement and emotional learning deficites (Freichel et al., 2007) should be investigated. These mice should be used to perform a brain region specific characterisation of α-Synucleinopathy. Furthermore the amygdala, the key region of the emotional learning circuitry, which is affected in PD and DLB patients, should be closer investigated for the effect of α-Synucleinopathy on neuronal function.

(1) Thereby synucleinopathy in affected brain regions had to be investigated and compared to young healthy, not yet affected mice, by proteinbiochemical analysis and histopathological investigation. This experiments uncover disease dependent proteinbiochemical modifications of αSyn, e.g. phosphorylation at the Ser129 residue, its intracellular distribution and other modifications of αSyn, e.g. aggregation at different extent, formation of detergent-insoluble and amyloid like αSyn forms. Proteinbiochemical fractionations will be used to isolate different αSyn species from different intracellular compartments, e.g. cytoplasm and nucleus.

(2) Correlation of present pSer129 αSyn with histopathological silver staining and stainings with the congophilic marker ThS should shed light on the pathologic effect of pSer129 αSyn positive structures, their form, LB-like / LN-like, and the status of aggregation, i.e. amyloidosis.

(3) Behavioural experiments should confirm functional deficits and correlate them to present α-Synucleinopathy. Staining for immediate early genes, e.g. the c-FOS protein, directly after neuronal activation should uncover a possible, α-Synucleinopathy dependent, lower neuronal activation in old impaired transgenic mice. Estimation of activated areas can be achieved with stereological quantifications of serial paraffin sections containing the brain regions, which are relevant for emotional learning.

(4) Furthermore experiments with neuronal cell models should show potential kinases involved in the α-Synucleinopathy relevant Ser129 phosphorylation of αSyn. The *in vivo* relevance of identified potential kinases for the Ser129 phosphorylation and therefore also for a possible influence on neuronal function should be investigated with histologic double stainings, with pSer129 αSyn antibodies of single or serial sections isolated from impaired animals suffering from α-Synucleinopathy.

Taken together, this work deals with the influence of synucleinopathy on the development of neuronal pathology and misfunction in a transgenic animal model for synucleinopathy.

2 Results

Aim of this work was the investigation of synucleinopathy in different brain regions of an [A30P] alpha-synuclein (αSyn) transgenic mouse model (Kahle et al., 2000, Kahle et al., 2001, Neumann et al., 2002, Freichel et al., 2007) expressing the transgene under the control of the CNS neuron-specific promoter Thy1. Particular attention was turned on the observation of phosphorylation of αSyn, its status of aggregation and its intracellular localisation in affected brain regions of aged mice. The localised synucleinopathy was correlated with functional impairment of affected brain regions.

2.1 General brain region-dependent-distribution of human [A30P]αSyn expressed under control of the Thy1-promoter in C57Bl6 mice

It was shown that a salient feature of mouse models expressing human wt- as well as A53T- and A30P-αSyn under control of the Thy1 promoter was the formation of somatodendritic accumulation of granular- and detergent insoluble αSyn throughout the brain and spinal cord (Kahle et al., 2000, van der Putten et al., 2000, Kahle et al., 2001, Rockenstein et al., 2002). The (Thy1)h[A30P]αSyn animal model used in this study also showed αSyn expression througout the brain (Figure 2.1 and Figure 2.2), therefore intracellular localisation of αSyn in respective brain regions was investigated.

General distribution of transgenic human αSyn in 4 months and 18 months old animals was visualised by histology staining performed with the rat monoclonal 15G7 antibody (Figure 2.1). Stainings of murine saggital brain sections for human αSyn confirmed the general expression of the protein in a variety of brain regions brainstem (BS), midbrain (MB), cerebellum (Ce), cortex (Cx), hippocampus (Hip), olfactory bulb (OB) of both 4 months (Figure 2.1 A) and 16 months (Figure 2.1 B) old transgenic animals. Brains of old transgenic mice showed in general a brighter staining signal in αSyn

positive regions, pointing to overexpression dependent higher amounts of the human αSyn protein in all brain regions of old mice. Detailed stainings are shown in chapter 2.4 and chapter 2.5.

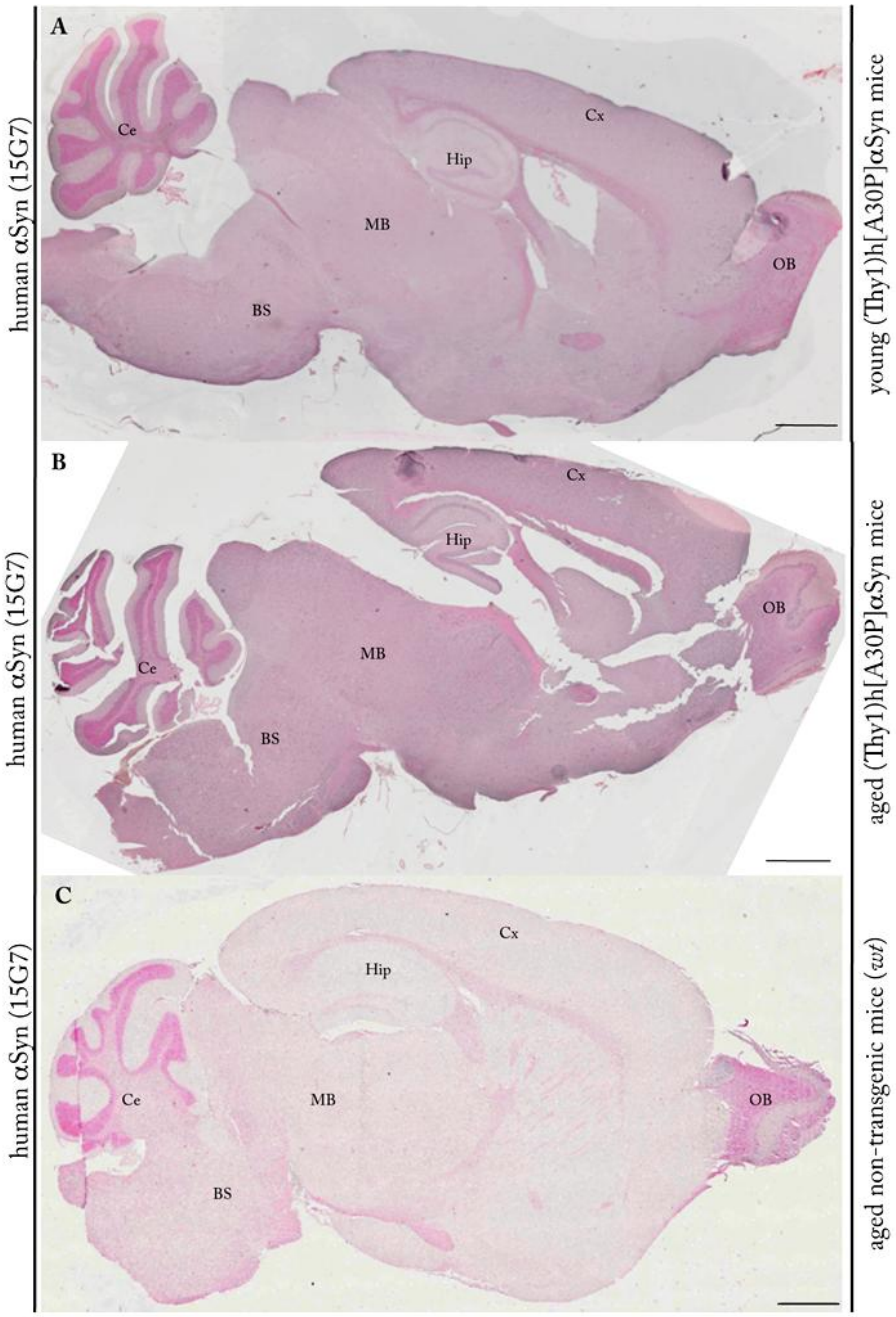

Figure 2.1 Expression of human [A30P]αSyn in homozygous transgenic mice.

Saggital sections of brains from transgenic 4 months (A), aged 18 months (B) and 22 months old wild type (wt) non-transgenic mice (C) were probed for transgenic human αSyn with the monoclonal rat antibody 15G7 and counterstained with nuclear fast red. Presence of αSyn (grey staining) was shown throughout the brain of 4 months and 18 months old transgenic animals (A and B). Except of the nuclear fast red staining, brains of aged non-transgenic mice did not show any αSyn signal with the 15G7 antibody (C). Brain regions: cerebellum (Ce), brainstem (BS), midbrain (MB), hippocampus (Hip), cortex (Cx) and olfactory bulb (OB) are indicated on each section. Scale bars correspond to 1000 µm.

The specifity of the 15G7 antibody was confirmed with histological stainings of Saggital sections of 22 months old non-transgenic C57Bl6 (wt) animals. No reactivity of the antibody was observed throughout the whole brain (Figure 2.1 C).

Presence of the transgenic human αSyn was visualised by western blot (Figure 2.2). 25 µg protein lysate from BS, Cx, Ce and the rest of the brain (Rest) of young and aged mice were loaded on a 12.5 % polyacrylamide-gel. Monomeric αSyn (17 kD band) was detected in all brain regions of both young and old transgenic mice. Apart from the monomeric αSyn, lysates of the BS of aged transgenic mice contained dimeric, trimeric and oligomeric αSyn (Figure 2.2). In Cx, Ce and the rest of the brain only the monomeric αSyn form was detectable. This confirmed the previously described age-dependent aggregation which takes place in only a subset of brain regions (Freichel et al., 2007).

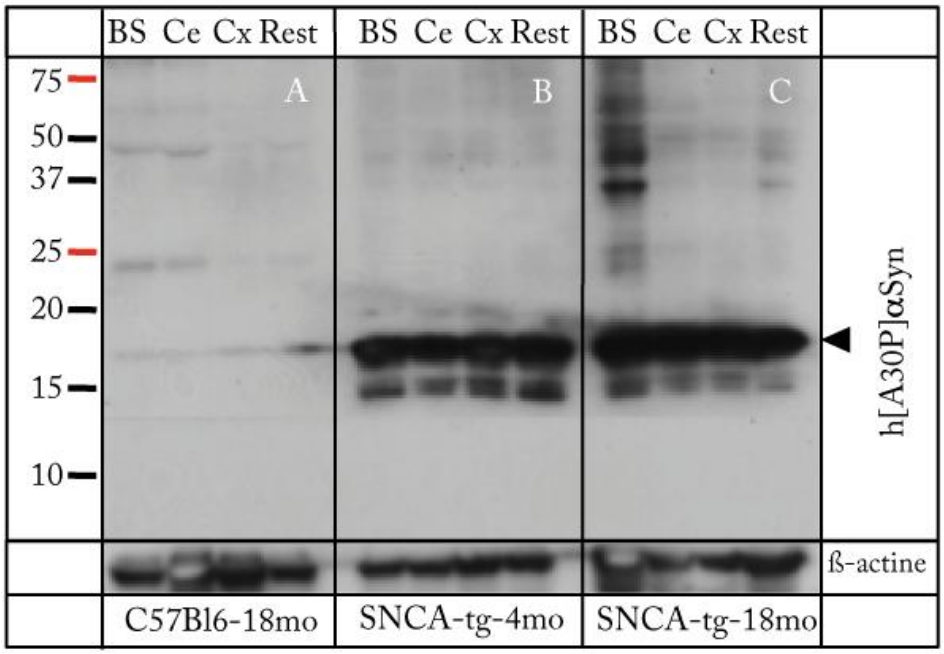

Figure 2.2 Detection of transgenic [A30P]αSyn in different brain regions of young and aged transgenic mice.

Tissue originating from 3 brainstem (BS), 3 cerebelli (Ce), 1 Cx, and 1 rest of the brain (Rest) of old wild-type (non transgenic) animals, young (SNCA-tg-4mo)- and aged symptomatic (SNCA-tg-18mo) mice was lysed and 25 µg of total protein was separated in an acrylamide gel via electrophoresis. αSyn was detected using an antibody (15G7) against human αSyn. Tissue originating from young transgenic animals (B) contained similar amounts of transgenic αSyn as the lysates from old transgenic mice (C). Lysates from old wild-type mice showed no signal after probing with 15G7 antibody (A). Representative results from 5 independent experiments are shown.

2.2 Biochemical investigation of the human [A30P]αSyn in the different brain regions of young and old [A30]αSyn transgenic mice

As formation of high molecular and oligomeric αSyn was observed especially in the BS of old [A30P]αSyn transgenic mice (Figure 2.2, C (BS) and (Kahle et al., 2001, Neumann et al., 2002)), solubility assays (Neumann et al., 2002) of BS, CE, Cx and the rest of the brain (Rest) isolated from old non transgenic (C57Bl6), young and old αSyn transgenic mice were performed (Figure 2.3). Tissue was lysed in Tris buffer, buffer insoluble material was disolved in Triton X-buffer and detergent insoluble material was collected in sarcosyl buffer. Fractions were subjected to SDS gel electrophoresis with 12% acrylamide gels, immunoblotted and probed with the human specific αSyn antibody 15G7. Young and old transgenic mouse tissue contain soluble monomeric αSyn in all brain regions probed (Figure 2.3, s1). Interestingly, BS and Ce of aged transgenic mice contained a reduced amount of soluble transgenic αSyn. Furthermore lysates of cerebellar tissue of old transgenic animals displayed an additionally high molecular band which was not visible in cerebellar lysates of young transgenic mice (Figure 2.3, s3, lines Ce respectively). In addition BS lysates of both young and old transgenic mice displayed similar high molecular αSyn lines, with comparable intensity (Figure 2.3 s2, s3, s4). Investigation of the insoluble fractions revealed presence of insoluble αSyn in cortical and rest of the brain tissue of both young and old transgenic mice (Figure 2.3 ins1). Consistent with the age-dependent worsening of neuropathology (Kahle et al., 2001, Neumann et al., 2002, Freichel et al., 2007), the amount of buffer-insoluble αSyn is increased in old transgenic mice (Figure 2.3 ins1, lanes BS respectively). Furthermore BS sarcosyl fractions of old transgenic mice contained a high molecular smear of insoluble and fibrillar αSyn (Figure 2.3, se5). In addition again only cortical and rest of the brain fractions of old transgenic mice displayed an αSyn positive signal at the size of monomeric αSyn in the sarcosyl fractions (Figure 2.3, se1 Cx and Rest respectively). As expected,

none of the fractions from wt non transgenic mice were positive for the human transgenic αSyn (Figure 2.3).

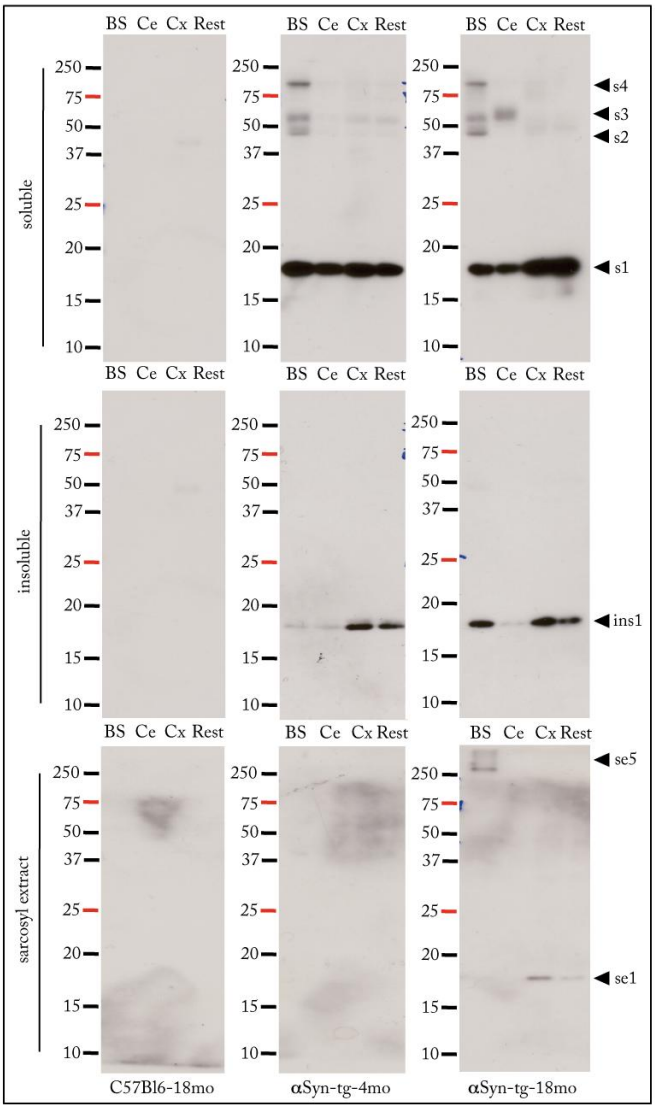

Figure 2.3 Solubility assays from different brain regions isloated from old non-transgenic, young and aged αSyn transgenic mice.

BS and Ce of 3 mice were pooled, both cortical hemispheres (Cx) of one brain and one rest of the brain (Rest) of old non transgenic (wt, C57Bl6), young (SNCA-tg-4mo) and old αSyn transgenic mice (SNCA-tg-18mo) were lysed in Tris buffer and subjected to fractionation with Triton X-100 and sarcosyl buffer. All samples of both young and old transgenic mice displayed the presence of monomeric αSyn in the soluble fraction, whereas the amount of αSyn in BS and Ce was reduced in respective lysates of old transgenic mice (s1, BS and Ce). In addition, cerebellar tissue of aged transgenic mice contained a high molecular smear wich is not present in the respective cerebellar Tris-buffer lysate of young trangenic mice (s3, Ce). Cortical and rest of the brain Triton-X fractions of young and old transgenic mice displayed comparable amounts of monomeric αSyn (ins1 Cx and Rest). Interestingly, amounts of insoluble αSyn were higher in BS of old transgenic mice compared to the amounts present in lysates of young animals (ins1, BS). Furthermore only BS, cortical and rest of the brain lysates of old trangenic mice contained αSyn in the sarcosyl extract (se5 and se1). As expected, solubillity assays with tissue from old non-transgenic (wt) mice showed no αSyn positive signals in any fractions.

2.3 General distribution of pSer-129 αSyn in (Thy1)h[A30P]αSyn transgenic mice

Phosphorylation of αSyn at Ser129 is a dominant protein biochemical modulation observed in familial and sporadic parkinsonian cases where synucleinopathies are involved (Fujiwara et al., 2002, Saito et al., 2003, Anderson et al., 2006, Waxman et al., 2008). Furthermore, pSer129 αSyn could be detected in several αSyn animal models (Kahle et al., 2002b, Neumann et al., 2002, Waxman et al., 2008). To investigate the importance of this modulation and its possible effect on αSyn aggregation and neurodegeneration, αSyn-phosphorylation and its intracellular localisation was investigated in young and aged [A30P]αSyn transgenic mice.

Saggital brain sections of 4 months and 18 months old transgenic mice, stained with an antibody specifically binding to αSyn phosphorylated at its Ser129, showed positive signals in the regions which were already shown to be positive for the human [A30P]αSyn (Figure 2.4 A and B). Noticeable much brighter Cx and Hipp staining of sections from old transgenic mice was seen and in addition very bright signal in the BS, MB and the glomerulus of the OB in the same animals (Figure 2.4 B) could be observed. Brain tissue from young transgenic mice displayed a weaker staining pattern or no signal in similar brain regions (Figure 2.4 A).

As visible in (Figure 2.4) the BS and MB of old αSyn transgenic mice contained a large amount of pSer129 αSyn-positive structures, whereas the same region in young transgenic mice was lacking the observed bright signal. At the same time cortical region of both, young- and old transgenic mice seemed to contain comparable amounts of pSer129 αSyn (Figure 2.4 A and B respectively).

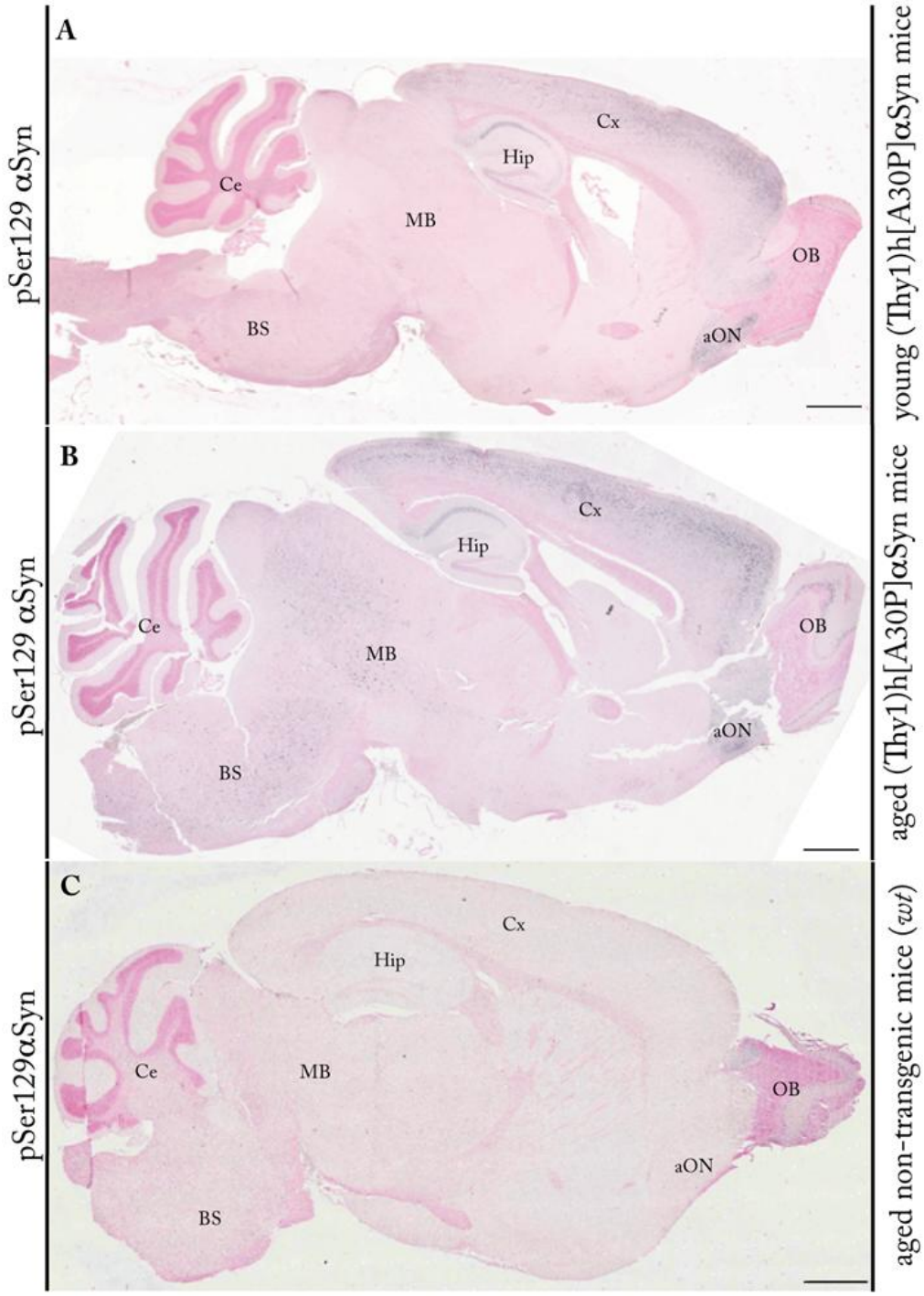

Figure 2.4 Distribution of pSer129 αSyn in young and aged transgenic mice.

Saggital sections of young transgenic, 4 months (A), aged transgenic 18 months (B) and old wild type 22 months (C) mice were probed for transgenic α-synuclein phosphorylated at its Ser129 residue (pSer129 αSyn) with the monoclonal rabbit antibody [EP1536Y] (abcam) and counterstained with nuclear fast red. Presence of phosphorylated αSyn (grey-/black staining) could be confirmed in all regions with transgenic αSyn expression both in 4 months and 18 months old transgenic animals (A-B). However, aged brains show a brighter signal for pSer129 αSyn (B) in all positive regions compared to the signal (grey/black staining) detectable in brains of young mice (A). Brains of aged non transgenic mice (wt) show with exception of the nuclear fast red staining no signal with the pSer129 αSyn antibody (C). Brain regions: Ce, BS, MB, Hip, Cx, OB and anterior olfactory nucleus (aON) are indicated on each section. Scale bars correspond to 1000 μm.

To confirm these observations and to detect possible forms of aggregated pSer129 αSyn BS-, cerebellar-(Ce), cortical- (Cx) tissue, as well as the rest of dissected brains of old wild-type-, young αSyn transgenic and old αSyn transgenic mice were lysed and lysates were loaded on tricine gels.

As expected, lysates originating from old wild-type mice contained no pSer129 αSyn (Figure 2.5 A). In contrast all lysates originating from old αSyn transgenic mice were positive for the pathologic pSer129 αSyn (Figure 2.5 C). In addition, lysates from BS and the rest of the brain (Rest) contained also different types of aggregated pSer129 αSyn (Figure 2.5 C, line BS and line Rest). All lysates from young transgenic mice contained only the monomeric αSyn phosphorylated at its Ser129 residue (Figure 2.5 B). In addition all detected signals were weaker than the signals detected in lysates from old transgenic mice.

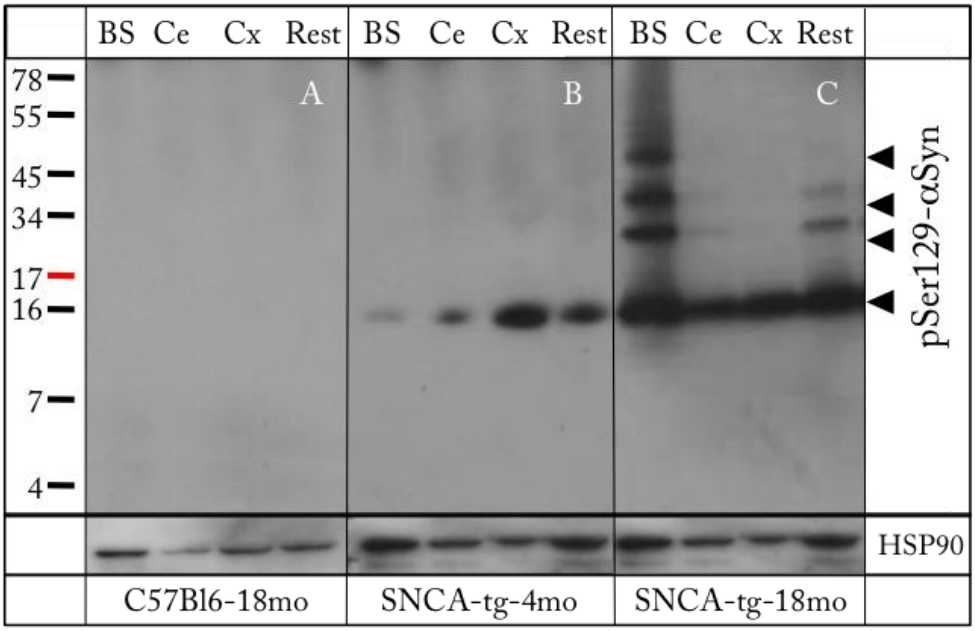

Figure 2.5 Investigation of pSer129 αSyn in lysates isolated from *BS, Ce, Cx* and the rest of the brains (Rest) of young and old αSyn transgenic mice.

BS, Ce, Cx and the rest of brains isolated from aged wild-type as well as from young transgenic and old endstage transgenic mice were lysed and 25 µg protein of each was subjected to western blotting with tricine gels (Novex). The antibody used was specific for αSyn phosphorylated at its Ser129 residue (Abcam, clone EP1536Y). As expected lysates from old wt animals contained no pSer129 αSyn (A). Lysates from old αSyn transgenic mice showed a strong signal for monomeric pSer129 αSyn in lysates of all brain regions included (C). In addition lysates from BS and the rest of the brain showed also the presence of different types of aggregated pSer129 αSyn (C, line BS and line Rest). In contrast, lysates of young mice showed weaker signals for pSer129 αSyn (C) with exception of cortical lysates (C, line Cx). Aggregated forms of pSer129 αSyn were not detectable in any of the lysates obtained from 4 months old αSyn transgenic mice. Representative results of 12 mice.

An exception turned out to be the cortical lysates of young transgenic mice, which showed a comparable signal to the one detected in cortical lysates of aged transgenic mice (Figure 2.5). These findings are consistent with the observations in histological stainings of saggital sections, originating from old wild type-, young αSyn transgenic- and old transgenic animals (Figure 2.4).

Old transgenic animals suffering from described synucleinopathy in MB, BS and spinal cord ((Kahle et al., 2000, Kahle et al., 2001, Neumann et al., 2002) and (Figure 2.1, Figure 2.2, Figure 2.4, Figure 2.5)), develop motor deficits measurable at an age of 16 months with the RotaRod test (Freichel et al., 2007). Motoric impairment starts with a decrease of the muscle tonus in the tail and the hind legs, leading to a shaky movement and an impairment of the animals in the grid-walk test. In this test mice are placed on the lid of their cage and the gait of the animals was observed for 1-2 minutes. Affected animals had a high tendency to miss the catching of grids and fall into the ripping of the cage lid. In a period of two to four weeks after detection of first symptoms these mice developed an endstage with paralysia of one or several extremities (Figure 2.6).

Figure 2.6 Consequence of synucleinopathy in homozygot transgenic [A30P]-αSyn mice.

Homozygous animals develop a motoric endstage (rigidity, tremor and paralysia) at an age between 16- and 22 months due to the synucleinopathy induced pathology (Figure 2.7, 2.8, 2.9, 2.10) in MB and BS areas. The depicted animal had to be sacrificed because of developing of paralysis in all 4 extremities.

2.4 Neuropathology in brain regions involved in motorical function

2.4.1 Distribution, intracellular localisation, aggregation and Ser129-phosphorylation of transgenic [A30P]αSyn in BS and MB: correlation with amyloidosis and silver staining

Investigation of MB and BS stainings with the 15G7 antibody revealed the presence of human αSyn mainly in somata of MB and BS cells of 18 months old transgenic mice (Figure 2.7 E-H). Cells of identical brain regions in 4 months old transgenic animals displayed the same somal localisation of the signal, but with a much weaker staining pattern (Figure 2.7 A-D). This result gives a hint to the age-dependent accumulation of human αSyn, which was already shown to be present in the applied animal model (Kahle et al., 2000, Kahle et al., 2001, Neumann et al., 2002. As expected, old wild type mice did not show any human αSyn positive cells in the MB or in the BS (Figure 2.7 I-L).

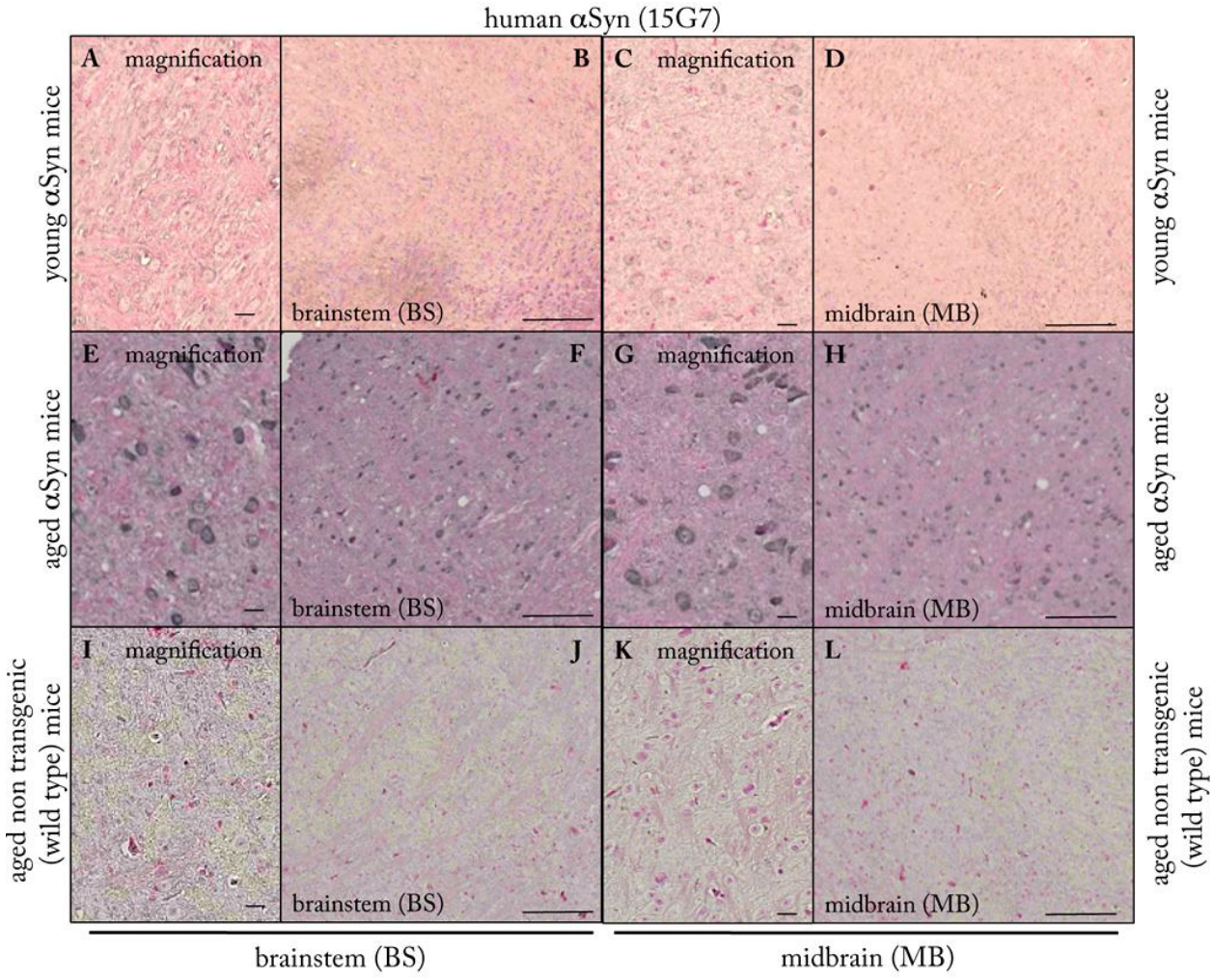

Figure 2.7 Distribution of human [A30P]αSyn in MB of young and aged αSyn transgenic mice.

Saggital MB and BS sections of 4 months transgenic (A-D), 18 months transgenic (E-H) and 22 months old wild type mice (I-L) were probed for transgenic α-synuclein (αSyn) with the monoclonal rat antibody 15G7 and counterstained with nuclear fast red. Human αSyn (grey staining) could be detected in 4 months and 18 months old transgenic animals (C, D). Furthermore positive cells in MB and BS of old transgenic animals showed a brighter αSyn signal (C) than tissue from young trangenic mice (compare E-H with A-D). Higher magnification showed mostly cytoplasmatic distribution of αSyn in MB and BS cells of young (A and C) and aged (E and G) transgenic mice. The MB and BS of aged non transgenic mice showed no αSyn signal (grey staining) but only the nuclear fast red staining (I-L). Scale bars in B, D, F, H, J and L correspond to 200 µm. Scale bars in A, C, E, G, I and K correspond to 20 µm.

Histological pSer129 αSyn staining of MB and BS containing sections of young and old transgenic mice revealed mainly weak staining of few cells in both brain regions of young transgenic mice (Figure 2.8 A-H). Higher magnification revealed pSer129 αSyn distribution in cytoplasmatic soma and branches of positive neurons (Figure 2.8 C-H). Stainings with the same antibody in similar brain regions of old transgenic mice revealed different

cytoplasmatic somal (Figure 2.8 L-S) and neuritic (Figure 2.8 K, -T, -N-O and R-S) staining patterns of numerous cells. Noticeable were the numerous pSer129 αSyn positive "Lewy Neurites" (Figure 2.8 K and –T). Furthermore there were cells detectable, which resided in different stages of synucleinopathy, displaying different amounts of pSer129 αSyn and different intracellular distribution patterns of the same protein (Figure 2.8 L-S). L to S suggest a possible pathway of how neurons end up to be filled with pSer129 αSyn containing oligomers and to form neuropathological swollen neurites which are typical for all diseases involving synucleinopathys (McNaught et al., 2002, Olanow et al., 2004, Jellinger, 2009). In the beginning [A30P]αSyn overexpressing cells display punctual localisation of pSer129 αSyn in the cytoplasm (Figure 2.8 L) which proliferate (Figure 2.8 M) until the soma and even parts of the dendrites are filled with pSer129 αSyn (Figure 2.8 N). After this stage affected cells trigger accumulation of pSer129 αSyn in much higher density (Figure 2.8 O) due to a possible induction of oligomerisation. This could explain the much brighter histological staining of cells in this stage. After induction of oligomerisation cells seem to have the tendency to concentrate pSer129 αSyn aggregates and orientate their transport in the direction of the centrosome (Figure 2.8 P) for a possible degradation, which seems to fail (Figure 2.8 Q). This results in an ongoing accumulation of pSer129 αSyn containing oligomers filling the cell soma (Figure 2.8 Q) and in the end even the branches of affected neurons (Figure 2.8 R and S). From this point onwards, neurons affected in this way should have functional impairments resulting in measurable physiological failures.

Specifity of the stainings in these brain regions was checked with appropriate stainings of sections from 22 months old wt mice, which revealed no reactivity with the pSer129 αSyn antibody (Figure 2.8 U and V).

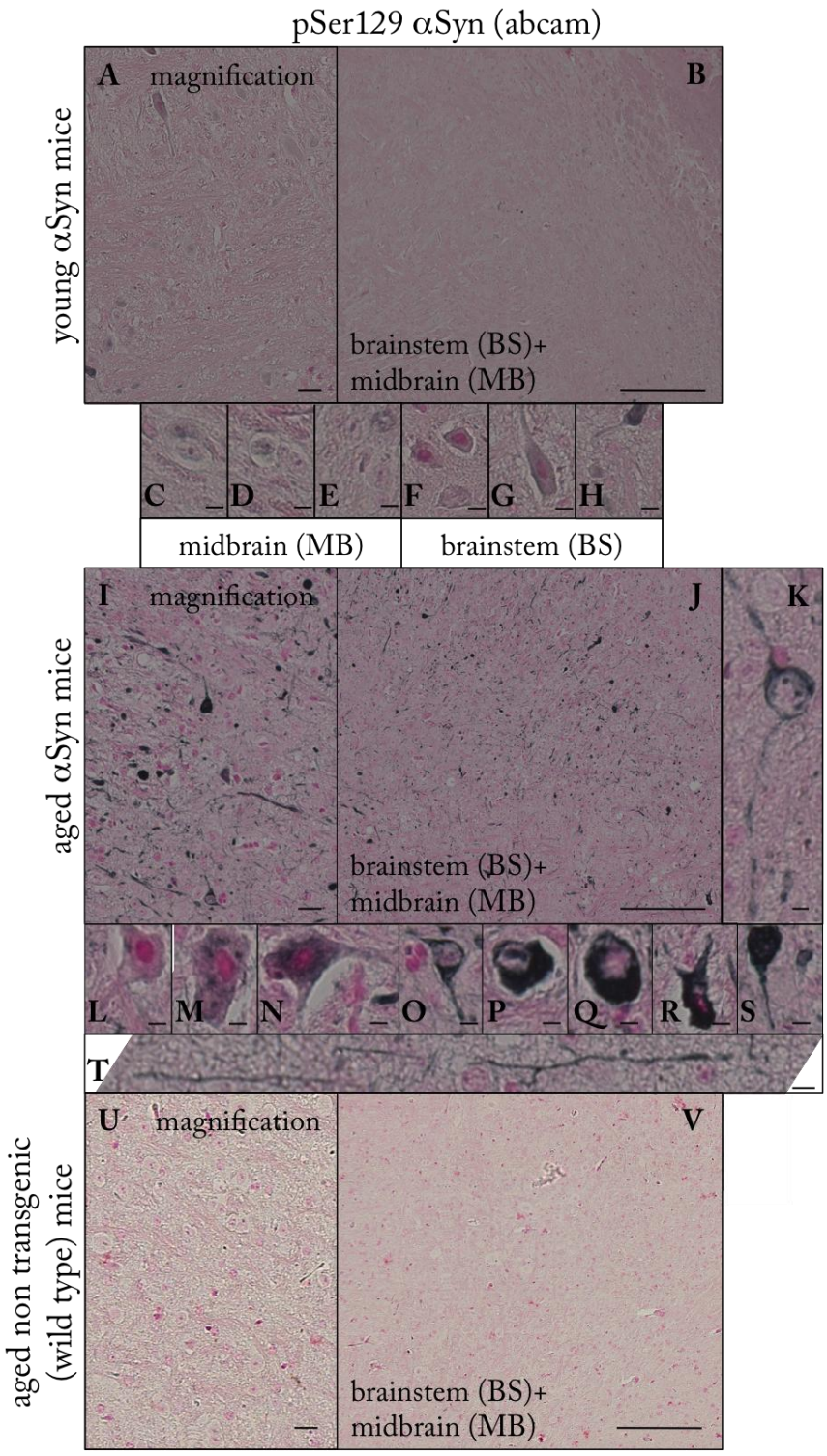

Figure 2.8 Distribution of pSer129 αSyn in BS and MB of young and aged αSyn transgenic mice.

Saggital sections containing MB and BS of 4 months transgenic (A-H), 18 months transgenic (I-T) and 22 months old wild type mice (U and V) were probed for transgenic αSyn phosphorylated at its Ser129 residue (pSer129 αSyn) and counterstained with nuclear fast red. Weak cytoplasmatic staining (grey staining) of few MB (C-E) and BS cells (F-H) could be detected in tissue of young mice. In contrast MB and BS of old (endstage) transgenic mice show pSer129 staining (grey-/black staining) in the cytoplasm (L-S) but also Lewy Neurite staining (K, O, S and T). BS and MB tissue of aged wt mice showed no positive signal with the pSer129 αSyn antibody (X-Y). Scale bars in B, J, and V correspond to 200 µm. Scale bars in A, I and U correspond to 20 µm. Scale bars in K-T correspond to 10 µm.

Amyloidosis in MB and BS areas of 4 months and 18 months old transgenic mice was checked with 0.1% thioflavine-S (ThS) stainings. As control, staining specifity was verified with ThS stainings of appropriate tissue, isolated from 22 months old wt mice.

ThS positive signals could by identified only in tissue from 18 months old transgenic mice, confirming existence of amyloidosis, only in tissue containing neurons with high levels of pSer129 αSyn with all its accompanied pathological attributes (Figure 2.9 C-D). Higher magnification of positive regions revealed, as already observed in stainings with the pSer129 αSyn antibody, cells containing morphologically different ThS positive structures (Figure 2.9 E-P). It was remarkable to observe that the presence of ThS positive structures localised only in the cell body and to lesser extent in neuronal branches. The picture series presented in Figure 2.9 E to -P demonstrates the possible pathway of how [A30P]αSyn overexpressing mouse neurons deal with ß-pleated aggregated αSyn, assuming that affected neurons induce transport of ß-pleated aggregated αSyn to the centrosome (McNaught et al., 2002, Olanow et al., 2004, Jellinger, 2009). At first affected neurons collect overexpressed transgenic αSyn into punctual cytoplasmatic ThS positive structures (Figure 2.9 E-G), which accumulate in the cytoplasm untill the whole soma seems to be filled (Figure 2.9 H). Affected neurons then trigger transport to structures resembling aggresomes (Figure 2.9 I-M) until formation of the "typical" spherical ThS positive structure is achieved (Figure 2.9 N-P).

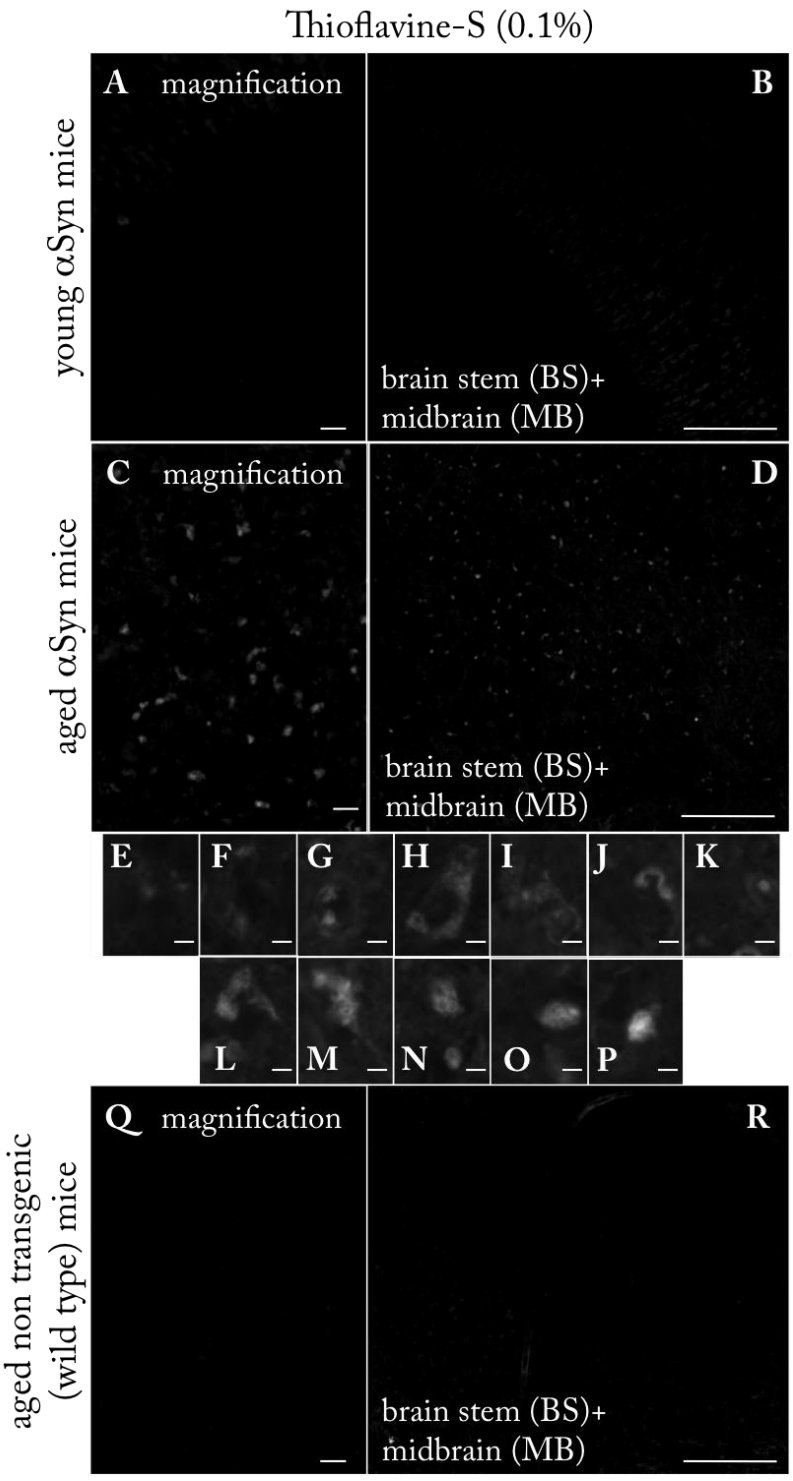

Figure 2.9 Amyloidosis in brain stem and MB of aged αSyn transgenic mice.

Saggital sections containing MB and BS of 4 months transgenic- (A and B), 18 months transgenic (C-P) and 22 months old wild type mice (Q and R) were stained with the congophilic dye Thioflavine-S (ThS) that specifically labels ß-pleated protein conformation. No ThS positive staining could be observed in BS and MB region of young trangenic mice (A and B) and old wt mice (Q and R). MB and BS tissue of aged transgenic mice show a high number of ThS-positive cells (white signal in D, C). Higher magnification shows cytoplasmatic localisation of ThS positive structures (E-P) and several possible stages of the formation of intracellular ThS positive inclusions (from E to P). Scale bars in B, D and R correspond to 200 µm. Scale bars in A, C and Q correspond to 20 µm. Scale bars in E-P correspond to 10 µm.

As already mentioned, amyloidosis was only detectable in MB and BS tissue of aged [A30P]αSyn transgenic mice. Similar tissue from 4 months young transgenic mice and 22 months old wt mice displayed no positive signal after staining with 0.1% ThS (Figure 2.9 A-B and Figure 2.9 Q-R respectively).

Gallyas silver staining of MB and BS containing sections of 4 months young and 18 months old [A30P]αSyn trangenic mice, as well as of 22 months old wt mice were performed to correlate the grade of pathology with detected synucleinopathy in respective brain regions. Pathological silver staining of MB and BS containing sections could only be detected in tissue of old [A30P]αSyn transgenic mice (Figure 2.10 C-S). The majority of detected structures in the MB regions had neurite-like morphology (Figure 2.10 E, J and K) sometimes with very long extensions (Figure 2.10 C). Few neurons had silver staining positive somata (Figure 2.10 E-I). In contrast majority of detected silver positive signals in BS belonged to positive neuronal somata (Figure 2.10 L, N, O). Sporadic neurite-like structures could be detected (Figure 2.10 P-S), however extended Lewy neurite-like morphology comparable to the structures detected in MB was absent in BS. Similar brain tissue of young transgenic mice as well as of 22 months old wt mice, was found to be negative for pathologic silver staining (Figure 2.10 A-B and Figure 2.10 T-V respectively).

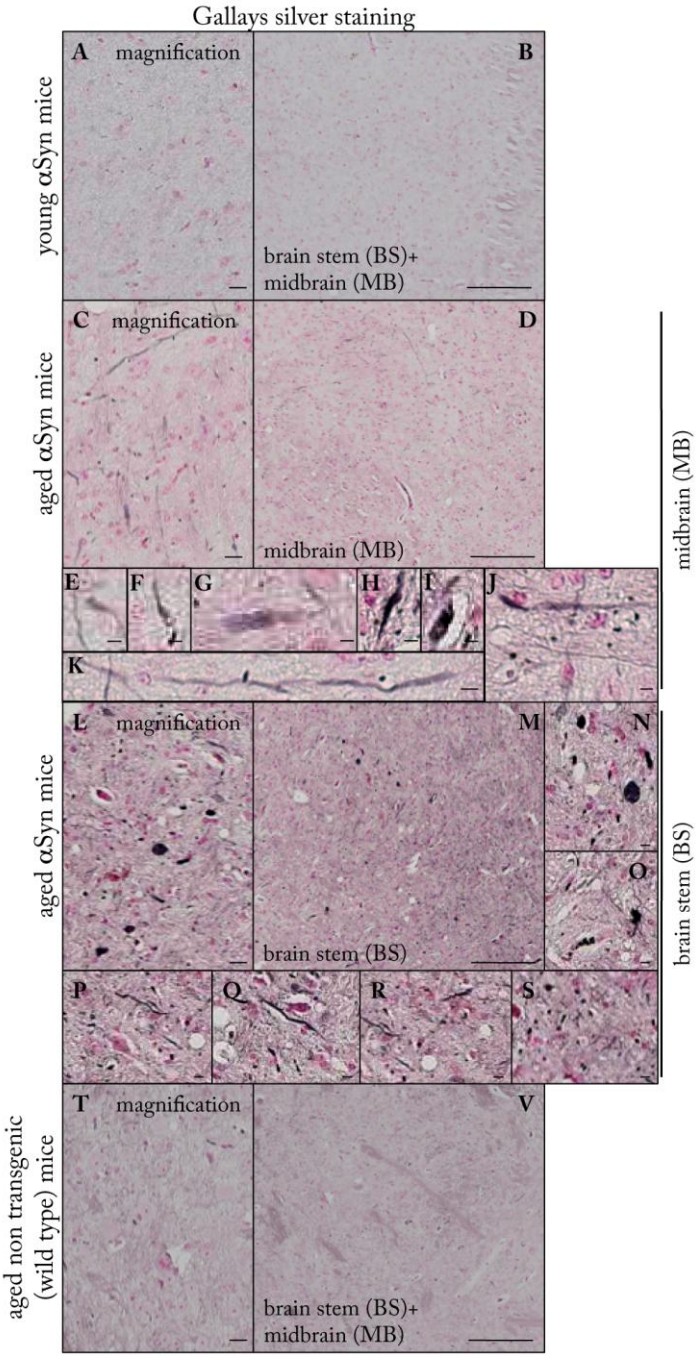

Figure 2.10 Investigation of neuropathology in BS and MB of young and aged αSyn transgenic mice.

Saggital sections containing MB and BS of 4 months transgenic (A and B), 18 months transgenic (C-S) and 22 months old wild type mice (V and T) were subjected to Gallyas silver staining. Neither BS and MB tissue of 4 months young transgenic mice (B and A), nor brain tissue with respective regions isolated from aged wt mice (T and V) were found to be positive for Gallyas silver staining. MB and BS containing sections of old αSyn transgenic mice were found to be highly positive for silver staining (grey-/black signals). In MB most of the staining included neurite like structures (C, J and K). Few MB-cells were stained with different intensity (E-I). In BS most silver staining positive cells had a strong signal (L-O). Silver positive Lewy Neurites in BS were shorter than the ones observed in MB but showed a much brighter staining (P-R). Scale bars in B, D, M and V correspond to 200 µm. Scale bars in A, C, L and T correspond to 20 µm. Scale bars in E-K and N-S correspond to 10 µm.

2.4.2 Distribution, intracellular localisation, aggregation and Ser129-phosphorylation of transgenic [A30P]αSyn in the Ce: correlation with amyloidosis and silver staining

As it is known that the Ce is involved in the finetuning of motorical coordination, this brain region isolated from the employed mouse lines was also included in the histopathological investigations described.

Histological investigation of human αSyn distribution in cerebelli of young and old transgenic mice revealed cytoplasmatic αSyn staining of cells in the granular layer and the cerebell lobule of old transgenic mice cerebelli (Figure 2.11 D and E). In old transgenic mice some cells which are part of the white matter, displayed accumulation of high amounts of somal transgenic αSyn (Figure 2.11 D). This staining pattern and pathological morphology was not visible in cerebelli of young transgenic mice (Figure 2.11 A-C). Only a small number of weak stained cells which are part of the cerebellar granular layer of young transgenic mice were positive for the human [A30P]αSyn (Figure 2.11 B).

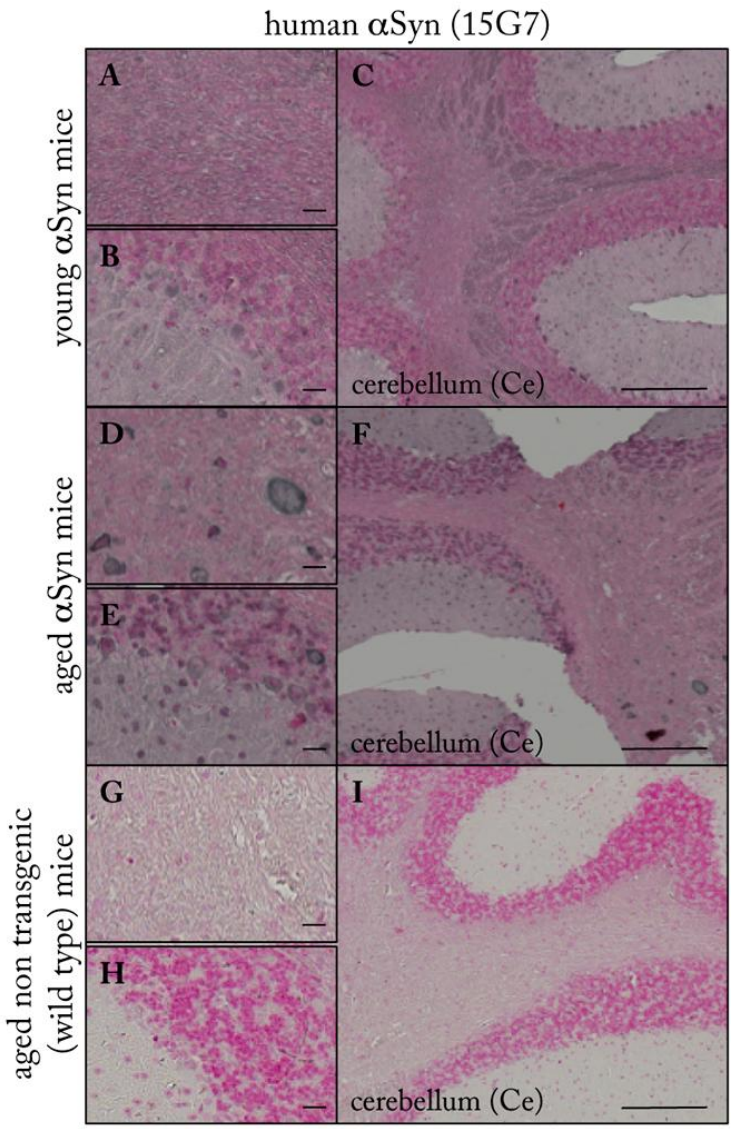

Figure 2.11 Distribution of human [A30P]αSyn in different regions of the Ce of young and aged αSyn transgenic mice.

Saggital cerebellar (Ce) sections of 4 months transgenic (A, B, C), 18 months transgenic (D, E, F) and 22 months old wild type mice (G, H, I) were probed for transgenic α–synuclein (αSyn) with the monoclonal rat antibody 15G7 and counterstained with nuclear fast red. Presence of human αSyn (grey staining) could be confirmed in granular region of 4 months (B) and 18 months old transgenic animals (E). However aged brains did show a brighter αSyn signal and a higher number of positive cells (E) compared to cerebellar tissue of young mice (B). Ce white matter of old transgenic animals showed strong positive signal for somal αSyn (D). The same region in young transgenic mice did not display any positive signal (A). Higher magnification revealed mostly cytoplasmic distribution of αSyn in cells of young (B) and aged (D and E) transgenic mice. Cerebellar tissue of aged non-transgenic mice displayed no αSyn signal with the 15G7 antibody (G, H and I), but was only stained by nuclear fast red. Scale bars in C, F and I correspond to 200 µm. Scale bars in A, B, D, E, G and H correspond to 20 µm.

Investigation of pSer129 αSyn staining in cerebellar tissue of young and old transgenic mice only revealed few neurite like structures in the cerebell lobule of old [A30P]αSyn transgenic mice (Figure 2.12 D). This staininig

could not be detected in tissue of young transgenic mice (Figure 2.12 B). Cerebellar granular layer of old transgenic mice was lacking any positive signals after histologic staining with the pSer129 αSyn specific antibody (Figure 2.12 E). In return the similar region in young transgenic mice contained few pSer129 αSyn positive cells (Fig. 2.4.4 A).

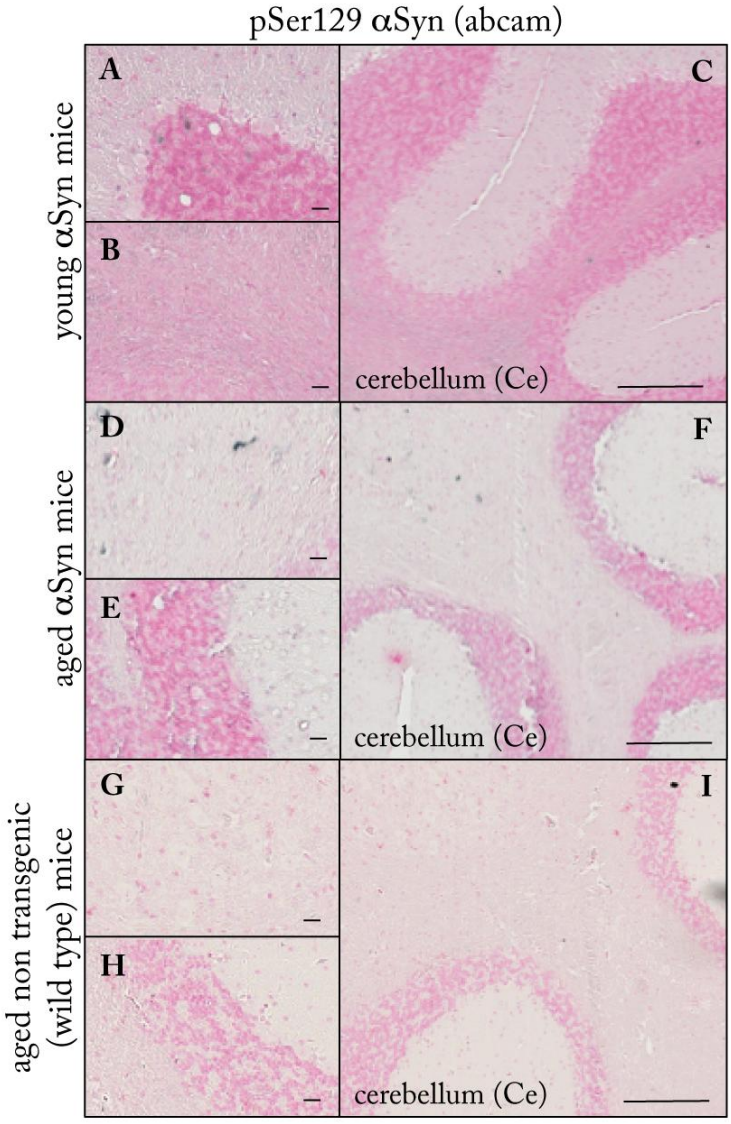

Figure 2.12 Distribution of pSer129 αSyn in the Ce of young and aged αSyn transgenic mice.

Cerebellar (Ce) sections of 4 months transgenic (A, B, C), 18 months transgenic (D, E, F) and 22 months old wild type mice (G, H, I) were probed for transgenic α-synuclein phosphorylated at the Ser129 residue (pSer129 αSyn) and counterstained with nuclear fast red. Weak cytoplasmatic staining of few granular neurons (grey-/black staining) was detected in young transgenic mice (A). Aged mice show few but stronger neurophilic and sometimes cytoplasmatic staining of cerebell lobule neurons (D). Tissue of aged wt mice shows with exception of the nuclear fast red staining no postitve signal with the pSer129 αSyn antibody (G-I). Scale bars in C, F and I correspond to 200 µm. Scale bars in A, B, D, E, G and H correspond to 20 µm.

ThS stainings of cerebellar tissue of young and old transgenic animals displayed few signals only in the cerebell lobule of old transgenic mice (Figure 2.13 D) in which pSer129 αSyn positive neurite like structures have been detected (Figure 2.13 D).

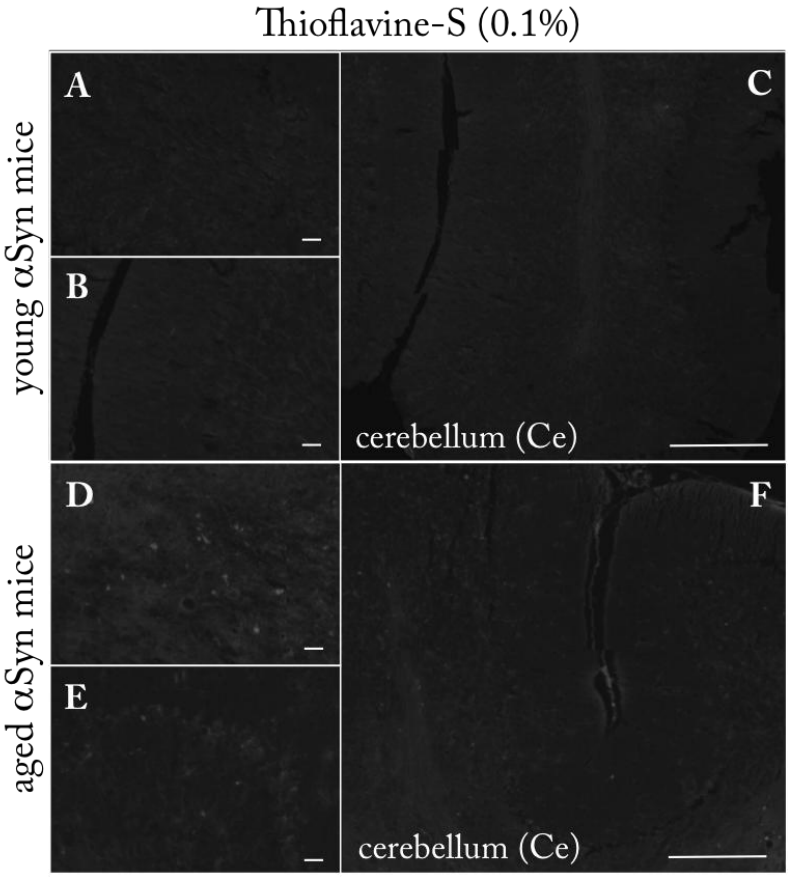

Figure 2.13 Investigation of amyloidosis in the Ce of young- and aged αSyn transgenic mice.

Saggital Cerebellar (Ce) sections of transgenic 4 months young mice (A, B) and transgenic 18 months aged mice (C, D) were stained with the congophilic marker thioflavine-S (ThS) which specifically labels β-pleated protein conformation. No ThS positive staining could be observed in any Ce region of young trangenic mice (A-C). In aged mice only in the cerebell white matter weak staining of few cells could be observed (D). Scale bars in C and F correspond to 200 µm. Scale bars in A, B, D and E correspond to 20 µm.

The neuropathology specific Gallyas silver staining of cerebellar tissue of 18 months old [A30P]αSyn transgenic mouse brain sections and of 22 months old wt mouse brain sections displayed no positive signals in any subregions of the cerebelli of both animal groups (Figure 2.14 A-C and D-F respectively).

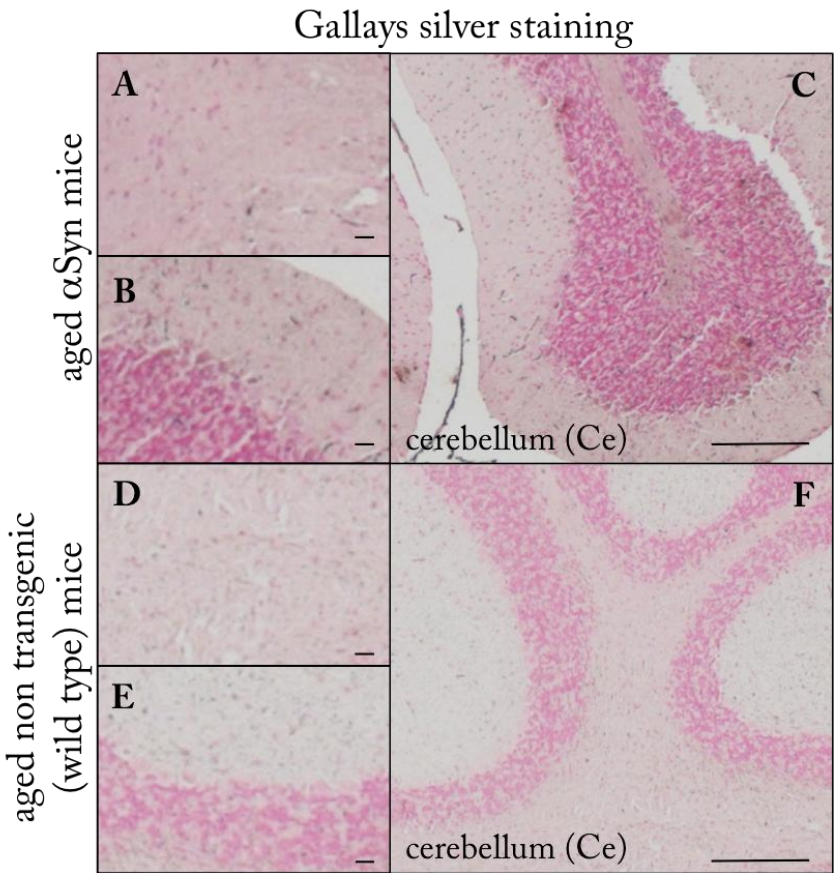

Figure 2.14 Investigation of neuropathology in the Ce of aged αSyn transgenic mice and aged wt mice.

Saggital cerebellar (Ce) sections of transgenic 18 months old mice (A-C) and 22 months old wt mice (D-F) were subjected to silver staining and counterstained with nuclear fast red. Neither the Ce tissue of aged transgenic mice (A-C), nor the Ce tissue of aged wt mice (D-F) displayed positive Gallyas silver staining. Scale bars in C and F correspond to 200 µm. Scale bars in A, B, D and E correspond to 20 µm.

2.5 Intracellular distribution of transgenic αSyn, Ser129 phosphorylation and neuropathology in the OB

Olfactory dysfunction is at least as common among Parkinsons disease (PD) patients as the resting tremor, which represents a cardinal motor feature of PD (Duda, 2004) and it often precedes the onset of the cardinal motoric symptoms of PD (Fleming et al., 2008). Furthermore it was shown that mice overexpressing wt human αSyn under control of the pan-neuronal Thy1 promoter develop olfactory deficits (Fleming et al., 2008). Therefore synucleinopathy and neuropathology of the OB was investigated in the Thy1h[A30P]αSyn mice used in this work.

Stainings of saggital sections of 4 months- and 18 months old transgenic as well as of 22 months old wt mice with the human αSyn specific 15G7 antibody, revealed cytoplasmatic αSyn in glomerular cells of the OB of transgenic animals (Figure 2.15 A-B, E-F, I-J). A high amount of αSyn positive cells and more intensive αSyn staining was observed in aged transgenic mice compared to the stainings of tissue isolated from young transgenic mice.

Closer investigation of the OB revealed positive signal for pSer129 αSyn in glomerular region of 4 months and 18 months old transgenic mice (C-D and G-H respectively). Tissue of aged mice contained, beside cells with weak and diffuse signals in soma, numerous cells with a bright staining in soma and branches (G). Positive stainings in 4 months old transgenic mice only contained cells with a weak and diffuse signal in somal cytoplasma (C). As expected, old wild type mice did not show any human αSyn positive cells nor any pSer129 αSyn signal in the OB (J-L).

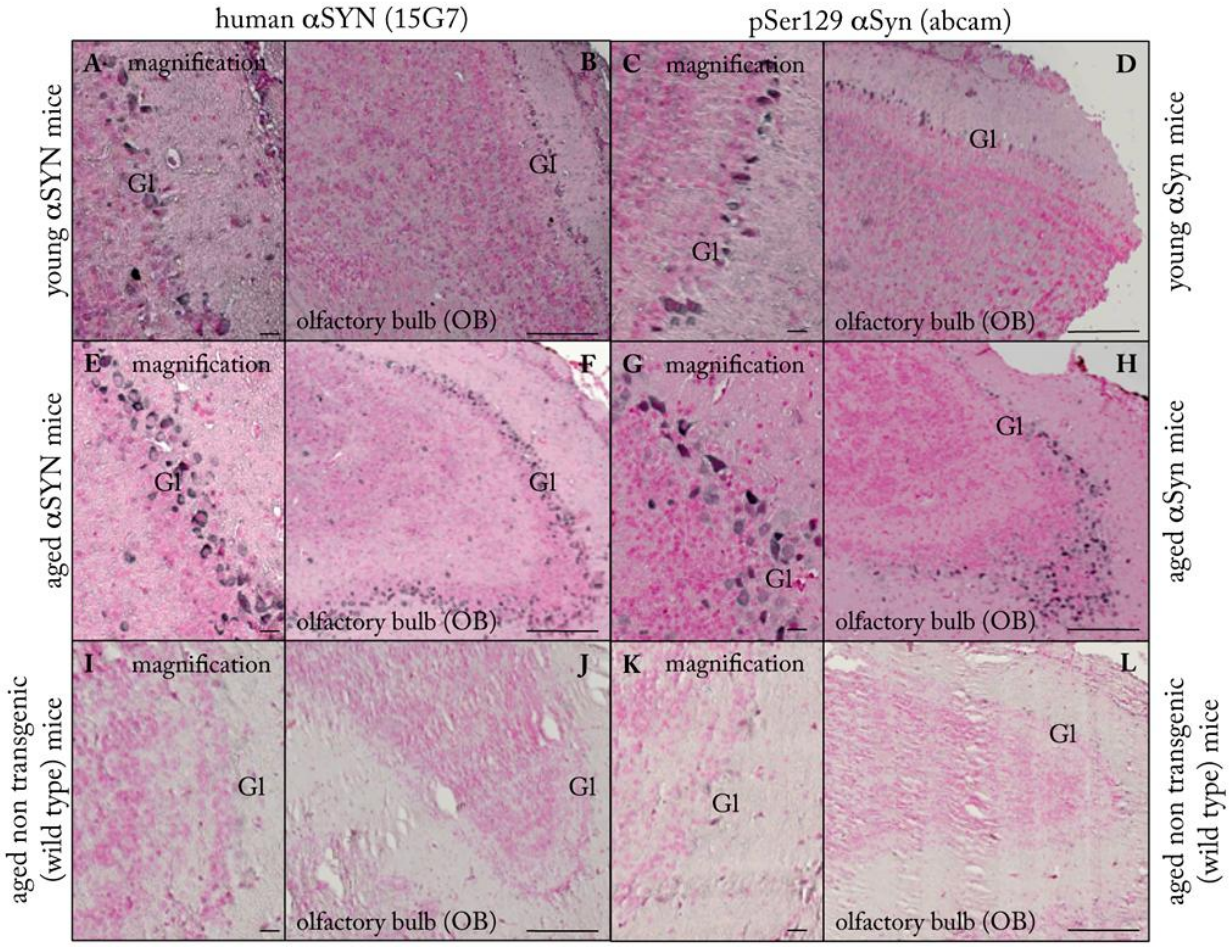

Figure 2.15 Distribution of human [A30P]αSyn in the OB of young and aged αSyn transgenic mice.

Saggital OB sections of transgenic young, 4 months (A-D), transgenic aged 18 months (E-H) and 22 months old wild type mice (J-L) were probed for human α-synuclein (αSyn) (A-B, E-F, I-J) and for transgenic α-synuclein phosphorylated at its Ser129 residue (pSer129 αSyn) (C-D, G-H, K-L). Presence of human αSyn (grey staining in A-B and E-F) and pSer129 αSyn (grey staining in C-D and G-H) could be visualised in glomerular region of 4 months and 18 months old transgenic animals whereas aged brains show a sligtly brighter αSyn signal in positive cells, compared to the tissue of young mice (compare E-F with A-B and G-H with C-D). Higher magnification showed the cytoplasmatic distribution of αSyn a pSer129 αSyn in glomerular cells (Gl) of young (grey staining in A and C) and aged (grey staining in E and G) transgenic mice. Except of the nuclear fast red staining, OB of aged non-transgenic mice show no αSyn signal with the 15G7 antibody (J-L). Scale bars in B, F, J and D, H, L correspond to 200 µm. Scale bars in A, E, J and C, G, K correspond to 20 µm.

Since the overexpressed human αSyn as well as pSer129 αSyn was found in both, young and old transgenic mice (although in different extend), the formation of ß-pleated aggregates (especially in the glomerular region) was investigated with 0.1% thioflavine-S (ThS) stainings of the OB of young and old transgenic mice. No ThS positive signal could be detected in the whole OB of 4 months old transgenic αSyn mice (Figure 2.16 A–B). In contrast, the

glomerular region of 18-months old transgenic mice displayed ThS positive neurons (Figure 2.16 C).

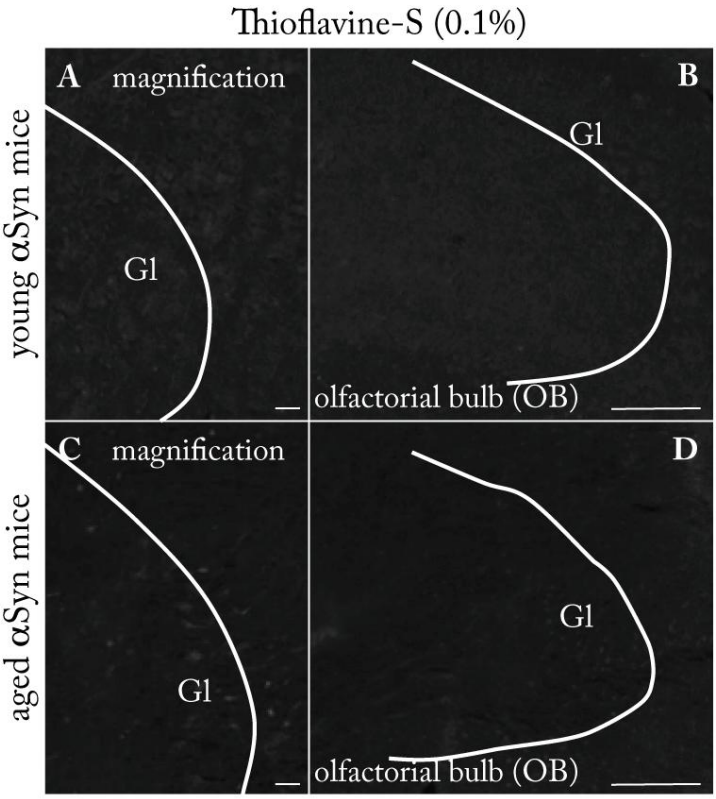

Figure 2.16 Investigation of amyloidosis in the bubus olfactorius of young and aged [A30P] αSyn transgenic mice.

Saggital OB sections of transgenic 4 months young mice (A, B) and transgenic 18 months aged mice (C, D) were stained with the congophilic marker Thioflavine-S (ThS) which specificaly labels ß-pleated protein conformation. Tissue of young transgenic mice, did not show any ThS positive structures (A-B). Glomerular neurons of old transgenic mice, on the other hand, were positive for the congophilic marker ThS (C-D). Scale bars in B and D correspond to 200 µm. Scale bars in A and C correspond to 20 µm.

To investigate the effect of Ser129 phosphorylated αSyn and/or ß-pleated aggregate formation on a possible development of neuropathology, brain sections of 18 months old [A30P]αSyn transgenic mice and 22 months old wt mice were subjected to Gallyas silver staining. Numerous glomerular neurons of old transgenic mice were positive after neuropathology specific silver staining (Figure 2.17 A and B). Higher magnification revealed mainly somal stainings of affected cells in brain tissue of 18 months old transgenic mice (Figure 2.17 A). Gallyas silver stainings of the similar brain region in old wt mice showed no neuronal staining (Figure 2.17 C and D).

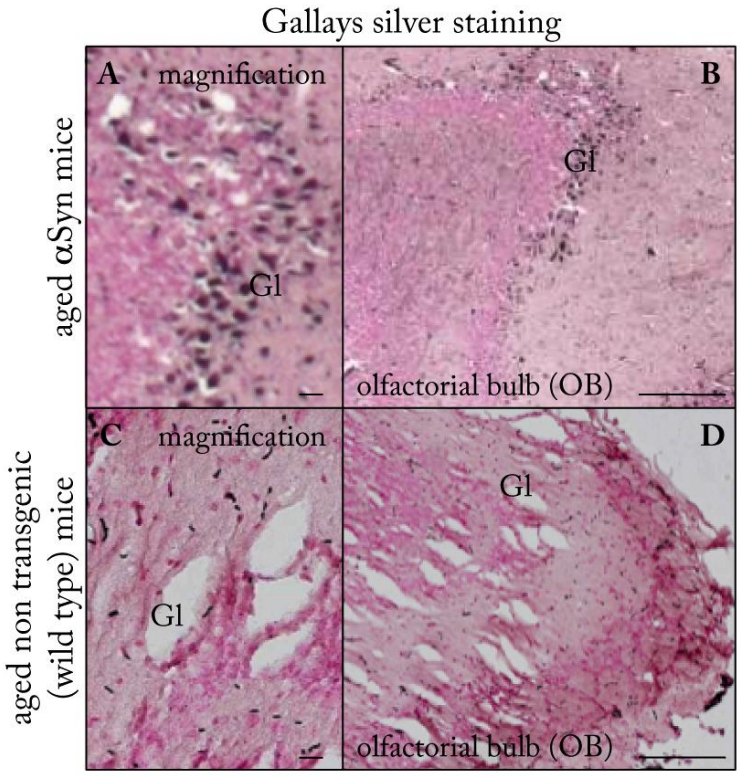

Figure 2.17 Investigation of neuropathology in the OB of aged αSyn transgenic mice and aged wt mice.

Saggital OB sections of 18 months old transgenic mice (A, B) and 22 months old wt mice (C, D) were subjected to silver staining and counterstained with nuclear fast red. Neuropathology (grey-/black staining) was detected in glomerular region of aged transgenic mice (B and A) but not in aged wt mice (D and C). Scale bars in B and D correspond to 200 µm. Scale bars in A and C correspond to 20 µm.

2.6 Neuropathology in brain regions involved in learning

2.6.1 Distribution, intracellular localisation, aggregation and Ser129-phosphorylation of transgenic [A30P]αSyn in the Cx: correlation with amyloidosis and silver staining

Investigation of cortical tissue of old and young [A30P]αSyn transgenic mice revealed a high number of human αSyn positive cells throughout the Cx of both 4 months and 18 months old mice (Figure 2.18 C and F respectively).

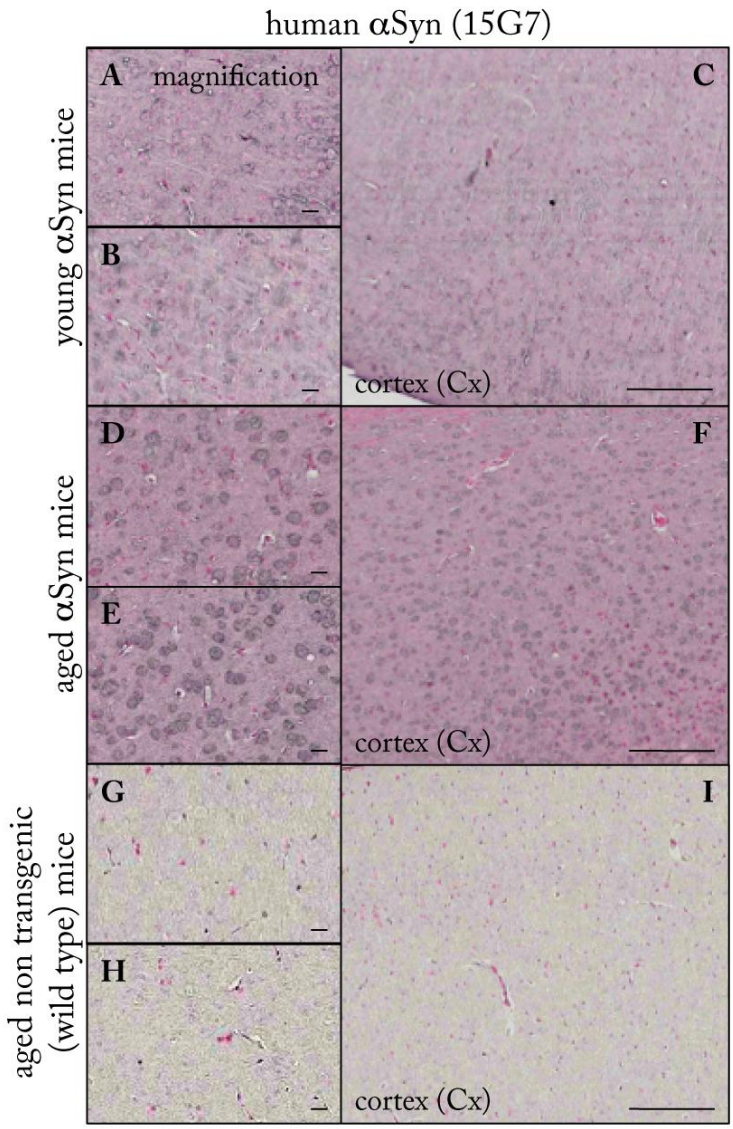

Figure 2.18 Distribution of human [A30P]αSyn in the Cx of young and aged αSyn transgenic mice.

Saggital Cx sections of 4 months transgenic (A, B, C), 18 months transgenic (C, D, E) and 22 months old wild type mice (G, H, I) were probed for transgenic α-synuclein (αSyn) with the monoclonal rat antibody 15G7 and counterstained with nuclear fast red.
Tissue from aged transgenic animals shows a similar number of αSyn positive cells (grey staining) like in young (A-C) transgenic mice (D-F). Positive cells in aged transgenic-mouse Cx show a stronger signal for mainly cytoplasmic αSyn (D, E) than the signal visible in young transgenic tissue (A, B). The Cx of aged non transgenic mice show no αSyn signal with the 15G7 antibody (G-I). Scale bars in C, F and I correspond to 200 µm. Scale bars in A, B, D, E, G and H correspond to 20 µm.

Higher magnification uncovers mainly a somal dirstribution of αSyn with stronger staining in the tissue of old transgenic mice (Figure 2.18 D and E) compared to the cortical staining of young transgenic mice (Figure 2.18 A and B). Investigation of pSer129 αSyn levels in cortical sections of young transgenic and aged transgenic as well as of aged wt mice revealed

numerous positive neurons throughout all regions of the Cx of young and old transgenic mice (Figure 2.19 B-D). Higher magnification showed somal and cytoplasmatic localisation of the pSer129 αSyn signal in both groups (Figure 2.19 A and –C respectively). Cortical tissue of old wt mice showed no positive signal after histological staining with the pSer129 αSyn antibody (Figure 2.19 E-F).

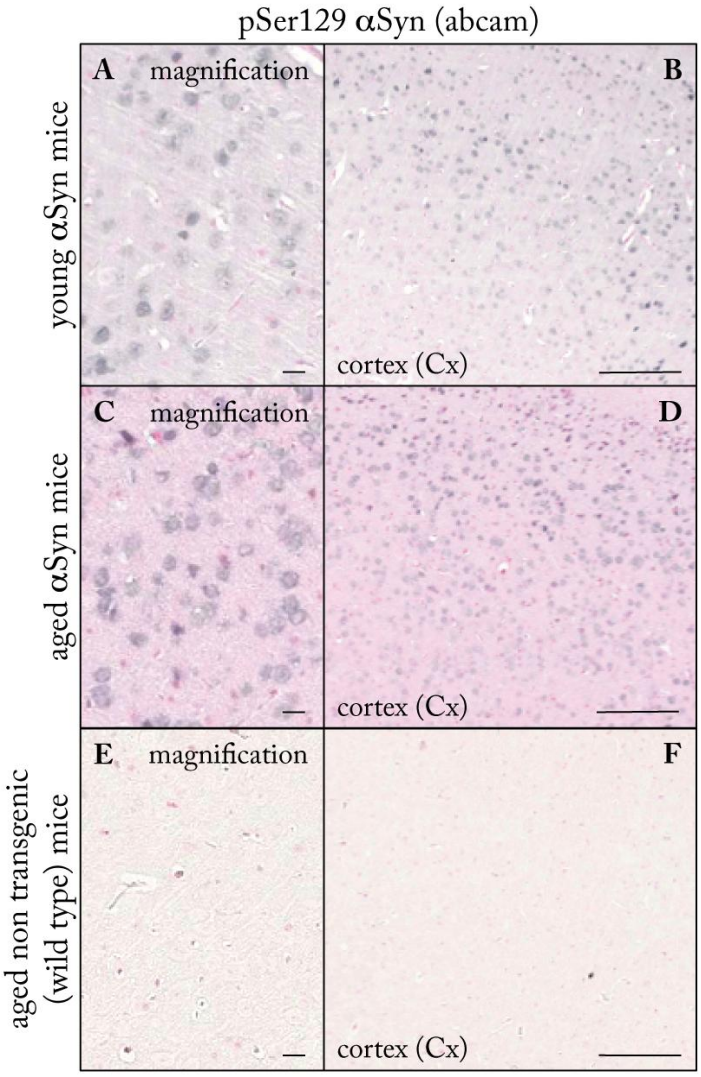

Figure 2.19 Distribution of pSer129 αSyn in the Cx of young and aged αSyn transgenic mice.

Saggital sections containing the Cx of 4 months transgenic (B and A), 18 months transgenic (D and C) and 22 months old wild type mice (F and E) were probed for transgenic α-synuclein phosphorylated at its Ser129 residue (pSer129 αSyn) and counterstained with nuclear fast red. Cytoplasmatic staining (A) of numerous cells (B) could be detected in cortical tissue of young transgenic mice (grey-/black staining). Staining of Cx tissue of aged transgenic mice displayed the same cytoplasmatic staining pattern of numerous neurons (C), but in a much stronger manner (D and C). Cx tissue of aged wt mice displayed no postitve signal with the pSer129 αSyn antibody (E and F). Scale bars in B, D, and F correspond to 200 µm. Scale bars in A, C and E correspond to 20 µm.

Cortical amyloidosis was investigated via 0.1% ThS staining of tissue isolated from 4 months young and 18 months old [A30P]αSyn transgenic mice. Gallyas silver staining was performed with similar tissue from 18 months old transgenic mice and 22 months old wt mice. Neither ß-pleated protein aggregates nor neuropathological silver staining positive neurons were detected in the cortical sections of all included animals (Figure 2.20 A-D and Figure 2.21 A-D respectively).

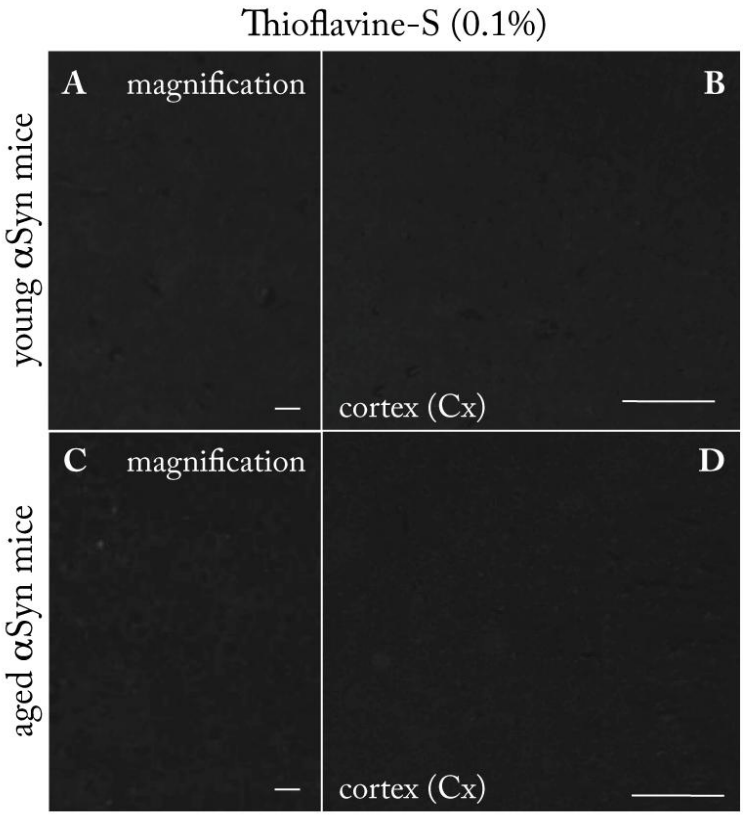

Figure 2.20 Investigation of amyloidosis in the Cx of young and aged αSyn transgenic mice.

Saggital cortical sections of 4 months young (A and B) and 18 months old transgenic mice (C and D) were stained with the congophilic marker Thioflavine-S (ThS) which specifically labels β-pleated protein conformation. No ThS positive staining was observed in any cerebellar region of young (A and B) and aged (C and D) transgenic mice. Scale bars in B and D correspond to 200 µm. Scale bars in A and C correspond to 20 µm.

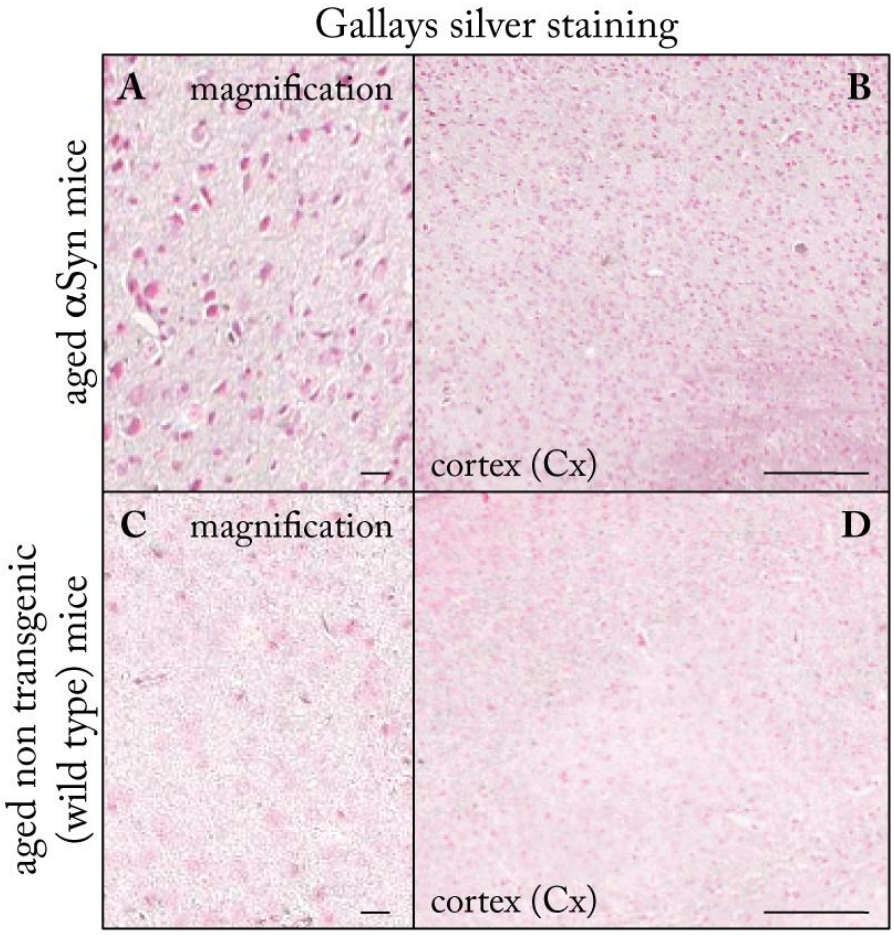

Figure 2.21 Investigation of neuropathology in the Cx of aged αSyn transgenic and aged wt mice.

Saggital cortical (Cx) sections of transgenic 18 months old mice (A and B) and 22 months old wt mice (C and D) were subjected to silver staining and counterstained with nuclear fast red. With exception of the nuclear fast red staining neither Cx tissue of aged transgenic mice (A and B), nor sections of aged wt mice (C-D) were found to be positive for the Gallyas silver staining. Scale bars in B and D correspond to 200 µm. Scale bars in A and C correspond to 20 µm.

2.6.2 Distribution, intracellular localisation, aggregation and Ser129-phosphorylation of transgenic [A30P]αSyn in the Hip: correlation with amyloidosis and silver staining

Histological stainings of Hip containing sections of young and old [A30P]αSyn transgenic mice with the 15G7 antibody uncovered positive signal in the subiculum (Sub.), CA1-, CA3-region and the dentate gyrus (DG) of 18 months old animals (Figure 2.22 E). Tissue of 4 months young transgenic mice revealed positive signals in the same hippocampal regions but in a much weaker staining pattern (Figure 2.22 A-D). Higher magnification revealed cytoplasmatic, somal stainings of cells in all αSyn positive regions of 18 months old mouse Hip (Figure 2.22 F, G and -H). Furthermore also synapses (granular layer) of CA1- and CA3-neurons were positive for human αSyn in old transgenic mice (Arrowhead in Figure 2.22 G and Figure 2.22 H). This synaptic staining pattern could not be observed in similar regions of young transgenic mice (Figure 2.22 C and -D). As previously observed in the other brain regions staining of sections of 22 months old wt mice with the same antibody showed no positive signal at all, confirming the specifity of the staining with the 15G7 antibody (Figure 2.22 I-L).

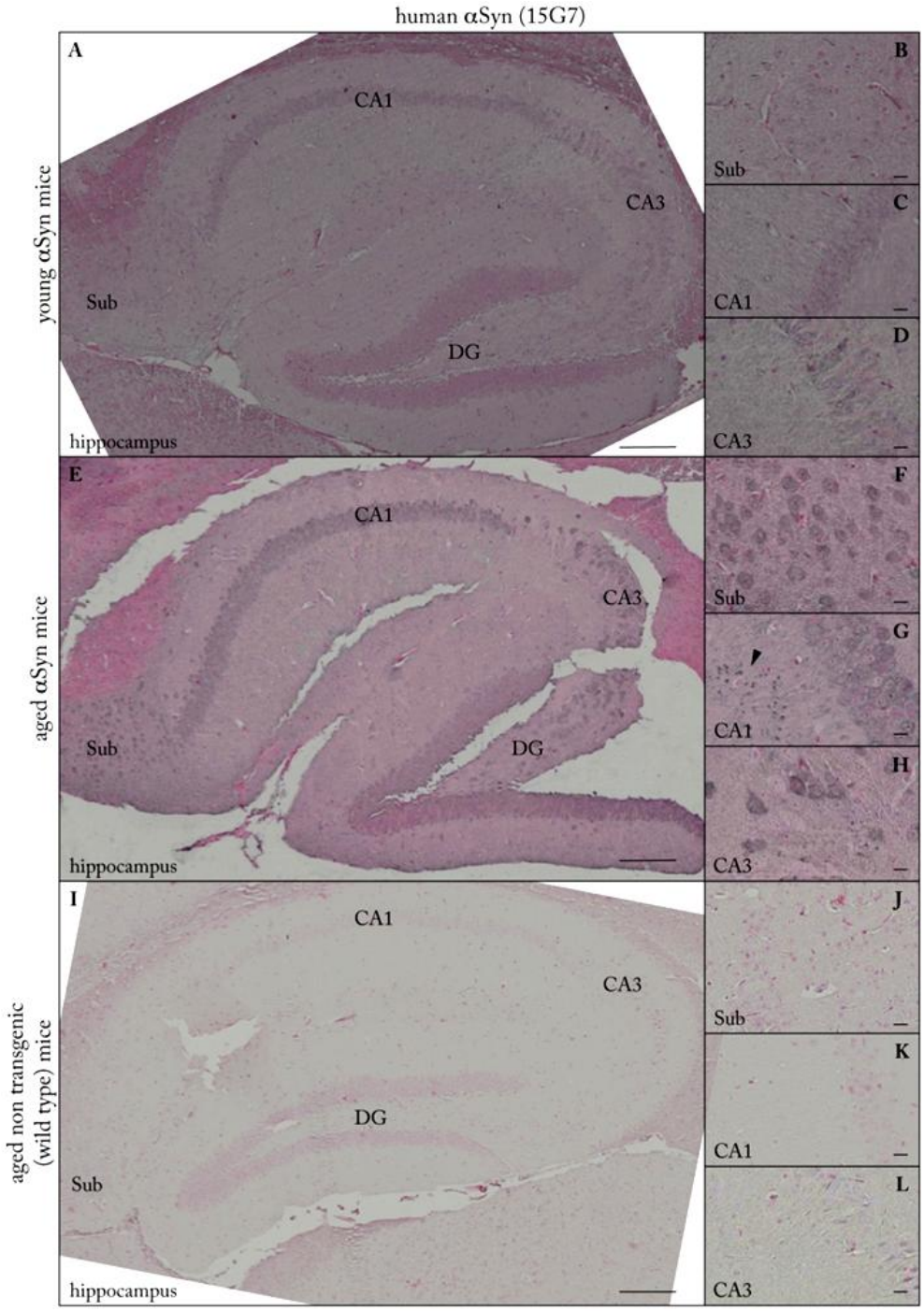

Figure 2.22 Distribution of human [A30P]αSyn in different regions of the Hip of young and aged αSyn transgenic mice.

Saggital hippocampal (Hip) sections of 4 months transgenic (A-D), 18 months transgenic (E-H) and 22 months old wild type mice (I-L) were probed for transgenic α-synuclein (αSyn) with the monoclonal rat antibody 15G7 and counterstained with nuclear fast red. Tissue from aged transgenic animals displayed a bright cytoplasmatic αSyn staining (grey staining in E) in the subiculum (grey staining in F), CA1- (grey staining in G), CA3-region (grey staining in H) and the gyrus dentate (grey staining in E). Furthermore synapses of CA1-neurons in aged transgenic mice were also positive for αSyn (arrowhead in G). Hip tissue from young transgenic mice showed weak and diffuse αSyn staining of few neurons in mentioned Hip regions (B-D). Hip of aged non-transgenic mice displayed no αSyn signal with the 15G7 antibody (I-L). Scale bars in A, E and I correspond to 200 µm. Scale bars in B-D, F-H and J-L corresponds to 20 µm.

Stainings with the human αSyn specific antibody 15G7 were positive in the hippocampal regions CA1 and CA3, as well as for the subiculum and the dentate gyrus (Figure 2.23). Investigation of pSer129 phosphorylation of transgenic αSyn in hippocampal brain regions of young and old transgenic mice revealed presence of pSer129 αSyn in both animal groups (Figure 2.23 A-H). Thereby neither intensity of the staining nor the number of positive cells did show any outstanding differences between the compared age groups. Interestingly, synapses of the CA1 and CA3 neurons, which were found to be positive for the overexpressed human [A30P]αSyn (Figure 2.22 G-H) in aged trangenic animals, were negative for pSer129 αSyn in the same animal group (Figure 2.23 G-H).

In accordance with previous results 22 months old wt mice did not show any pSer129 αSyn positive stainings throughout the whole hippocampal area (Figure 2.23 I-L).

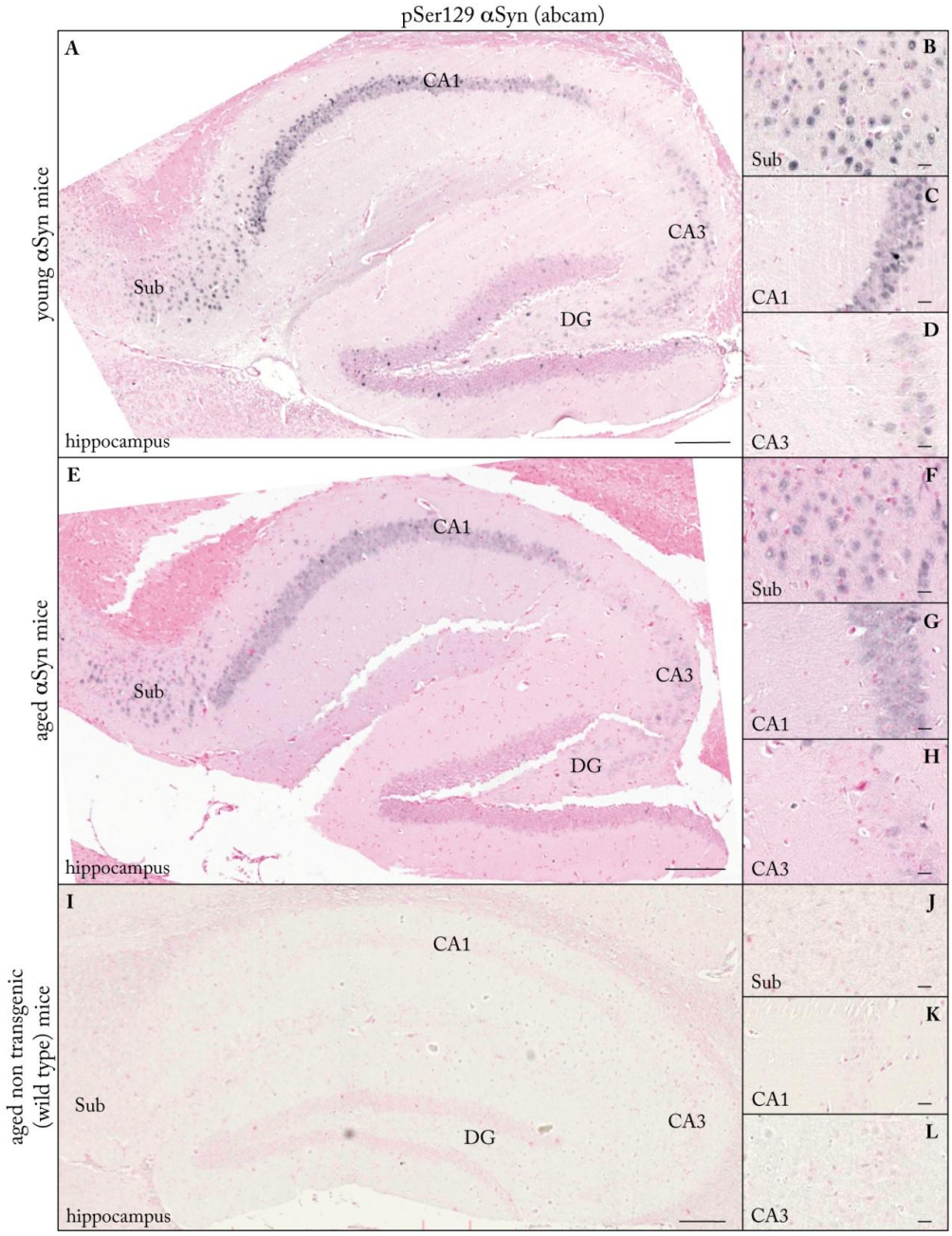

Figure 2.23 Distribution of pSer129 αSyn in the Hip of young and aged αSyn transgenic mice.

Saggital sections containing Hip of 4 months transgenic (A-D), 18 months transgenic (E-H) and 22 months old wild type mice (I-L) were probed for transgenic α-synuclein (αSyn) phosphorylated at the Ser129 residue (pSer129 αSyn) and counterstained with nuclear fast red. Tissue from young and aged transgenic animals shows a bright cytoplasmatic pSer129 αSyn staining (grey-/black staining) in the subiculum (B and F), CA1- (C and G), CA3-region (D and H) and the gyrus dentate (A and E). Scale bars in A, E and I correspond to 200 µm. Scale bars in B-D, F-H and J-L correspond to 20 µm.

Investigation of hippocampal amyloidosis with ThS staininig of sections isolated from young and old [A30P]αSyn transgenic animals showed no positive signals in investigated regions of the two included animal groups

(Figure 2.24 A-D and Figure 2.24 E-H respectively). Gallyas silver staining of similar brain regions was performed with tissue isolated from 18 months old transgenic mice and 22 months old wt animals. None of the hippocampal tissue investigated (neither of wt nor of transgenic mice) showed neuropathological positive silver staining in the hippocampal region (Figure 2.25 A-D and Figure 2.25 E-H, respectively).

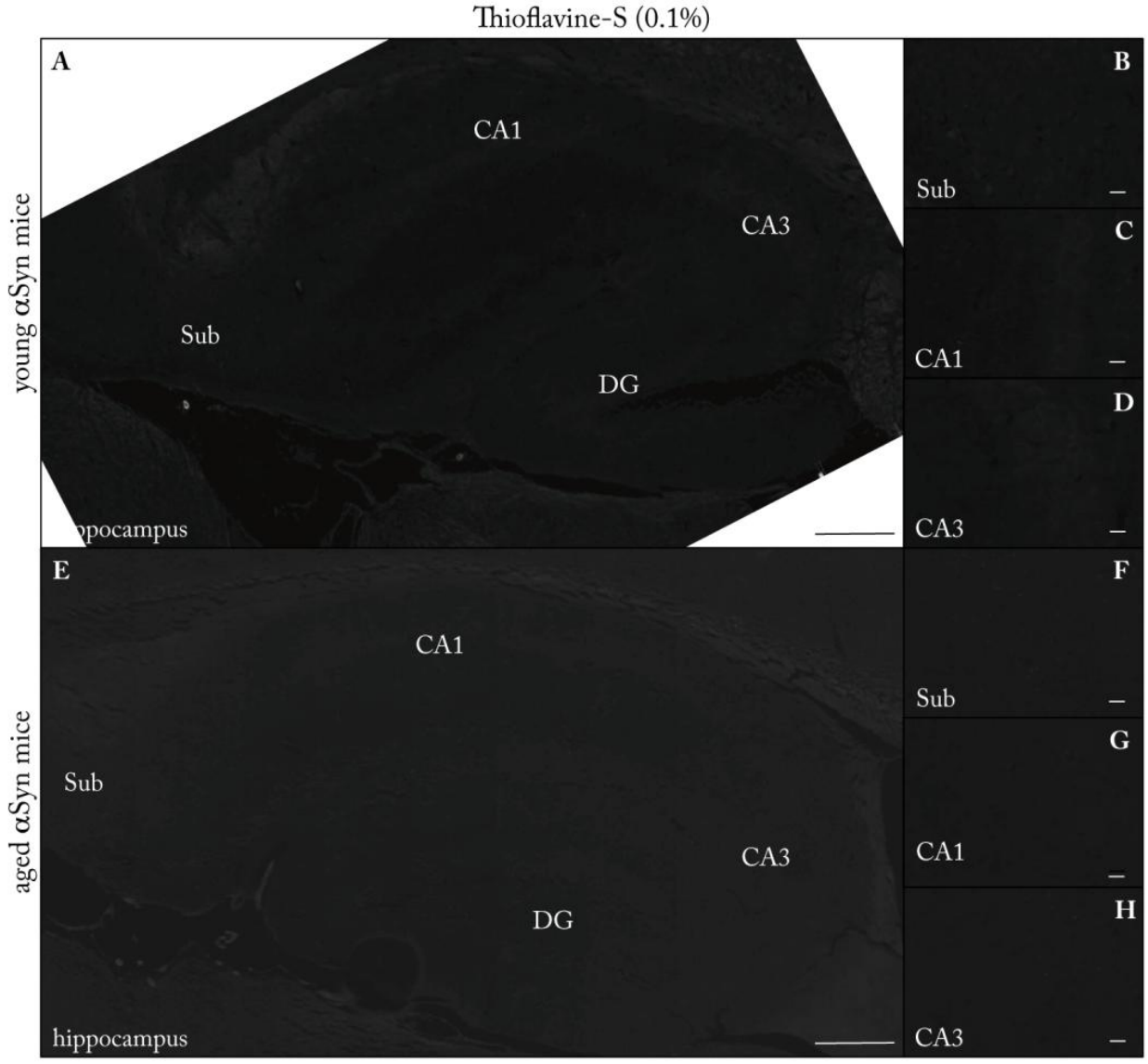

Figure 2.24 Investigation of amyloidosis in the Hip of young and aged αSyn transgenic mice.

Saggital Hip containing sections of transgenic 4 months young mice (A-D) and transgenic 18 months old mice (E-H) were stained with the congophilic marker Thioflavine-S (ThS) which specifically labels ß-pleated protein conformation. Neither the tissue of young transgenic mice, nor Hip tissue of aged transgenic mice displayed ThS positive stainings in this area. Scale bars in A and E correspond to 200 µm. Scale bars in B-D and F-H correspond to 20 µm.

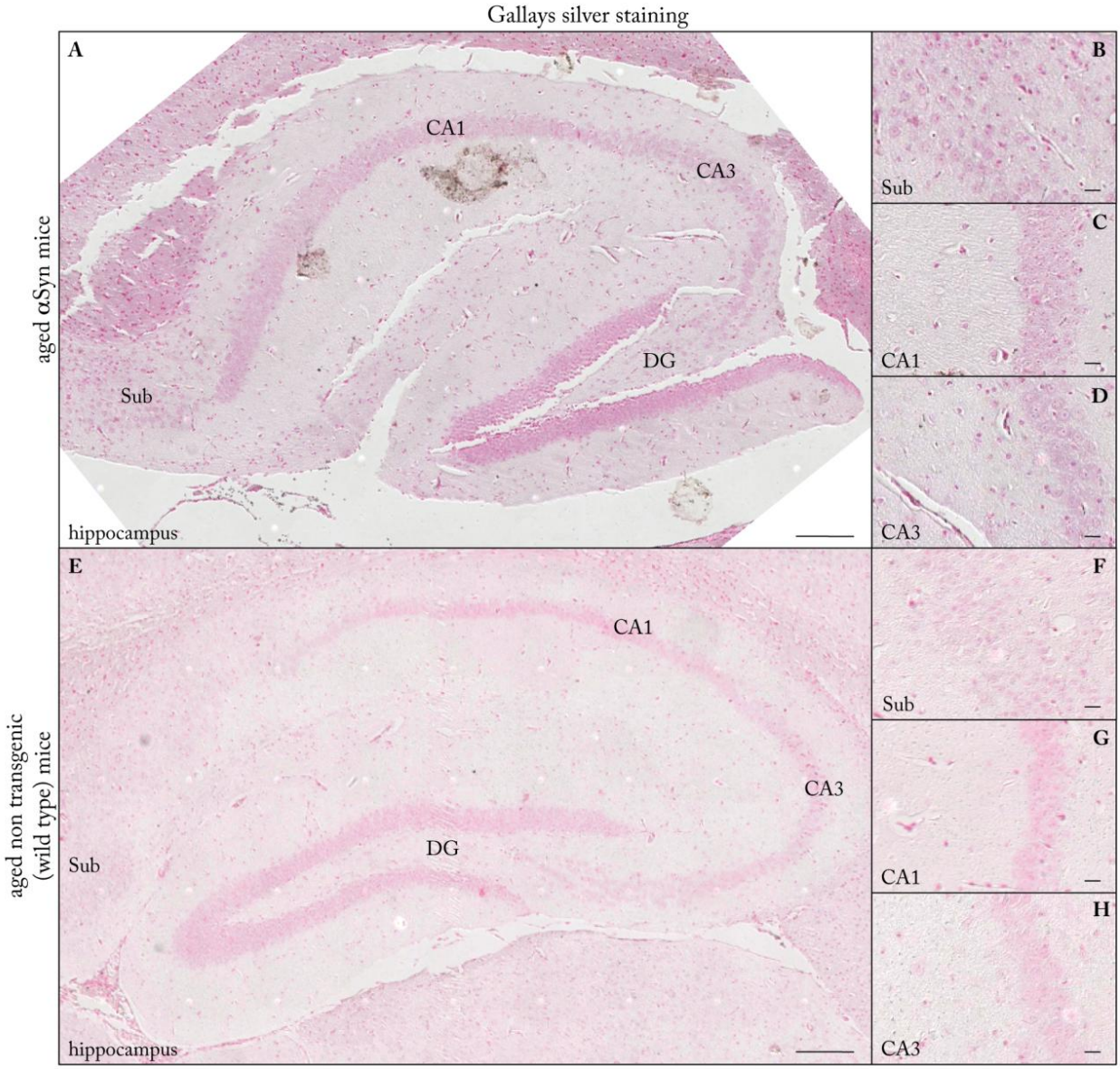

Figure 2.25 Investigation of neuropathology in the Hip of aged αSyn transgenic and aged wt mice.

Saggital hippocampal (Hip) sections of transgenic 18 months old mice (A-D) and 22 months old wt mice (E-H) were subjected to silver staining and counterstained with nuclear fast red. Neither Hip tissue of aged transgenic mice (A-D), nor of aged wt mice (E-H) was found to be positive for the Gallyas silver staining. Scale bars in A and E correspond to 200 µm. Scale bars in B-D and F-H correspond to 20 µm.

2.7 Impairment of context and emotional learning in aged transgenic (Thy1)h[A30P]αSyn mice

Transgenic αSyn mice expressing the protein under control of the Thy1 promoter were shown to develop motoric impairment (van der Putten et al., 2000, Fleming et al., 2004, Freichel et al., 2007) or disturbance of olfaction (Fleming et al., 2008). The [A30P]αSyn overexpressing mice used in this study were shown to develop in addition impairment of emotional learning (Freichel et al., 2007, Schell et al., 2009) at a much earlier timepoint than the onset of motoric disturbance (Freichel et al., 2007). Therefore an aim of this study was the investigation of the functional impairment induced by synucleinopathy in the amygdala, which is the key brain region involved in emotional learning processes.

4 months young and 18 months old [A30P]αSyn overexpressing mice were trained to associate a light/tone cue (conditioned stimuli (CS)) with fear, by exposure for one second to two 0.6 mA footshocks (unconditioned stimulus (US)) directly after the presentation of the CS (Figure 2.26, upper graphic). In each training session this process was repeated for 8 times for each animal trained. Furthermore in the course of the training session the general activity of trained animals was gradually decreasing during the CS (light-/tone cue) phase, until a reduction to nearly zero before the exposure to the last US (footshock) (Figure 2.26 B, activity graph, activity between activity peaks). Interestingly at the onset of the presentation of the last CS (light-/tone cue), the activity of the trained animal was showing an enhanced training dependent learning effect. Rectangle in the upper left corner of the activity graph demonstrates that trained transgenic mice, independent of age, nearly explore the whole available area of the conditioning box during the training session (Figure 2.26 B).

Control groups (non-trained animals) were deployed to a similar program which was lacking the exposure to the US (footshocks) (Figure 2.26 A, upper graphic and upper bar in activity graph). As expected all animals,

independant of age, showed in general normal exploration behaviour during the training, indepenedant of presence or absence of the CS (light-/tone cue) (Figure 2.26 activity graph). Furthermore included animals explored almost the whole available area in the fear conditioning box (Figure 2.26 rectangle in upper left corner of activity graph).

Investigation of total percentage of explored area of all trained groups showed a similar exploration of all groups during first phase, inependant of age (Figure 2.26 C, phase 1). After exposure to the first US, training groups of old and young mice have a high tendency to a reduced exploration, which starts to be significantly reduced compared to non trained animals, after exposure to the third US (Figure 2.26 C, phase 4). The exploration of these groups remains significantly decreased until the end of the training, although all aged groups, inependant if trained or not, always show the tendency to a decreased exploration (Figure 2.26 C phase 2-8).

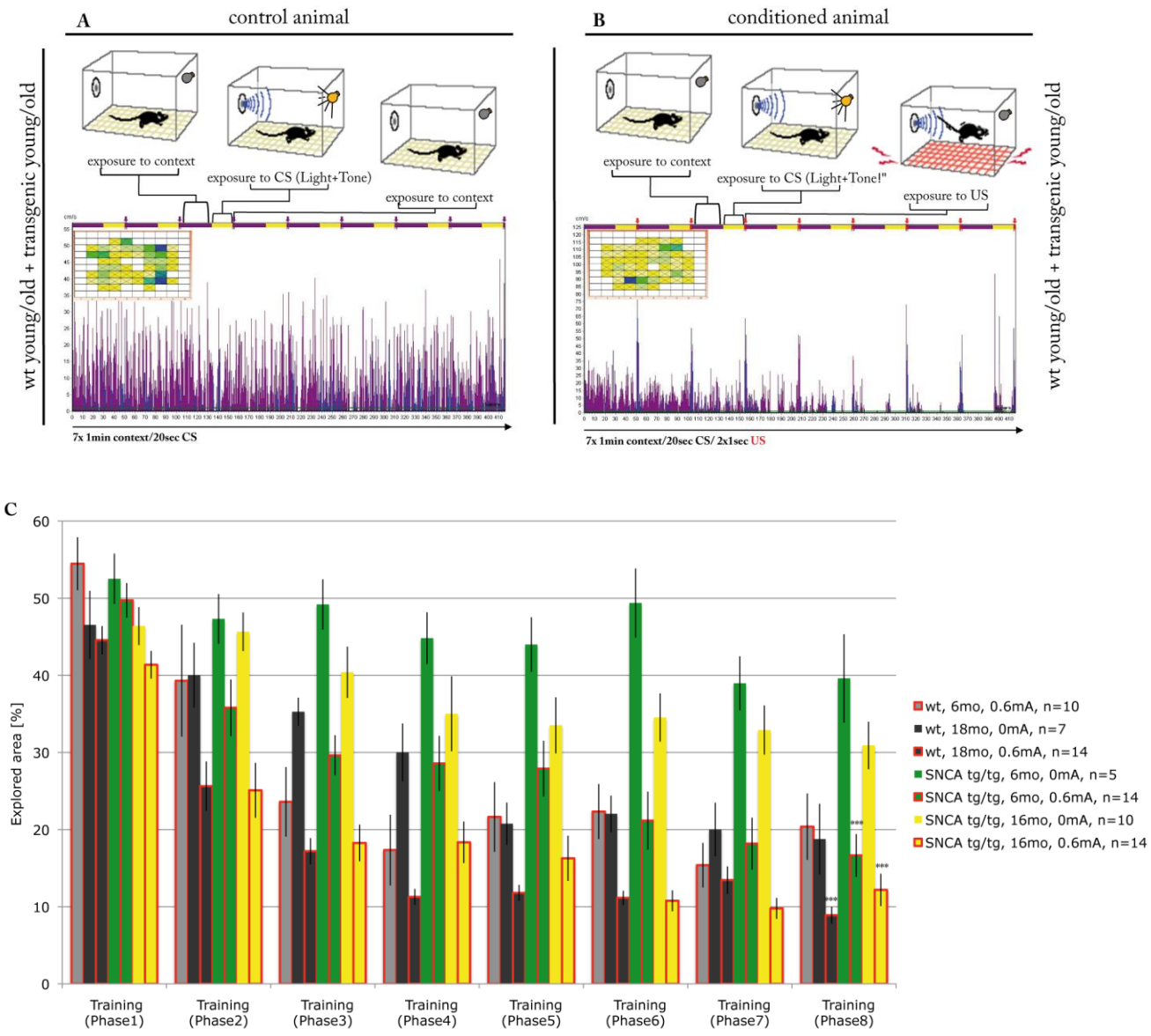

Figure 2.26 Fear conditioning training of young and aged αSyn transgenic mice.

Young and aged transgenic, as well as wild type mice were trained in a 6 min conditioning session, in which control animals received no (A) and trained animals received 2 x 0.6 mA scrambled foot shock (B) for 1 sec, signaled by a 20 sec light/tone cue immediately prior to the shock (upper graphics in A and B). Pink/yellow/red line included in the upper part of the activity graph (Figure 2.26 B) demonstrates the 8 fear conditioning phases which contain; break: pink line; exposure to CS (light-/tone- cue): yellow line; exposure to US (footshocks): red line (conditioned groups) or lacking of US for control animals. The activity graph below points out the high activity of the animals directly after each exposure to the footshocks (Figure 2.26, high activity peaks in the activity graph).
None of the shocked animals displayed continuous movement and exploratory behaviour during the whole training session (activity graph in A). Animals exposed to foot shocks had an advancing decrease in activity with ongoing training (activity graph in B), due to a decrease of exploration activity and an increase of freezing time spent between exposure to foot shocks (C). Nearly the whole available area of the conditioning box was visited by the animals, independent of age and genotype (rectangle in left upper corner of activity graph in A and B). ***p<0.0001.

The hippocampal CA1 and CA3 regions, as well as the dentate gyrus and the subiculum of both young and old transgenic mice, were positive for the overexpressed human αSyn and pSer129 αSyn (Figure 2.22 and Figure 2.23). Furthermore non phosphorylated, transgenic, synaptic αSyn was only detected in the molecular part of the hippocampal CA1 region of old transgenic mice with cognitive impairment (Figure 2.22 B-D and F-H and Figure 2.23 B-D and F-H). Due to this findings, hippocampal function dependent context learning (Tsoory et al., 2008, Langston et al., 2010) was checked for all groups. Therefore 24 h after training, control and trained mice of both ages were exposed for 3 minutes to the same context, which was used in the training session (Figure 2.27 A and B, upper graphic) and explored area of available space was recorded. Control animals, which were only exposed to the CS (light-/tone cue) during the training, showed just the normal exploration behaviour (Figure 2.27 A, activity graph) and nearly visited the whole available area (Figure 2.27 A, rectangle in the upper left corner of activity graph). Conditioned young and old groups, which were exposed to the CS (light-/tone cue) and to the US (footshocks) in the training, spent most of the time freezing (Figure 2.27 B, activity graph), and showed startle reactions (jumping) (Figure 2.27 B, rectangle in the activity graph, interrupted visited areas). Consequently this behaviour led to a significantly reduced exploration of trained young and old animals (Figure 2.27 C, red framed bars), whereas old trained mice showed a tendency to explore more, and therefore to spend less time freezing, compared to young trained mice (Figure 2.27 C, yellow- and green red-framed bars respectively).

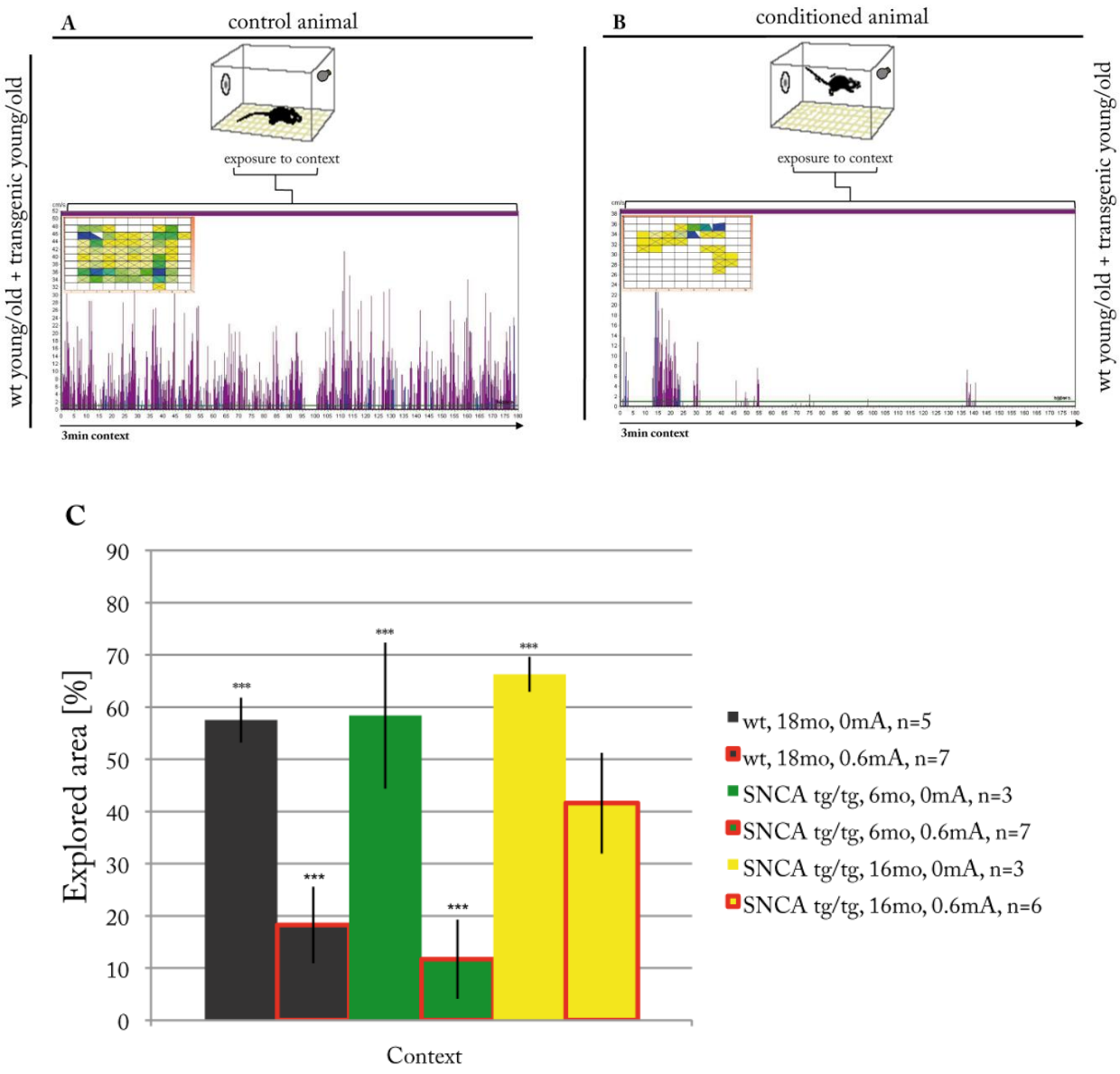

Figure 2.27 Context-test of young and aged αSyn transgenic mice.

24 h after training mice were assessed for context learning in the same context used for the training for a time period of 3 min (upper grapics in A and B). None shocked animals displayed normal exploration behaviour and activity independent of age and genotype (activity graph in A), and inspected nearly the whole available area of the conditioning box (rectangle in left upper corner of activity graph in A).
Mice exposed to foot shocks (old and young transgenic and wt animals) spent most of the time freezing, therefore measured activity was low (activity graph in B). Furthermore explored area was also reduced (rectangle in left upper corner of activity graph in B). All conditioned groups (independent of age and genotype) recognized the conditioning context (C), but old trangenic animals displayed a tendency for a higher exploration activity and therefore spent less time freezing (C) compared to the young conditioned group. ***p<0.0001; **p<0.001

In order to assess cued learning, which is dependent on amygdala function (Maren, 2001), 6 h after the context learning test, mice were exposed to a different context. The wall-color, floor plate and embedding material were changed, but the same CS (light-/tone cue) as used in the training session was presnted for a period of 3 minutes (Figure 2.28 A and B, upper graphics and pink/yellow/pink bar above the activity graph). Explored area was measured during the first phase which was a two minutes break, second phase included a 3 minutes exposure to the CS and the third phase was a one minute break (Figure 2.28 A and B, pink/yellow/pink bar above activity graph). Non-trained control animals showed normal exploration behaviour and explored most of the available area, independent of age or presence or absence of the CS (Figure 2.28 A, activity graph including rectangle in the upper left corner and Figure 2.28 D, yellow and green bars). Young conditioned mice displayed a similar activity during the breaks, but in contrast to the none conditioned control groups, this animals directly reduced activity and exploration when presentation of CS began due to the onset of freezing behaviour (Figure 2.28 B, second phase of the activity graph). Old conditioned transgenic animals showed a similar reaction as the young conditioned mice after onset of CS, but to a lesser extent (Figure 2.28 C, second phase of the activity graph). Therefore time spent freezing was reduced for this group of animals and the percentage of explored area was higher for the old conditioned transgenic animals than for the young conditioned transgenic mice (Figure 2.28 D, yellow- and green-red framed bars respectively).

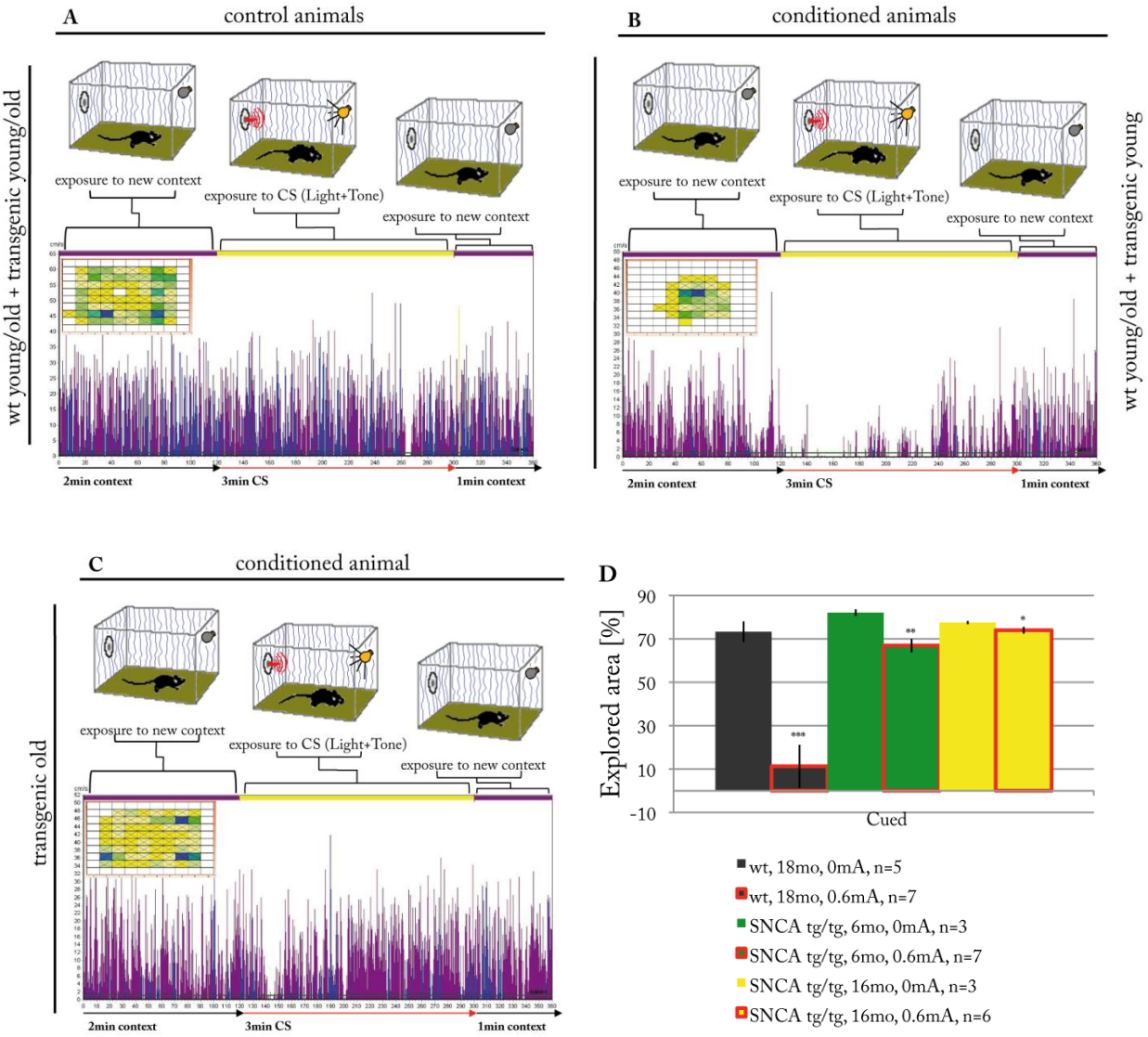

Figure 2.28 Cued-test of young and aged αSyn transgenic mice.

Six hours after examination of context learning, cued learning was checked. Therefore all animals were placed into a different context and exposed to the same light and tone cue (condition stimuli (CS)) used in training (upper graphics in A, B and C). Exploration behaviour and activity were measured 2 min before onset of light- and tone cue, during a 3 min exposure to the conditioning cues and for 1 min after exposure to the cues (upper grapics in A, B and C). Non-trained animal groups (inependent of age and genotype) exhibit consistent exploration behaviour and activity throughout the whole measurement, independent of presence or absence of conditioning light/tone cue (activity graph in A). Also all this animal groups inspected nearly the whole available area of the conditioning box (rectangle in left upper corner of activity graph in A). With exception of aged transgenic mice all trained animals showed a direct interruption- and a general low activity and exploration behaviour, directly after onset and during the whole exposure to the light/tone cue (activity graph in B). Furthermore explored area of these conditioned groups was much lower (rectangle in left upper corner of activity graph in B) than the area measured from non conditioned (rectangle in A) and aged transgenic conditioned mice (rectangle in left upper corner of activity graph in C). Apart from the exploration of nearly the whole available area, aged αSyn transgenic mice displayed a consistent exploration behaviour and activity comparable to the measurements of the non-shocked groups (inependent of presence or abence of the conditioning stimuli). The only exception is a short interruption of activity directly after the onset of the light/tone cue (activity graph in C).
With exception of the aged conditioned transgenic αSyn mice all conditioned animals recognised the condition stimuli and showed the expected reduction of activity and exploration due to the onset of freezing behavior in the CS-presentation phase (D). Old conditioned transgenic mice explore nearly the same percentage of area as non trained animals (D). ***p<0.0001; **p<0.001; *p<0.02

2.8 Histological investigation of synucleinopathy in brain regions involved in context and emotional learning

Old transgenic animals showed a reduced, amygdala-dependent, cued learning after fear conditioning and a tendency for an impaired, Hip function-dependent, context learning (Chapter 2.7). Histological investigation of coronar sections with the human αSyn specific antibody 15G7, revealed presence of [A30P]αSyn in coronar amygdala containing sections of young and old transgenic mice (Figure 2.29 C-D). Furthermore described presence (Figure 2.22) of transgenic αSyn in the Hip could be shown again with the staining of coronar sections (Figure 2.29 C-D). Higher magnification of aged transgenic mouse tissue revealed bright cytoplasmatic staining in the main output region of the amygdala and the lateral hypothalamus (Figure 2.29 K). Furthermore numerous basal amygdala and lateral amygdala cells containing cytoplasmatic "nuclear localised" signals could be identified (Figure 2.29 L). The amygdaloid central nucleus of old transgenic mice contained also few transgenic αSyn positive cells with weak somal staining pattern (Figure 2.29 M). Higher magnification of similar brain regions in coronar sections of young transgenic mice revealed diffuse and weak staining of few neurons in all examined brain regions (Figure 2.29 H-J).

As expected, staining of similar sections of 22 months old wt animals with the human specific αSyn antibody showed no signal throughout the whole tissue (Figure 2.29 F).

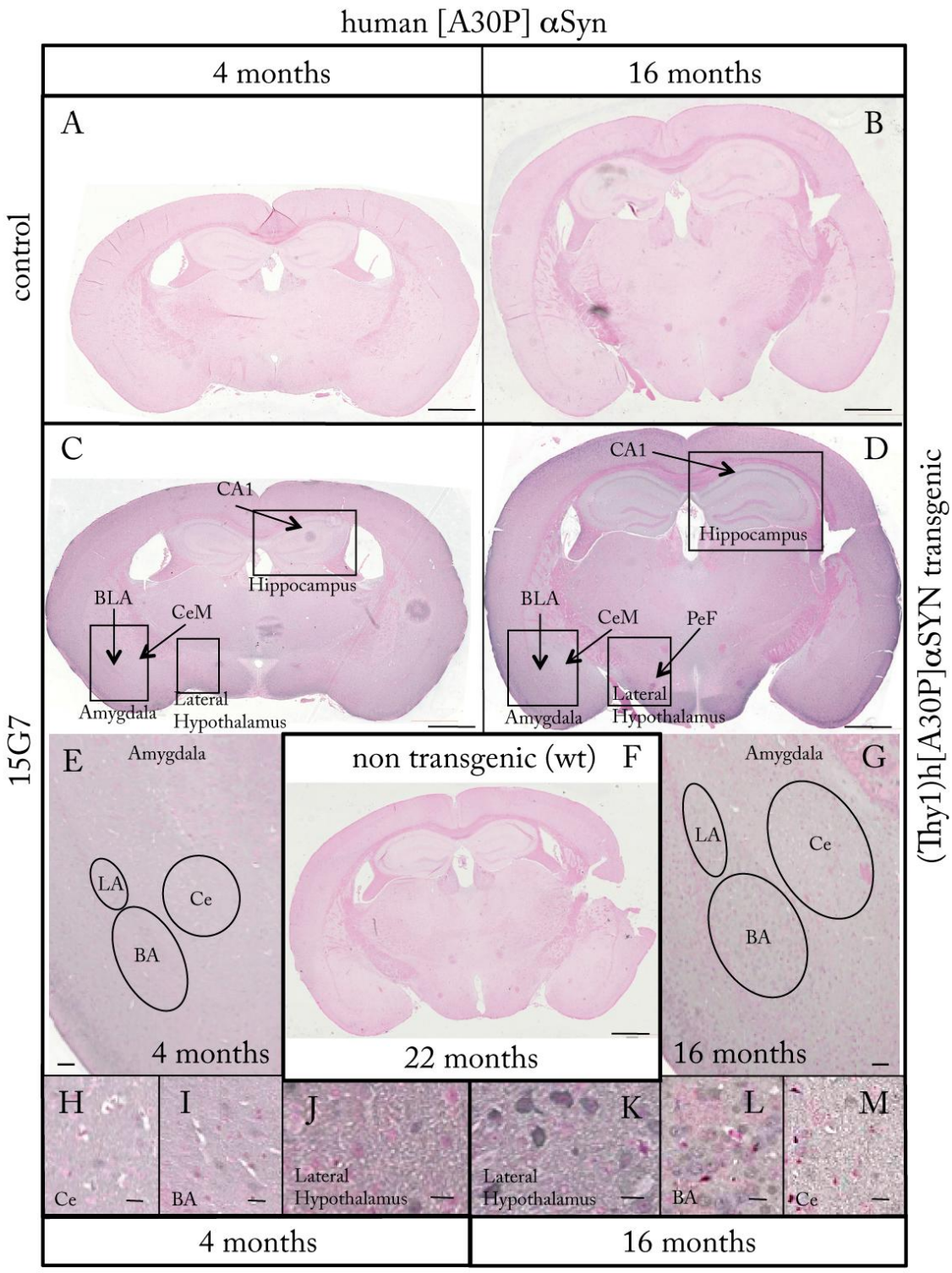

Figure 2.29 Human [A30P]αSyn in brain regions involved in context and fear conditioning learning.

Coronar sections of transgenic young (A-C), aged (B-D) and wild type (F) mice were probed for transgenic α-synuclein (αSyn) with the monoclonal rat antibody 15G7 (B-E) or only with secondary antibody (A-B). Presence of human αSyn (grey-/black staining) could be confirmed in 4 months and 16 months old transgenic animals (C-D) whereas aged brains show a brighter α Syn signal (D) compared to the signal detected in brains of young mice (C). Brains of aged non transgenic mice show no signal with the 15G7 antibody (E). Scale bars in A-D and F correspond to 1000 µm. Scale bars in E and G correspond to 200 µm. Scale bars in H-M correspond to 20 µm.

Histology of coronal sections from young and old transgenic mice with the pSer129 αSyn specific antibody stained the majority of cortical tissue (Figure 2.30 A-B), as well as hippocampal CA1 and CA3 regions (Figure 2.30 C-E), in both young and old transgenic mice. However positive signals in coronar tissue of young animal seemed to be weaker than the signals visible in similar tissue of old transgenic mice (Figure 2.30 A-B). Nevertheless in cortical cells pSer129 αSyn could be detected in soma and neuronal branches, whereas in hippocampal CA1 and CA3 region pSer129 αSyn was detected only in neuronal somata (Figure 2.30 E).

The staining of amygdala showed different, region dependant staining patterns in young and old transgenic mice. The lateral- (LA) and basolateral amygdala (BA) of old [A30P]αSyn transgenic mice contained numerous pSer129 αSyn positive neurons (Figure 2.30 F-G), which showed a "nuclei-localised" staining pattern (Figure 2.30 H). This staining was much weaker and more diffuse in similar regions of young transgenic mice (Figure 2.30 F). Closer investigation of the amygdaloid central nucleus (Ce) of old transgenic mice revealed pSer129 αSyn positive structures, reminiscent of the Lewy neurites detected in BS and MB of old motorically impaired transgenic mice (Figure 2.30 L and –K). This staining pattern could not be detected in the central nucleus of young trnagenic mice (Figure 2.30 I). Higher magnifications revealed few cells with weak somal staininig (Figure 2.30 J).

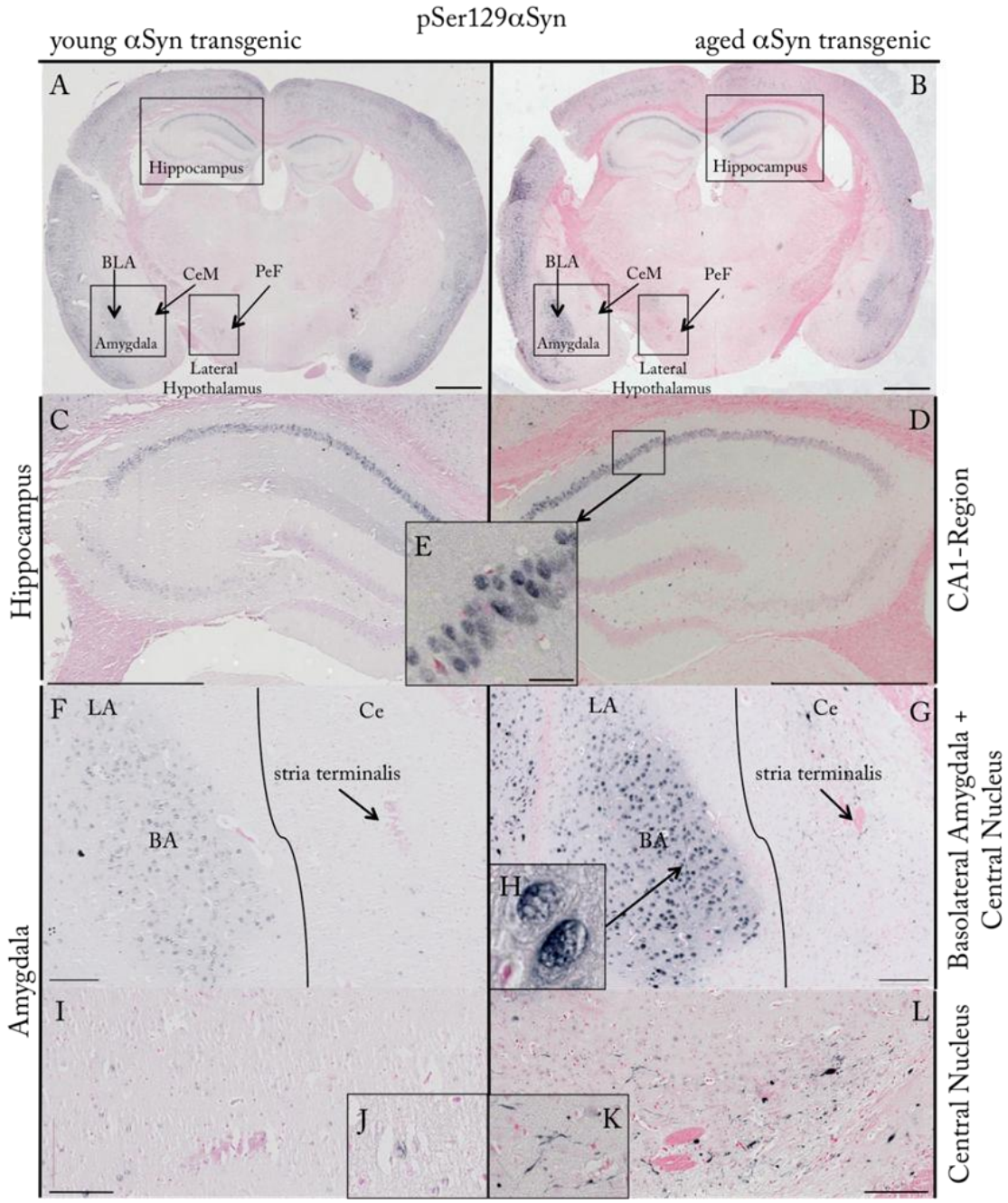

Figure 2.30 Histological investigation of amygdala synucleinopathy in young and aged α-synuclein transgenic mice (modified from (Schell et al., 2009)).

Coronar sections of transgenic young (A, C, F, I, J) and aged transgenic mice (B, D, E, G, L and K) were probed for transgenic α-synuclein phosphorylated at its Ser129 residue (pSer129 αSyn) and counterstained with nuclear fast red. Presence of pSer129 αSyn (grey-/black staining) could be confirmed in 4 months (A) and 16 months old transgenic animals (B) in hippocampal CA1 region (C and D), basolateral amygdala (BLA) (F and G), and the central nucleus of the amygdala (I and L). Higher magnification displayed cytoplasmatic and nuclear like pSer129 αSyn staining pattern in hippocampal CA1 region (E) and the basolateral amygdala (BLA) (H) of young and old transgenic animals, in which staining of old transgenic tissue (especially of the BLA) shows a much brighter signal than the signal detected in tissue of young mice. Higher magnification of the central nucleus revealed the most outstanding difference between synucleinopathy in young transgenic (J) and old transgenic mice (K): While tissue of young transgenic animals displayed weak cytoplasmatic staining of scattered cells, old transgenic animals have numerous Lewy neurite like pSer129αSyn positive structures in the central nucleus of the amygdala (K). Scale bars in A-D correspond to 1000 µm. Scale bars in F-G, I-L correspond to 100 µm. Scale bar in E corresponds to 20 µm.

Investigation of amyloidosis in the amygdala was performed with ThS stainings (0.1%) of coronal sections isolated from old wt- and αSyn transgenic mice. None of the sections contained any positive signals for the congophilic marker ThS (Fig. 2.6.3).

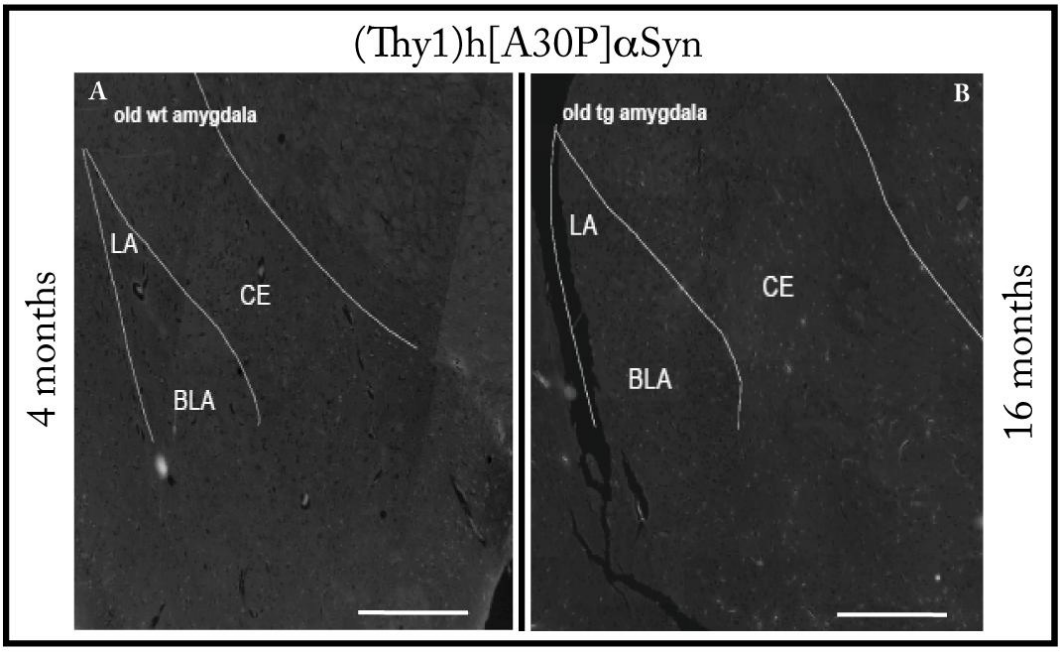

Figure 2.31 Histological investigation of amygdala amyloidosis in young and aged α-Synuclein transgenic mice.

Coronal sections of aged wt and αSyn transgenic mice containing the neuroplasticity and emotional learning relevant lateral amygdala and basal amygdala as well as the amygdaloid central nucleus (which is the main output region of the amygdala) were stained with the congophilic marker Thioflavine-S (ThS) which specifically labels β-pleated protein conformation. No ThS positive staining could be observed in any of the reviewed sections originating from old wt (A) and old αSyn transgenic animals (B). Scale bars correspond to 500 µm.

2.9 Intracellular distribution of Ser129 phosphorylated αSyn in αSyn and GRK5 transiently tranfected HEK293E cells

To confirm the nuclear like staining pattern which was detected particularly in the basolateral amygdala (BLA) and to investigate general distribution of pSer129 αSyn in cell culture, HEK293E cells were transiently co-transfected with αSyn and its kinase GRK5 (Arawaka et al., 2006). Triple-label confocal microscopy confirmed increase of pSer129 αSyn in cells cotransfected with αSyn and GRK5 with two different pSer129 αSyn antibodies (Figure 2.32 C and O). Interestingly this signal was localised to the nucleus as already observed in the BLA-cells of brain slices from αSyn transgenic mice (Figure 2.32 F-G). GRK5 signal could be detected in the plasma membrane while αSyn was scattered throughout the cytosol (Figure 2.32 A-B, E-F and Figure 2.32 M-N, Q-R). Cells co-expressing αSyn and a kinase-dead mutant GRK5 showed no positive signal for pSer129 αSyn (Figure 2.32 G and S). Specifity of nuclear pSer129 αSyn staining was checked by eliminating phosphorylation via phosphatase treatment (Figure 2.32 K). Thus, the kinase GRK5 phosphorylates αSyn at its Ser129 residue in this cell culture model and pSer129 αSyn is transported to the nucleus.

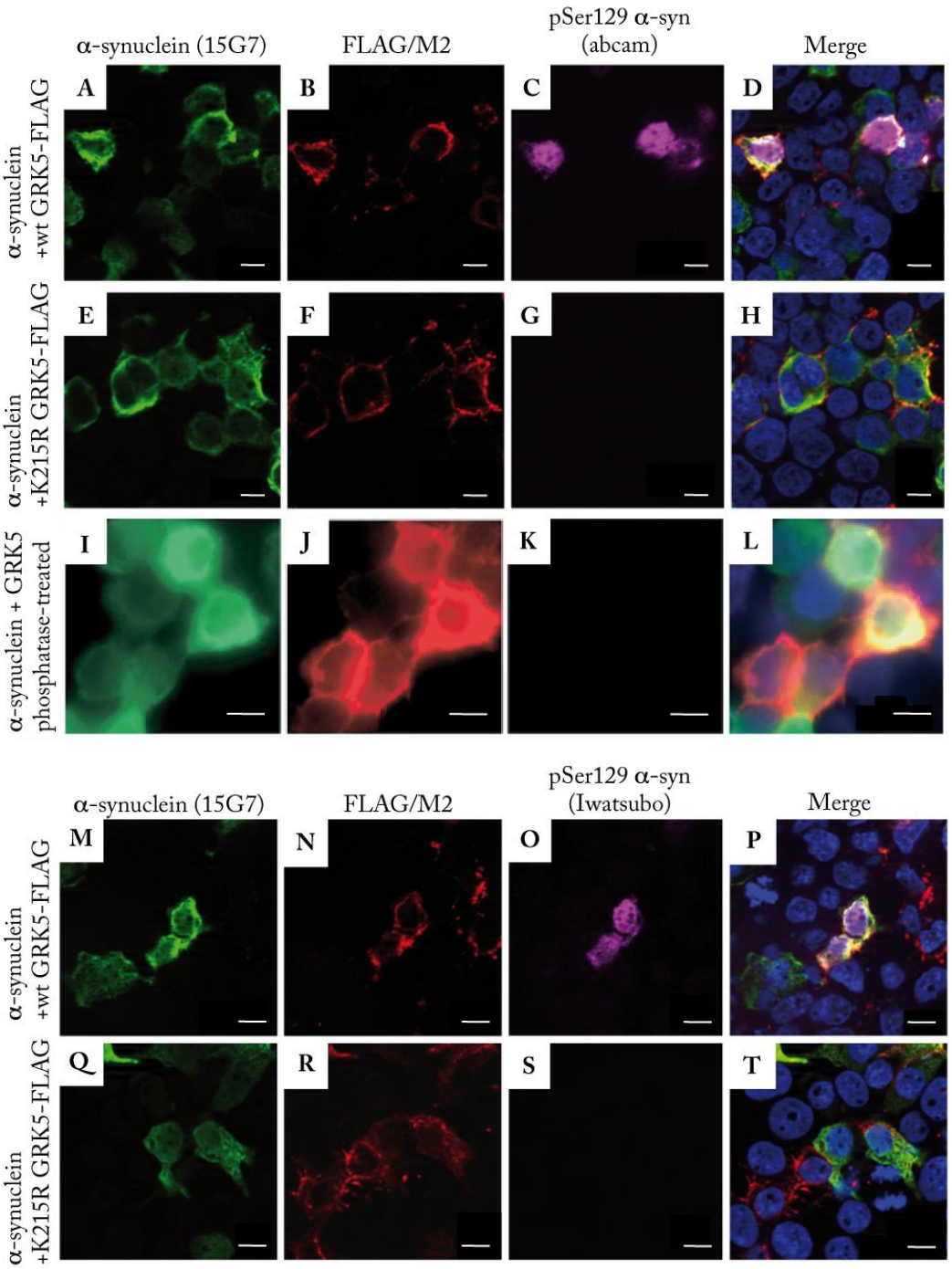

Figure 2.32 Nuclear pSer129 αSyn in HEK-cells cotransfected with αSyn and its kinase G protein-coupled receptor kinase 5 (GRK5) (modified from (Schell et al., 2009), generated by T. Hasegawa).

HEK293E cells were transiently transfected with plasmids encoding untagged wild-type αSyn together with either wild-type GRK5-FLAG (A–D, I–P) or kinase-dead [K215R]GRK5-FLAG (E–H, Q–T). After 2 days of incubation cells were fixed and triple-stained with rat anti-αSyn (green; A, E, I, M, Q), mouse anti-FLAG to visualize GRK5 (red; B, F, J, N, R) and rabbit monoclonal anti-PSer129 (pink; C, G, K) or rabbit polyclonal anti-PSer129 (pink; O, S). Note that both wild-type and mutant GRK5-FLAG are localised at the cell membrane while most of the total anti-αSyn signal is scattered throughout the cytosol. In contrast, the anti-PSer129 signal from both antibodies is enriched in the nucleus in a strictly GRK5 activity-dependent manner (C, G and O, S). Phosphatase treatment abolished the PSer129 signals (K). Merged images include Hoechst nuclear counterstains (blue; D, H, L, P, T). Scale bars in A-H and M-T correspond to 20 µm, scale bars in I-L correspond to 10 µm.

As specifity of nuclear pSer129 αSyn staining was confirmed with histology of αSyn transgenic brain tissue (Figure 2.30) and with immunofluorescent stainings of transfected cells (Figure 2.32), it was hypothesised that pSer129 αSyn or just the C-terminal part of αSyn containing the phosphorylated Ser129 could be tranlocated into the nucleus to influence / regulate transcription (Maroteaux et al., 1988, Goers et al., 2003, Kontopoulos et al., 2006). To verify this hypothesis, BS and Cx of young and old αSyn transgenic mice were isloated, fractionated in nuclear and cytoplasmatic fractions and subjected to western blotting with tricine gels (Novex) to identify small proteins to the size of 4 kD (Figure 2.33).

All cytoplasmatic fractions originating from both brain regions of young and old transgenic mice displayed the presence of monomeric pSer129 αSyn. Furthermore there was a high molecular smear visible in the fraction originating from the BS of old transgenic mice.

Nuclear fractions originating from cortices of young and old αSyn mice displayed weak bands at the hight of monomeric pSer129 αSyn. Nuclear BS fractions originating from old αSyn mice displayed weak signals for monomeric pSer129 αSyn and a high molecular smear. Nuclear BS fractions originating from young transgenic αSyn mice were pSer129 αSyn negative.

Detection of HSP90 in all nuclear fractions demonstrated a contamination of all this fractions with cytoplasma fraction. This finding points to the very probable cytoplasmatic origin of the pSer129 αSyn detected in nuclear fractions.

Nevertheless detection of this blots with the pSer129 αSyn specific antibody revealed no small fragments in any of the fractions of young and old transgenic animal tissue (Figure 2.33). Separation of the proteins received by these fractionations with the Wildfang-Blot system could not uncover any nuclear fraction specific pSer129 αSyn signals (data not shown).

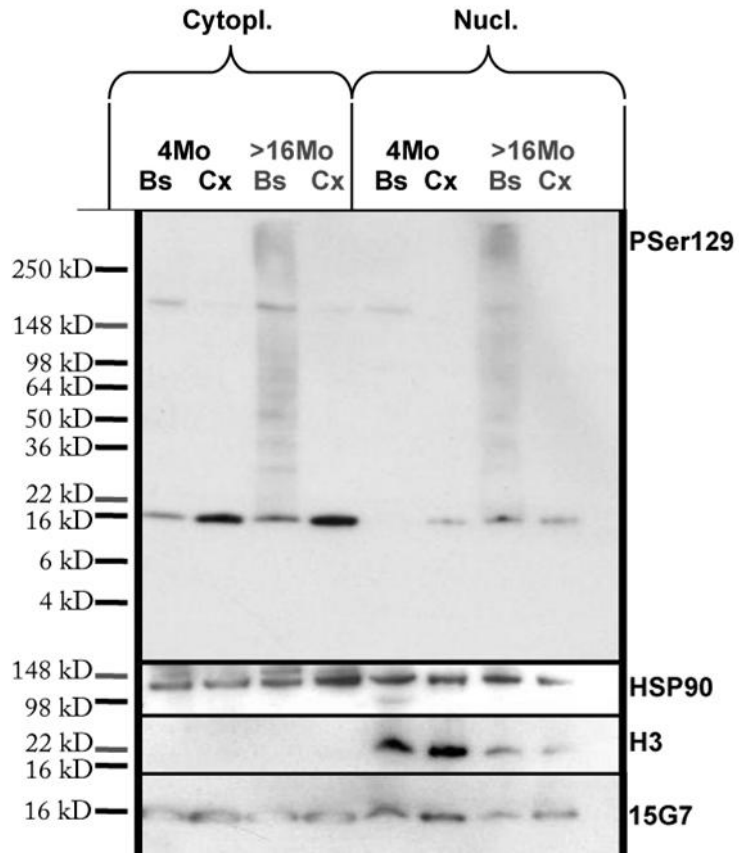

Figure 2.33 Investigation for nuclear pSer129 αSyn fragments in nuclear fractions isolated from brain stem and Cx of young and old αSyn transgenic mice.

Brain stem and Cx isolated from young mice and old, endstage, transgenic mice were subjected to nuclear fractionation and western blotting with tricine gels (Novex). Antibodies used were specific for pSer129 αSyn, transgenic human[A30P]αSyn (15G7), heat shock protein 90 (HSP90) as a cytoplasmatic marker and histone H3 as a marker for nuclear fractions. Detection with the pSer129 αSyn antibody displayed similar amounts of monomeric pSer129 αSyn in cytoplasm of young and old cortical neurons. Lysates isolated from cytoplasm of BS neurons of old transgenic mice contained in addition to the normal length pSer129 αSyn a high molecular smear which could not be detected in similar lysates of young transgenic mice. Signals detected in nuclear fractions resulted with high probability from a general contamination with the cytoplasmatic fraction (HSP90 signal). No small pSer129 αSyn fragments could be detected in any of the isolated fractions.

2.10 Phosphorylation of the Ser129 αSyn residue by Polo-Like-Kinase-2 and -3 in primary hippocampal neurons

Neurological diseases like Parkinson's disease (PD) or dementia with Lewy bodies (DLB) are characterized by the accumulation of pSer129 αSyn in neuronal bodies and dendrites (Kahle et al., 2001, Fujiwara et al., 2002, Anderson et al., 2006), therefore it is important to investigate which kinases and phosphatases are involved in this physiological and pathological modification process. This knowledge would help to advance the

development of adequate models to investigate the role of αSyn-Ser129 phosphorylation in survival and death of affected neurons as well as the development of synucleinopathy. Previously it was shown that the kinases Polo-like kinase-2 (PLK2) (Inglis et al., 2009) and PLK3 are involved in the *in vivo* Ser129 phosphorylation of αSyn in primary hippocampal neurons (Inglis et al., 2009, Mbefo et al., 2010) and Figure 2.34. In order to confirm this, primary hippocampal neurons were treated with PLK2 and PLK3 specific siRNA and stained for αSyn and pSer129 αSyn (Figure 2.34, (Mbefo et al., 2010)). Indeed, silencing of either PLK2 and PLK3 clearly decreased the pSer129 αSyn signal without having any effect on total αSyn levels.

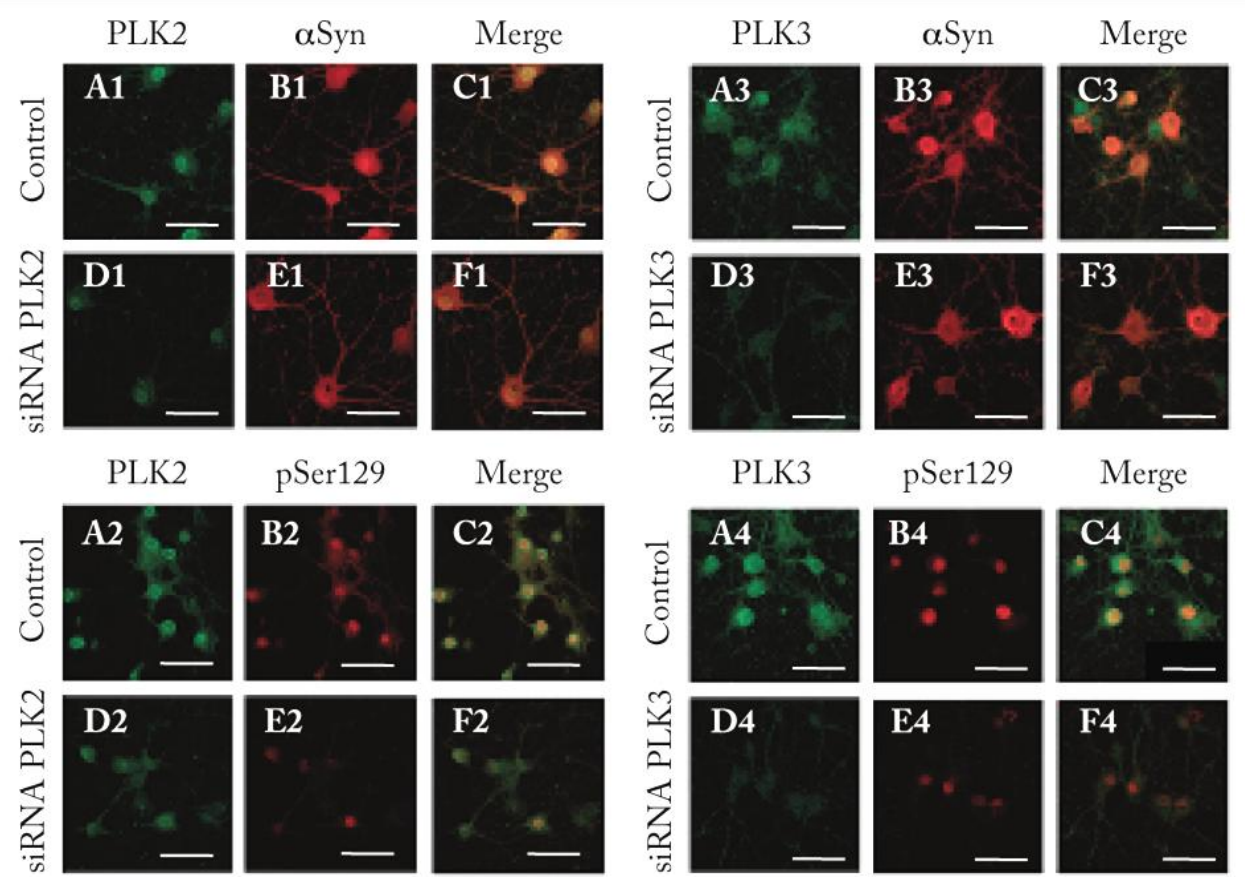

Figure 2.34 Silencing of PLK2 and PLK3 in primary hippocampal neurons and its effect on the phosphorylation of αSyn at the Ser129 residue (adopted from (Mbefo et al., 2010)).

Primary hippocampal neurons were treated with siRNA for PLK2 (D1-F1 and D2-F2) and PLK3 (D3-F3 and D4-F4), and colocalisation with αSyn (A1-C1 and A3-C3) and pSer129 αSyn (A2-C2 and A4-C4) was investigated. Silencing of PLK2 (D1-F1) and PLK3 (D3-F3) has no effect on neither αSyn levels nor its distribution in primary neurons, but absence of PLK2 as well as of PLK3, leads to a reduction of pSer129 αSyn levels (D2-F2 and D4-F4 respectively) in the same cell type. Scale bars correspond to 100 µm. (Figure originally produced and published by (Mbefo et al., 2010))

2.11 Colocalisation of αSyn and pSer129 αSyn with PLK2 and PLK3 in (Thy1)h[A30P]αSyn transgenic mice

Silencing of either PLK2 or PLK3 in primary hippocampal neurons lead to a clearly decreased phosphorylation of αSyn Ser129.

To assess a possible colocalisation of pSer129 αSyn with PLK2 and PLK3 in brains of αSyn transgenic mice, 4 µm serial sections of endstage αSyn mice were stained with pSer129 αSyn, PLK2 and PLK3 antibodies. Due to high unspecific background staining from high lipofuscin amounts in especially neurons of aged mice, performing of fluorescent stainings was avoided.

Staining of saggital sections showed a wide distribution of PLK2 and PLK3 throughout the brain, whereas both kinases were generally localised in the neurophil. Furthermore several neuronal subpopulations showed enriched somal stainings for PLK3 and nuclear staining patterns for PLK2. As shown in Figure 2.23, hippocampal sections of aged αSyn transgenic mice are highly positive for pSer129 αSyn in the CA1- and CA3-region, as well as in the dentate gyrus and subiculum (Figure 2.35 E). Interestingly subicular neuronal cell bodies were also positive for PLK3 (Figure 2.35 D). Neocortical staining showed somal and nuclear staining pattern with the pSer129 antibody (Figure 2.35 J). Stainings with both PLK2 antibodies resembeled the nuclear pSer129 positive stinings observed in the neocortex (Figure 2.35 G-H). Histological investigation with the PLK3 antibody showed mainly a neurophil staining pattern (Figure 2.35 I). The two findings that PLK2 tends to colocalise with pSer129 αSyn in neuronal nuclei and that PLK3 has a tendency to show a more neuritic distribution are consistent with the findings in primary hippocampal cultures (Figure 2.34). Investigation of possible colocalisation of pSer129 αSyn Lewy-like pathology with PLK2 or PLK3 in BS neurons, showed no specific staininig of the antibodies directed against the kinases (Figure 2.35 K-O). Neutralisation of PLK2 antibody reduced staining in the neuropil and in cell bodies (Figure 2.35 A, -F, and –K), confirming specificity of the staining.

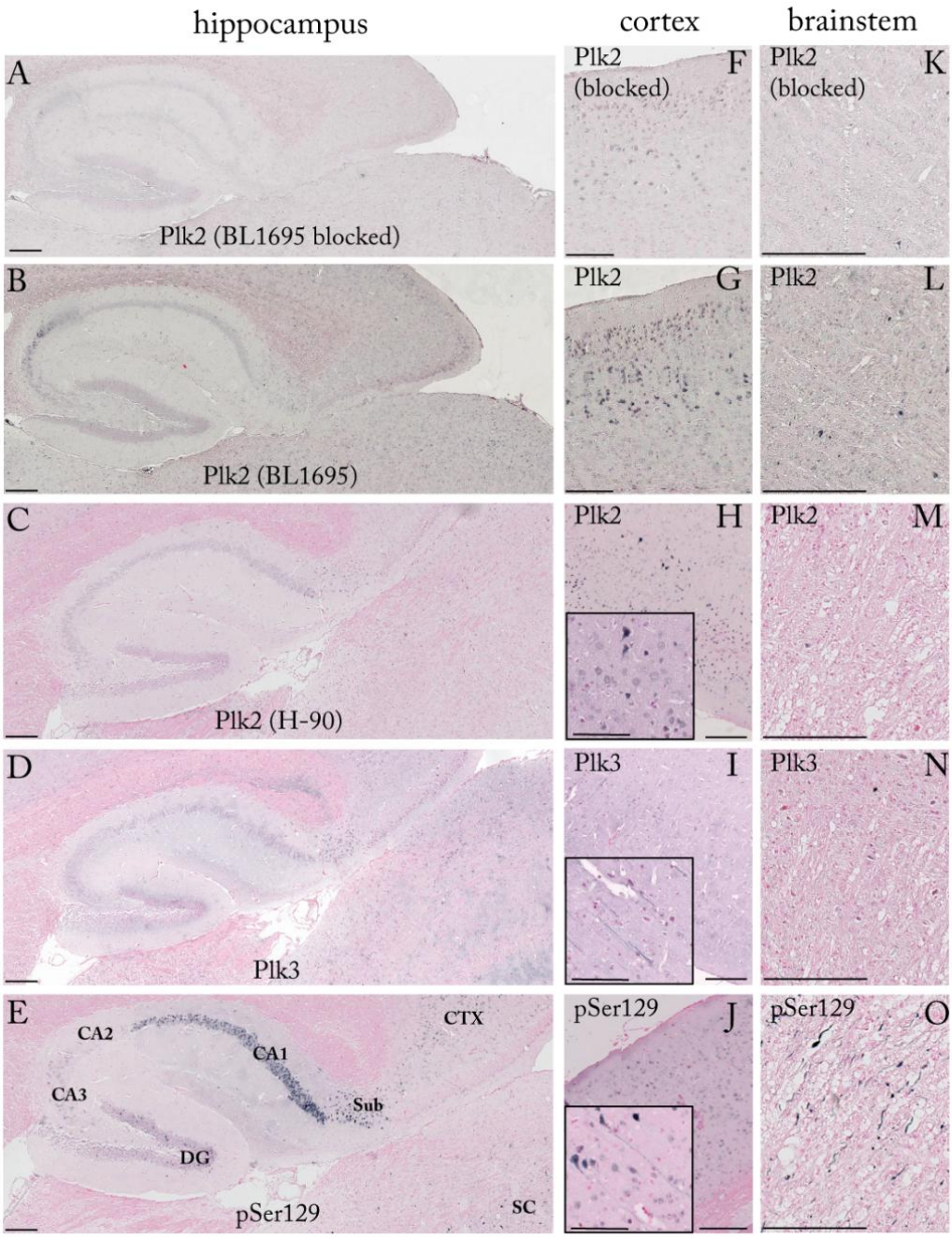

Figure 2.35 Colocalisation of pSer129 αSyn with PLK2 and PLK3 in aged transgenic (Thy1)h[A30P]αSyn mice (modified from Mbefo et al., 2010).

For µm thick serial paraffin sections of 12 months old αSyn transgenic mice were stained with a pSer129 αSyn antibody (E-O), two different PLK2 antibodies (B-M) and a PLK3 specific antibody (D-N). pSer129 αSyn (grey-/black staining) could be detected in hippocampal CA1-, CA2-, CA3- region, subiculum and the dentated gyrus (E). Furthermore BS sections contained Lewy pathology (O) and neuronal cellbodies in the neocortex were found to be positive for pSer129 αSyn (J). PLK3 stainings (grey staining) were localised more diffusely in the neurophil of hippocampal CA1-, CA3- and subicular neurons (D) as well as in neocortical neurons (I). In the BS no positive PLK3 staining could be detected (N). PLK2 stainings (grey-/black staining) were more prominent in nuclear region of neocortical neurons (G and H). Hippocampal staining pattern was weaker (B and C) than the staining observed with the PLK3 antibody (D). BS sections contained no PLK2 positive staininig (M and N). Specifity of staining was checked via a preabsorbtion of PLK2 antibodies with recombinant PLK2. Preabsorbed antibodies failed to stain any structures in the Hip (A), neocortex (F) and BS (K) confirming the specifity of the staining. All scale bars correspond to 200 µm.

2.12 Colocalisation of pSer129 αSyn with the polo-like-kinases-2 and -3 in brain regions involved in context and emotional learning

Next we investigated if PLK2 or PLK3 could be involved in the Ser129 phosphorylation of transgenic [A30P]αSyn which was detected in brain regions involved in context and emotional learning. 4 µm coronar paraffin sections of old transgenic mice containing Hip and amygdala were stained with antibodies against pSer129 αSyn, PLK2 and PLK3 to investigate intracellular colocalisation. Cytosolic pSer129 αSyn staining pattern of hippocampal CA1- and CA3-region was also observed after stainings with PLK2 antibodies, whereas CA3-region displayed a much stronger and the CA1-region a much weaker signal (Figure 2.36 A and –D respectively). Stainings with the PLK3 antibody displayed a neurophil staining pattern only in the CA3-region, while the rest of hippocampal tissue remained negative (Figure 2.36 G). Observation of the basolateral amygdala confirmed the "nuclear" staining pattern with the pSer129 αSyn antibody (Figure 2.36 B). Stainings with the PLK2 antibody displayed a very high colocalistion of PLK2 (Figure 2.36 E) with the pSer129 αSyn in BLA neurons (Figure 2.36 B). PLK3 stainings displayed positive signal in the neurophil of the BLA (Figure 2.36 H), similar to the staining already observed in cortical tissue (Figure 2.36 I). pSer129αSyn positive Lewy Neurite like staining of the central nucleus remained negative after staining with PLK2 and PLK3 specific antibodies (Figure 2.36 C, F and I respectively), reminding of the observations recorded after staining of BS tissue (Figure 2.35 K-O).

Taken together in CA1- and CA3-region of the Hip as well as in the basolateral amygdala, PLK2 tended to colocalise with pSer129 αSyn in nuclear regions of positive neurons, wheras PLK3 stainings remained restricted to the neurophil. This observation was consistent with the stainings of cortical tissue and with the findings in primary hippocampal cultures.

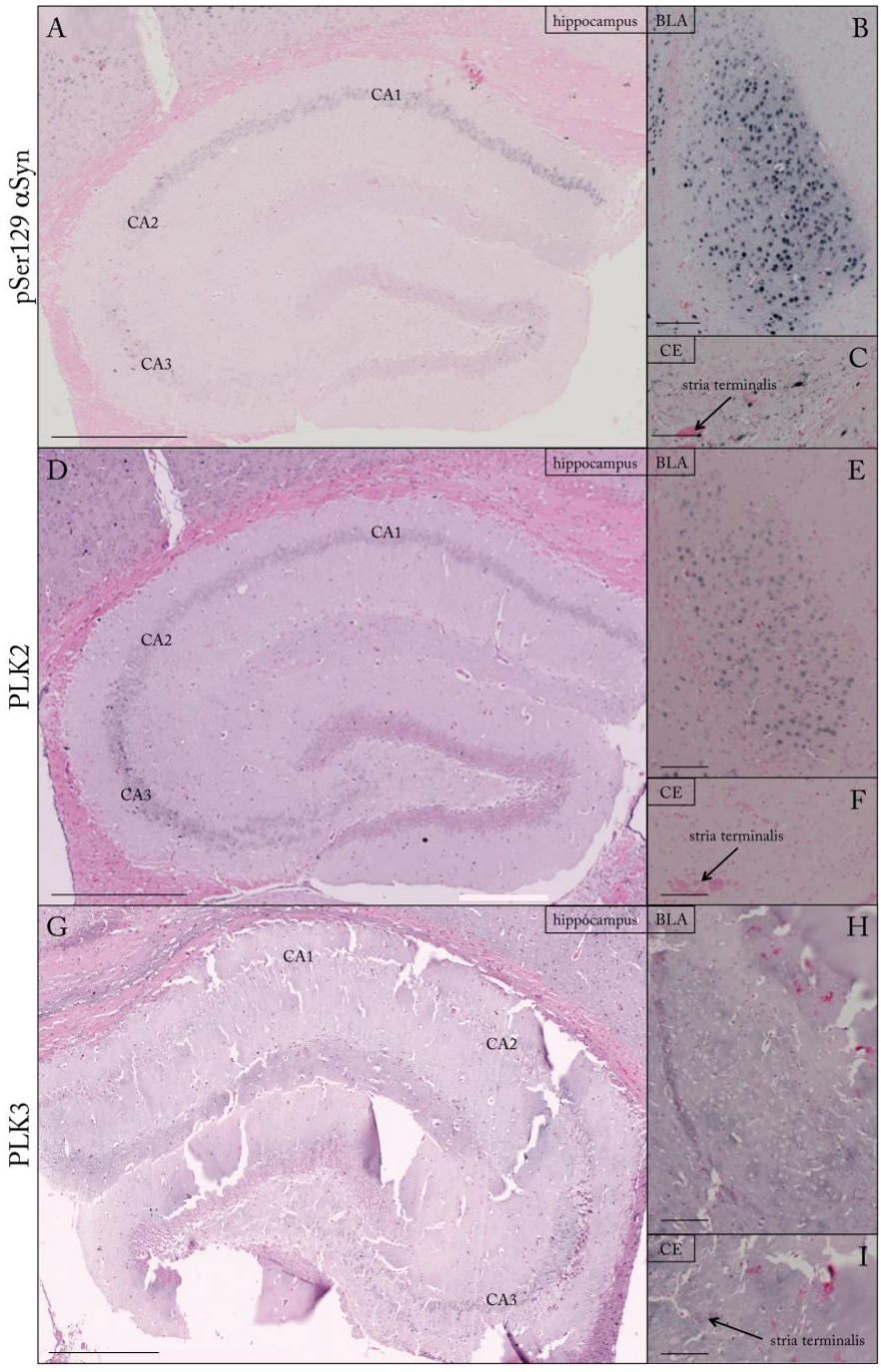

,

Figure 2.36 Colocalisation of pSer129 αSyn with PLK2 and PLK3 in Hip and amygdala of aged transgenic (Thy1)h[A30P]αSyn mice.

Four µm coronar sections of old [A30P]αSyn trangenic mice were stained with nuclear fast red and with antibodies specifically binding to pSer129 αSyn, PLK2 and PLK3 in order to identify intracellular colocalisation of pSer129 αSyn with its kinases PLK2 and PLK3 (grey-/black stainings). Hippocampal staining showed colocalisation of pSer129 αSyn and PLK2 in neuronal soma of hippocampal CA1- and CA3-region (A and D). PLK3 stainings displayed weak neurophil staining only in the CA3-region of the Hip (G). Neurons of the BLA display a very strong nuclear localised signal after staining with pSer129 αSyn antibodies (B). This signal colocalised with the signals visible after staining with PLK2 antibodies (E). Stainings with PLK3 specific antibodies displayed signal only in the neurophil (H). Central nucleus (CE) of the amygdala showed pSer129 αSyn positive, Lewy Neurite like stainings (C) reminiscent of the morphology of the structures visible in the BS. This region showed no positive stainings after staining with PLK2- and PLK3 specific antibodies (F and I respectively), again reminding of the results observed after stainings of the BS. Scale bars in A, D and G correspond to 200 µm and in B, C, E, F, H and I to 100 µm.

2.13 Reduced activation of BLA-neurons after Fear-Conditioning of aged and cognitively impaired (Thy1)h[A30P]αSyn transgenic mice

The synucleinopathy observed in the amygdaloid basolateral (BL) region and the central nucleus (Ce) of aged αSyn transgenic mice (Figure 2.30 G-H page 57) might have a negative influence on the activation of neurons in the BLA, and therefore negatively influence the learning relevant neuroplasticity in this brain region. Furthermore processed information leaving the BLA might not be transfered by the Ce due to presence of pSer129 αSyn in its neuronal branches (Figure 2.30 K-L page 57). To closer investigate this hypothesis, young and old αSyn transgenic mice, as well as old wt animals were involved in fear conditioning training and sacrificed 40 min to 60 min after the training. Brains were isolated, fixed in 4% PFA in PBS and used for histology. 4 µm brain sections were stained with an antibody directed against the immediate early protein FOS (Radulovic et al., 1998). As expected all conditioned animals, independent of transgene and age, had a higher amount of FOS positive signal in the BLA and interestingly also in the Ce (Figure 2.37 J-R), when compared with the unconditioned contrlol groups (Figure 2.37 A-I). Comparison between the different conditioned groups showed that conditioned aged transgenic mice (Figure 2.37 M-O) had a much lower activation of the BLA region after fear-conditioning, when compared to young transgenic animals (Figure 2.37 J-L), or old wt mice (Figure 2.37 P-R).

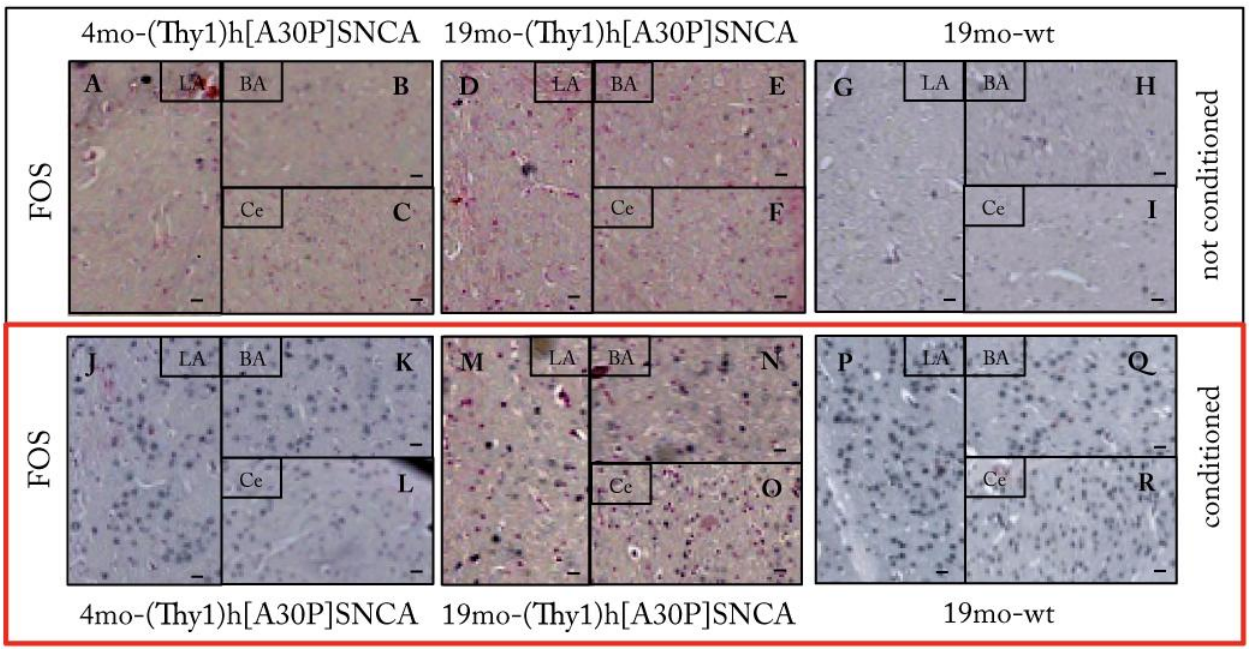

Figure 2.37 Expression of FOS protein in the emotional learning circuit after fear conditioning of αSyn transgenic and wt mice.

Animals were trained as described in chapter 2.4 and in the material and methods part. 40 - 60 min after training all animals were sacrificed. Staining with anti FOS antibody (grey-/black staining) revealed high number of positive BA- and LA-neurons in conditioned young SNCA-transgenic (J-L) and conditioned old wt mice (P-R) but not in conditioned old SNCA-transgenic mice (M-O). Control groups, independent of age and transgene, showed no particular positive FOS stainings in amygdala region (A-I). The red staining in all pictures represents the counterstaining with nuclear fast red. Scale bars correspond to 20 µm.

Quantification of FOS positive area in all animal groups was conducted with the stereoinvestigator software based on the quantification method described by B. F. Calvalieri. For each animal seven objectives, each containing one row with 3 sections, were included into the counting. First objective always contained the first parts of the BLA when cutting from the Ce to the olfactory bulb. Last objective always contained the last visible part of the BLA. Young transgenic animals and old wt mice had a significant increase of FOS positive signal after conditioning, whereas old αSyn transgenic mice displayed only a trend but not a significant increase after conditioning in both BLA (Figure 2.38 A) and in the Ce (Figure 2.38 B). Interestingly the increase of the FOS positive signal in the BLA of conditioned young transgenic mice is not as high as detected in BLA of old

wt mice. Conversely these groups show now difference in the elevation of FOS signal in the Ce (Figure 2.38 B).

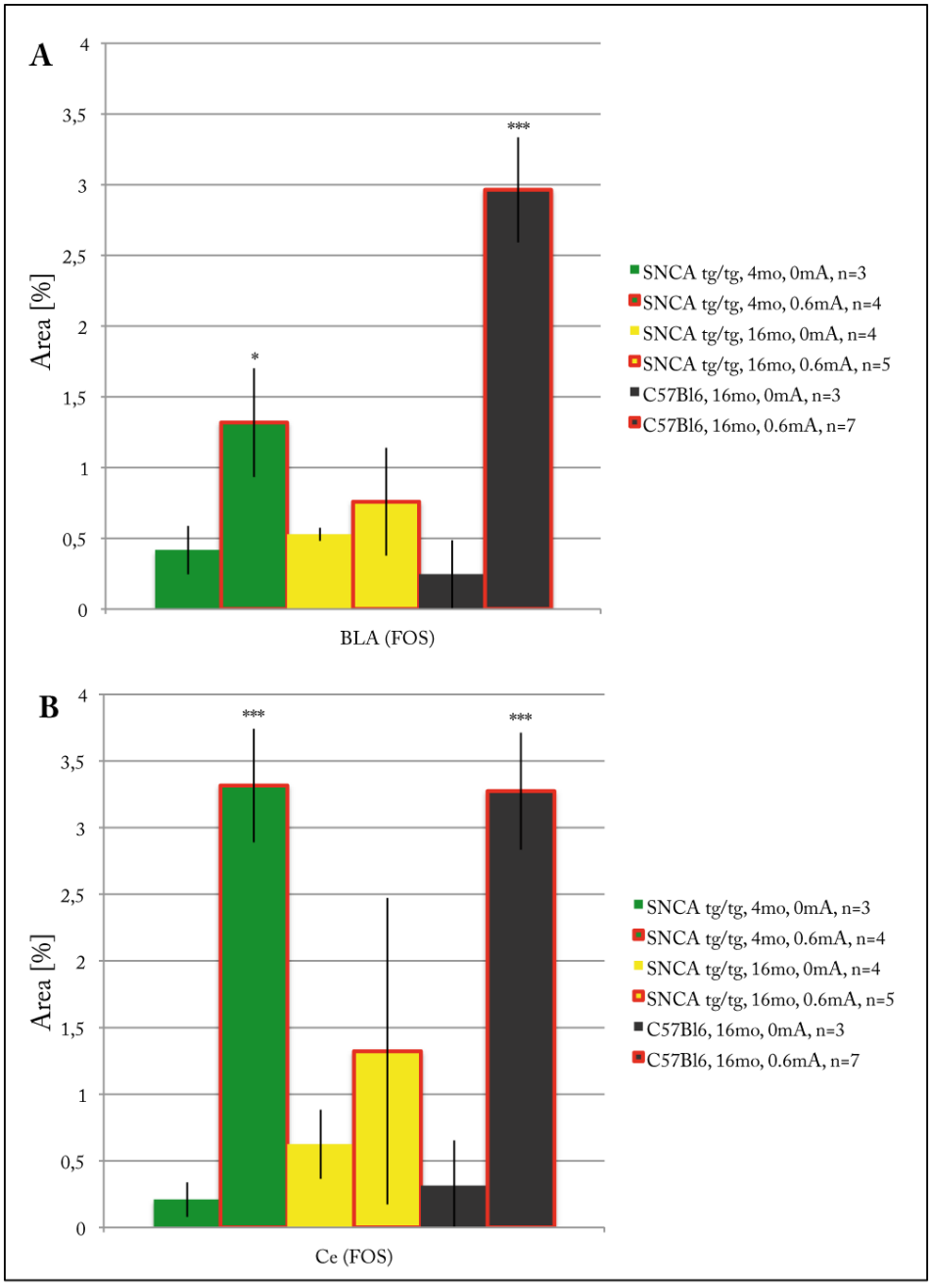

Figure 2.38 Quantification of expression of FOS protein in the emotional learning circuit after fear conditioning of αSyn transgenic and wt mice.

Percentage estimation of FOS positive area was conducted with the software stereoinvestigator based on the method described by B. F. Cavalieri. Results displayed a significant upregulation of FOS in the BLA (A) and Ce (B) of the amygdala in young transgenic (green bars with red line) and old wt mice (black bar with red line) when compared to the not conditioned control animals (green and black bar respectively). Old transgenic mice showed just the tendency to a higher number of FOS positive neurons after conditioning (yelow bars with red line in A and B), which remained not significant after compairing with the results obtained from old transgenic not conditioned controls (yellow bars in A and B). ***p<0.0001; *p<0.02

2.14 Absent upregulation of PLK2 in the Amygdala after Fear-Conditioning of old (Thy1)h[A30P]αSyn mice

It was shown that PLK2 signals colocalise with pSer129 αSyn signal in Cx (Figure 2.35 G-H and J respectively), BLA (Figure 2.36 E and B respectively), as well as in the subiculum (Figure 2.35 A-C and –E respectively). In addition it was found, that PLK2 is involved in homeostatic plasticity (Kauselmann et al., 1999, Pak et al., 2003, Seeburg et al., 2008a, Seeburg et al., 2008b) and therefore has an influence on learning. Therefore PLK2 stainings of amygdala containing coronar sections of all animals involved in the fear conditioning training (Figure 2.26, Figure 2.38, Figure 2.40) were also analysed. After fear conditioning training (Chapter 2.7), the brains were isolated and preparated as previously described (Chapter 2.11). Interestingly PLK2 signals detected in tissue of conditioned young transgenic and old wt mice were increased after training (Figure 2.39 J-L and P-R respectively), when compared to the results obtained from stainings of non-conditioned animals of the same groups (Figure 2.39 A-C and G-I respectively). Old αSyn transgenic animals on the other hand showed emotional learning deficits and displayed no increase in PLK2 signal intensity after conditioning (Figure 2.39 M-O) when compared to the non-conditioned control group (Figure 2.39 D-F).

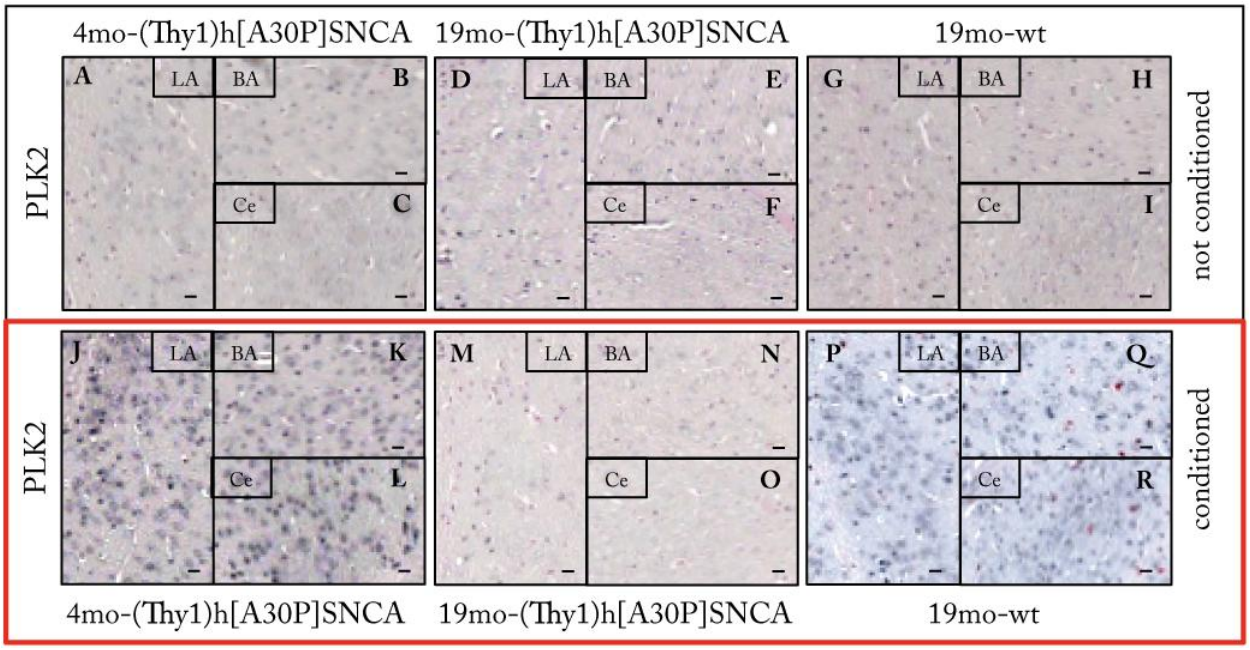

Figure 2.39 Expression of PLK2 (grey-/black staining) in the amygdala after fear conditioning of young αSyn transgenic, old αSyn transgenic and old wt mice.

Animals were trained as described in chapter 2.7 and in the material and methods part. 40 - 60 min after training all animals were sacrificed and brains were isolated and fixed in 4% PFA in PBS. Staining with anti PLK2 antibody (1:250) revealed a high number of positive BA- and LA-neurons in conditioned young SNCA-transgenic (J-L) and conditioned old wt mice (P-R) but not in conditioned old SNCA-transgenic mice (M-O). Control groups, inependent of age and transgene, showed a weak neuronal cytoplasmatic staining in amygdala region (A-I). Red color in all pictures represents nuclear fast red staining. Scale bars correspond to 20 µm.

Quantification of PLK2 positive areas in all animal groups was conducted as already described for FOS protein in chapter 2.13. Young αSyn transgenic (Figure 2.40 A and B, green bars) as well as wt mice (Figure 2.40 A and B, black bars) displayed a significant increase of PLK2 signal in the amygdaloid basolateral area (BL) and the central nucleus (Ce) (Figure 2.40 A and B, red surrounded green- and black- bars respectively). Interestingly the old αSyn transgenic animals, which showed defficites in emotional learning, displayed the tendency to a reduced PLK2 signal in BLA and CE after conditioning compared to non-conditioned control animals (Figure 2.40 A and B, red surrounded yellow bars).

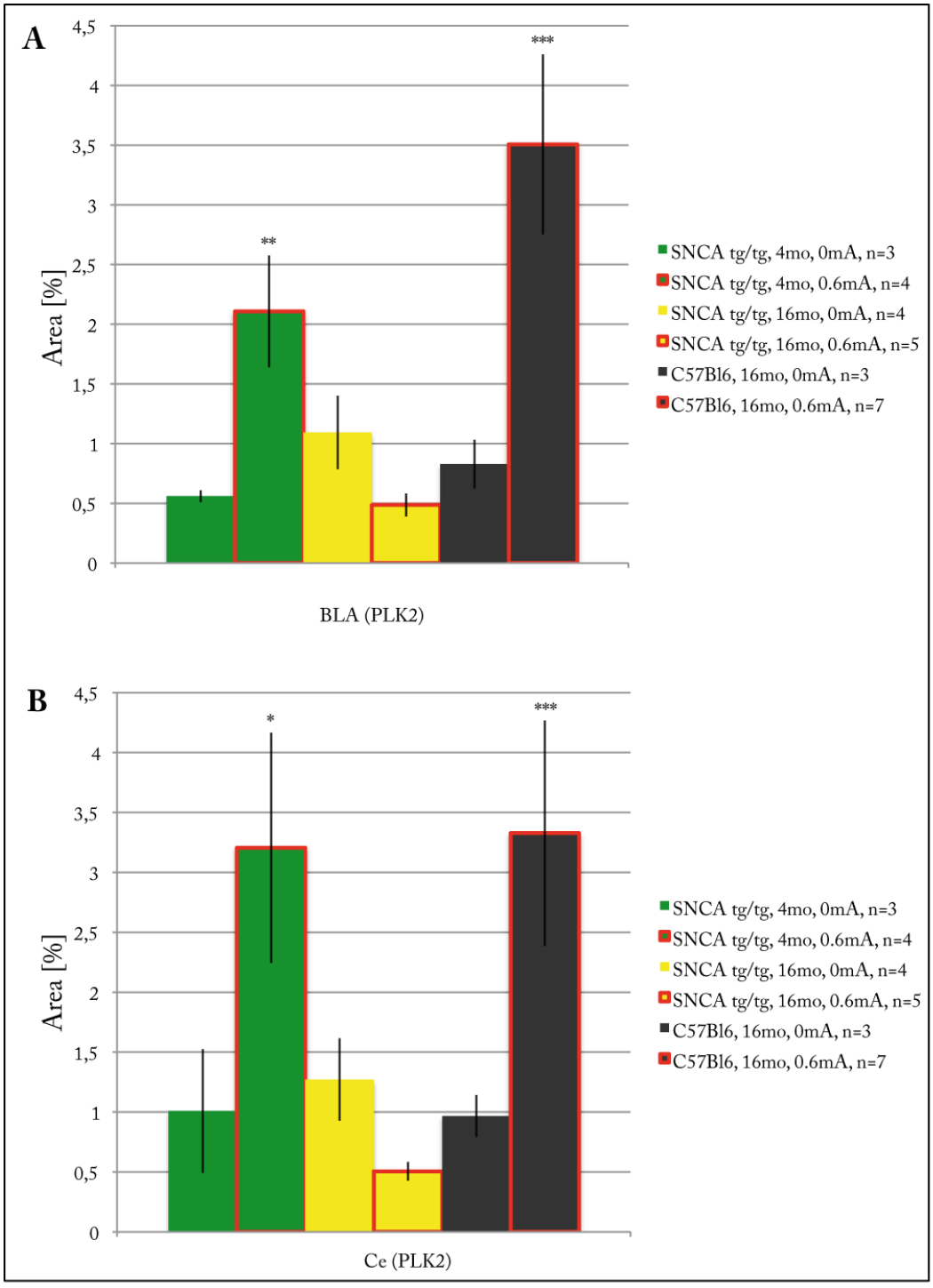

Figure 2.40 Quantification of PLK2 positive neurons in the amygdala after fear conditioning of young αSyn transgenic, old αSyn transgenic and old wt mice.

Percentage estimation of PLK2 positive area was conducted with the software stereoinvestigator based on the method described by B. F. Cavalieri. For each animal seven slides, each containing one row with 3 sections, were included into the counting. First slide always contained the first parts of the BLA when cutting from the Ce to the bulbus. Last slide always contained the last visible parts of the BLA respectively. Results show a significant higher percentage of PLK2 positive cells in the BLA (A) and Ce (B) in young αSyn transgenic (green bars with red line) and old wt mice (dark bars with red line) when compared to the not conditioned control animals (green and dark bars respectively). In contrast the quantity of PLK2 detectable in the same regions of old conditioned animals was not significantly increased (yellow bars in A and B). ***p<0.001; **p<0.01; *p<0.02

3 Discussion

Synucleinopathies like Parkinson's disease and dementia with Lewy bodies are neurological disorders of the elderly (Trenkwalder et al., 1995). Neuropathological characterisation of these diseases has revealed presence of Lewy bodies and Lewy neurites, which are intraneuronal inclusions mostly composed of αSyn fibrils (Spillantini et al., 1997, Arawaka et al., 1998, Takeda et al., 1998, Arai et al., 2000). αSyn itself is phosphorylated at Ser129 (Okochi et al., 2000). This posttranslational modification of αSyn, which is also observed in αSyn transgenic animal models (Kahle et al., 2002b, Neumann et al., 2002, Schell et al., 2009), is known as the pathological hallmark of neuropathological lesions in synucleinopathys (Fujiwara et al., 2002).

In this study a (Thy1)h[A30P]αSyn mouse model developing motorical impairment and impairment of fear conditioning learning (Freichel et al., 2007, Schell et al., 2009) was used to investigate correlations between emerging synucleinopathy, amyloidosis, as well as Gallyas silverstaininig positive pathology and functional deficiency of different neurologic systems (e.g. the motoric system or the emotional learning circuit). Main focus of attention was laied on the correlation of detectable pathology with functional deficiency of the Hip and the amygdala, the regions involved in context- and emotional learning.

Staining of saggital brain sections revealed diverse pSer129 αSyn staining patterns, which partially colocalised with positive ThS and Gallyas silver staining. General pSer129 αSyn immunoreactivity increased with age in all positive brain regions of (Thy1)h[A30P]αSyn transgenic mice. pSer129 αSyn positive Lewy Bodies and Lewy Neurites were observed in BS and MB of old transgenic mice with motoric impairment, whereas BS and MB of motorically not affected young transgenic mice only showed weak somal stainings of few cells. Investigation of amyloidosis and Gallyas silver staining pathology in

these brain regions showed highly positive brain stem and MB staining of old transgenic mice and, as expected, no positive staining in brain tissue of healthy, young transgenic and wild type mice.

Interestingly cortical and hippocampal areas, as well as basolateral amygdala (BLA) nuclei displayed a somal and nuclear pSer129 αSyn immunoreactivity in old transgenic mice. This was also present in a weaker staining pattern also in young, pre-symptomatic mice, but not in wild type controls. Investigation of amyloidosis and pathological Gallyas silver staining were found to be negative in these brain regions. Furthermore, to confirm that pSer129 αSyn tends to accumulate in the nucleus, cell culture experiments were performed, in which this finding could be assessed.

Another finding in the fear conditioning learning impaired (Thy1)h[A30P] αSyn transgenic mice was the identification of age-dependent neuritic-terminal pSer129 αSyn pathology in the medial parts of the central amygdala (CeM) and in one of its projection areas, the lateral hypothalamus (LH). Unlike the ThS-positive Lewy-like neuropathology detected in the BS of old transgenic mice, neuropathology detected in CeM and the LH was found to be ThS-negative.

As Ser129 αSyn phosphorylation seems to be the main posttranslational modification of αSyn in human synucleionopathies as well as in αSyn transgenic animal models, a main interest was the identification of natural kinases and phosphatases regulating αSyn phosphorylation. In this work it was shown, that αSyn can be phosphorylated by GRK5 in HEK293E cells where it shows nuclear accumulation. Recent works showed that Polo-like-kinases (PLKs), which are known to be involved in the regulation of the cell cycle (Barr et al., 2004, Dai, 2005, Xie et al., 2005, van de Weerdt et al., 2006), are phosphorylating αSyn *in vivo* (Inglis et al., 2009, Mbefo et al., 2010). In this work histological investigation of [A30P]αSyn transgenic mouse brain tissue revealed, that PLK2 might be involved in the pathologic Ser129 phosphorylation of αSyn associated to the nucleus, whereas PLK3

colocalises with pSer129 αSyn detected in the neurophil (Mbefo et al., 2010). This observation was prominent in cortical areas and the BLA, regions which are involved in synaptic plasticity. Accordingly this finding could be confirmed also with cell culture experiments of primary hippocampal neurons in which PLK2 and PLK3 specifically colocalised with pSer129 αSyn in various subcellular compartiments (e.g. cytoplasm, nucleus and membranes) (Mbefo et al., 2010).

Taken together, αSyn becomes phosphorylated at its Ser129 residue in distinct parts of the brain of (Thy1)h[A30P]αSyn mice. Animals with motoric deficits show an age- dependent formation of Lewy like pathology with classical amyloidosis and silver positive stainings in the BS and MB. Only in those mice impaired in fear learning, pSer129 αSyn positive Lewy like pathology could be detected in the CeM, as well as in one of its projection areas, the LH. Notably, although Freichel et al. detected silver staining pathology in these regions (Freichel et al., 2007), none of these regions contained signs of amyloidosis. In these affected animals the cortical areas and the BLA, which are involved in neuroplasticity, showed an age-dependent increase of nuclear pSer129 αSyn (Schell et al., 2009). Ser129 phosphorylated αSyn was specifically correlated with the localisation of PLK2, which was shown to phosphorylate αSyn *in vitro* and *in vivo* (Inglis et al., 2009, Mbefo et al., 2010). Furthermore it has been shown that levels of PLK2 are significantly increased in brains of Lewy body- and Alzheimers disease patients (Mbefo et al., 2010).

These results suggest a necessity for further studies on the development of synucleinopathys and the correlation of their different stages (e.g. pSer129 αSyn phosphorylation with or without amyloidosis and pathologic silver staining) with neuro-cellular misfunction and resulting neurosystemic failures. Furthermore it is important to elucidate the role of interactions between PLK2 and αSyn in normal biology, as well as their involvement in Parkinson’s disease and other synucleinopathys.

3.1 Expression of human [A30P] αSynuclein (αSyn) in the mouse under control of the CNS neuron-specific Thy1 promoter: biochemistry of synucleinopathy in a model organism

A prominent feature of the Thy1-αSyn-mouse-models has been shown to be the formation of somatodendritic accumulations of detergent insoluble αSyn in the spinal cord and throughout the brain (Kahle et al., 2000, van der Putten et al., 2000, Kahle et al., 2001, Rockenstein et al., 2002, Maskri et al., 2004).

The (Thy1)h[A30P]αSyn mice used in this study displayed already in young age the formation of insoluble αSyn in a variaty of brain regions e.g. BS, cerebellum (Ce) and Cx (Cx). Interestingly, detected amounts of insoluble protein were different in the investigated brain regions and cortical lysates displayed the highest amounts of insoluble αSyn in young transgenic mice. Nevertheless the presence of insoluble αSyn is not associated with any severe phenotype in the Thy1h[A30P]αSyn mice (Neumann et al., 2002). This observation is consistent with the finding that detergent-insoluble αSyn clinically does not correlate with measured parameters of Lewy-Body (LB) dementia patients (Klucken et al., 2006). Furthermore the amounts of insoluble protein did not increase in an age-dependent manner in cortical brain regions, as there was no clear difference in amounts of insoluble cortical synuclein between young and old transgenic mice. The same observation was true for lysates isolated from cerebellar tissue, although the amount of isolated insoluble αSyn protein was low in both young and aged transgenic mice. Solubility assays of BS isolated from both age groups displayed different results. Interestingly, despite the presence of overexpressed, monomeric αSyn in all investigated brain regions, only the lysates from BS isolated from old transgenic mice contained high molecular αSyn species. Sarcosyl BS extracts, which contain fibrillar and amyloid proteins, displayed positive αSyn signals only on the high molecular level and only in extracts isolated from old transgenic animals. The acquired fibrillar amyloid conformation of αSyn was confirmed by stainings with the

congophilic marker Thioflavine-S (ThS). These observations are consistent with results from other studies which could additionally demonstrate the proteinase K resistance of the BS amyloid αSyn in old transgenic mice (Neumann et al., 2002). Furthermore, it could be shown that the appearance of these αSyn species coincides not only with the appearence of pSer129 αSyn positive Lewy Bodies and Lewy Neurites but also with the appearence of the pSer129 αSyn high molecular smear in lysates isolated from BS of old transgenic mice. Moreover it could be shown that the presence of pathologic pSer129 αSyn (Okochi et al., 2000, Fujiwara et al., 2002) coincides with the arise of oxidated and ubiquitinylated forms of αSyn (Neumann et al., 2002). Thus the fibrillisation of αSyn occurs together with biochemical modifications of the protein, develops in an age- dependent manner and is brain region specific. Cerebellar and cortical tissue are not affected by this type of synucleinopathy, although transgenic as well as Ser129 phosphorylated αSyn are detectable in an age-dependent manner in these brain regions.

Interestingly only cortical sarcosyl extracts from aged transgenic animals contained an αSyn form, that was not detectable in extracts from young transgenic mice. Histological investigation of cortical tissue isolated from aged transgenic mice with pSer129 αSyn antibodies showed numerous cells displaying somal, nuclear and weak neuritic staining patterns. In contrast, the staining pattern observed in tissue isolated from young transgenic mice was much weaker and less prominent for nuclear pSer129 αSyn staining. These observations confirm that the neuronal responses to the stress induced by αSyn overexpression are neuron- and brain region specific and therefore result in different forms of synucleinopathy. These differing synucleinopathy forms have different effects on the function of affected neurons and therefore also on the function of the affected brain regions.

3.2 Ser129-phosphorylation of αSyn: Cellular distribution and kinases involved in phosphorylation process

The phosphorylation of the Ser129 residue in αSyn (Okochi et al., 2000) is the proteinbiochemical modulation, which is present in all neurodegenerative diseases in which αSyn is involved (synucleinopathys) (Fujiwara et al., 2002). The animal model used in this work displays presence of pSer129 αSyn in numerous brain regions in which overexpression of the [A30P]αSyn transgene was confirmed (Kahle et al., 2001, Neumann et al., 2002). In most of the pSer129 αSyn positive brain regions an age-dependent increasing of intensitiy of the pSer129 αSyn staining was observed. At the same time formation of age-dependent neuropathological structures (Lewy Bodies and Lewy Neurites) could be observed in histological pSer129 αSyn stainings of the amygdaloid central nucleus and at a later point of time of the BS. This observations could also be confirmed on the proteinbiochemical level with western blot and solubility assays with BS tissue isolated from different aged transgenic mice.

Interestingly some brain regions, although overexpressing the transgene, Ce, Cx, Hip and the basolateral amygdala, did not show the severe age-dependent formation of Lewy pathology and amyloidosis, which was observed in the BS of old transgenic mice. In Cx, hippocampal CA1 and especially in the basolateral amygdala (BLA) the only age dependant change was a weak increase in the intensity of the pSer129 αSyn staining. Furthermore, this brain region showed a unique nuclear pSer129 αSyn staining, which was already present in young transgenic animals, which did not suffer from any obvious neuronal deficits, e.g. motoric coordination, emotional- and spacial-, or context-learning, but already displayed a worse performance in context and emotional learning when compared to wild type mice. This staining was confirmed with two different antibodies and could be diminshed by phospatase treatment, confirming the specifity of the immunoreaction. Furthermore, this staining pattern was also desribed in a [A53T]αSyn mouse model that overexpresses the transgene under control of

the rat tyrosine hydroxylase promotor (Wakamatsu et al., 2007). In this animal model the phosphorylation of αSyn at the Ser129 residue was assigned to casein kinase 2 (CK2), and could be demonstrated by colocalisation of CK2 with αSyn in neurons. *In vitro* studies previously have shown that the Ser129 αSyn is phosphorylated by CK2 (Okochi et al., 2000, Ishii et al., 2007, Waxman et al., 2008). In this work HEK293E cells were cotransfected with αSyn and its kinase GRK5 (Arawaka et al., 2006). Although αSyn was scattered throughout the cytosol and GRK5 was localised to the plasma membrane, detected pSer129 αSyn was localised in the nucleus. Cells transfected with the kinase dead GRK5 were lacking pSer129 αSyn positive signals.

As high levels of nuclear pSer129 αSyn were present in areas with high plasticity, e.g. BLA, Cx and Hip (all areas with high neuronal plasticity) of both young transgenic and aged impaired transgenic mice, a transcriptional regulation of neurotransmission was hypothesised for pSer129 αSyn. Perhaps is pSer129 αSyn or only the c-terminal cleaved part of the protein translocated into the nucleus, where it interacts with histones, influences their acetylation and therefore modulates neurotoxicity (Goers et al., 2003, Kontopoulos et al., 2006).

To closer investigate this hypothesis cytoplasm-nuclear fractionations were performed with tissue from both young and old transgenic mice. The used tissue originated from BS, which does not contain neurons with nuclear pSer129 αSyn and from Cx, which contains numerous neurons with pSer129 αSyn. Unfortunately these experiments could not reveal a nuclear fraction specific αSyn form. However solubility assays performed with BS, Ce and Cx from young and aged transgenic mice, displayed an αSyn form which was present only in amyloid fractions of the Ce of aged transgenic mice.

A recent study showed that PLK2 is involved in the *in vivo* phosphorylation of αSyn at the Ser129 residue (Inglis et al., 2009). PLK2 knock out mice displayed a 70% reduced Ser129 αSyn phosphorylation suggesting that

especially this kinase must have a crucial effect on the posttranslational modulation of αSyn. Experiments where PLK2 and PLK3 were silenced in primary hippocampal neurons could show an inhibition of Ser129 αSyn phosphorylation (Mbefo et al., 2010). The same study could show that levels of PLK2 were increased in Alzheimer disease and Lewy body disease patients. In the transgenic mice used in this work colocalisation of PLK2 and PLK3 with αSyn could be observed in the Hip, subiculum, Cx and the BLA, which is in all regions with neuronal plasticity. PLK3 stainings were only visible in the neuropil, but PLK2 stainings displayed similar close intracellular localisation as the pSer129 αSyn stainings. Especially in the BLA, the neuroplastical region of the amygdala, PLK2 stainings nearly showed an identical nuclear staining pattern as detected with the pSer129 αSyn antibodies. This finding is very interesting as it is confirmed that PLK2 and PLK3 take part in the dendritic spine remodeling, homeostasis and synaptic plasticity (Kauselmann et al., 1999, Seeburg et al., 2005, Seeburg et al., 2008b) and therefore are expressed in response to synaptic activation. Another study could show that PLK2 is crucial for neuronal differentiation (Draghetti et al., 2009). Taken together these results show that PLK2 does not only play a key role in the modulation of synucleinopathy by phosphorylating αSyn at the Ser129 residue, but also possibly play a key role in learning related neuroplasticity. Therefore learning related PLK2 and PLK3 expression were checked in the amygdala of healthy young transgenic and aged emotional learning impaired transgenic mice. This issue will be discused in chapter 3.4.

3.3 Neuropathology and impairment of different neural systems affected by synucleinopathy

There are differences concerning the onset of functional impairment of different neuronal systems in the (Thy1)h[A30P]αSyn mice (Freichel et al., 2007) e.g. functional deficits of the emotional learning are already measurable as early as the age of 12 months, whereas onset of motorical impairment is detected at a much higher age (18-22 months). Due to this different onset time points of malfunction in the different neuronal systems, it was important to investigate the neuropathology in the brain regions related to the misfunction and to compare them to brain regions that do not develop any obvious misfunction althoug having a similar [A30P]αSyn transgene overexpression.

3.3.1 Context and emotional learning system neuropathology and disfunction

Investigation of human brain material made clear that the cental amygdaloid nucleus is a predilection site for α-Synucleinopathy (Braak et al., 1994, Marui et al., 2002). Furthermore clinical manifestations of non-demented Parkinson's disease patients could be correlated to αSyn pathology in subnuclei of the amygdala (Harding et al., 2002). 30% - 60% of demented PD and Alzheimer's disease patients suffer from αSyn lesions in the amygdala (Hamilton, 2000, Mikolaenko et al., 2005) which is more severely affected in α-Synucleinopathy patients (Braak et al., 1994, Marui et al., 2002, Zaccai et al., 2008).

At an age of 12 months cognitive impairment was the earliest measured disorder in the animal model used in this work. Animals affected displayed reduced performence in the Morris water maze, the active avoidence and the fear conditioning task (Freichel et al., 2007). In this work the age-dependent impairment of contextual- and fear-conditioned learning could be confirmed (Schell et al., 2009).

It is known that a functional amygdala is crucial for a functional emotional learning (LeDoux, 2000, Maren, 2001, Holahan et al., 2004). Neuropathological investigation of this brain region in young and old transgenic animals displayed an age-dependent increase of intesity of the staining for the overexpressed [A30P]αSyn in several parts of the fear conditioning system. Most prominent were the basolateral amygdala, the key region for amygdaloid neuroplasticity and the lateral hypothalamus, which connects the amygdala to the hormonal system (LeDoux et al., 1988) and represents the main output region of the amygdala (Killcross et al., 1997, Goosens et al., 2001). Immunostainings with pSer129 αSyn specific antibodies displayed numerous intensive and age-dependent stainings in neuronal nuclei of the BLA. Furthermore only in aged cognitively impaired animals the medial central amygdaloid nucleus (CeM) displayed pSer129 αSyn lesions resembling dystrophic neurites and axon terminals. Similar structures were found in the CeM of human dementia with Lewy bodies (DLB) patients (Iseki et al., 2005). Interestingly the detected pSer129 αSyn pathology in the CeM of aged transgenic mice did not correlate with amyloidosis. This finding together with the fact that the neuropathology in the CeM of aged transgenic mice comes along with functional impairment in a early point of life in the transgenic mice, point to the induction of a negative effect of the CeM synucleinopathy on the function of affected neurons in the CeM (LeDoux et al., 1988, Rizvi et al., 1991). An other study used the induction of the immediate early gene product cFos as a marker of activation of neurons, in order to demonstrate the involvement of the CeM in the classical fear conditioning (Radulovic et al., 1998). The classic fear conditioning was used in this work to investigate the possible lower neuronal activation of CeM neurons in 12 months old cogntively impaired αSyn transgenic mice.

In addition to the detected impairment in emotional lerning, old transgenic mice also displayed a significantly reduced contextual fear learning. It is known that this type of learning requires a functional Hip and amygdala

(Killcross et al., 1997, Goosens et al., 2001). Therefore hippocampal tissue of young and old transgenic animals was also included in the neuropathological and histological investigations. Stainings with pSer129 αSyn antibodies displayed positive signals in the hippocampal subiculum, CA1, CA3 region and the dentate gyrus in both young and old transgenic mice and to a simmilar extent. Remarkable was the nuclear pSer129 αSyn staining of neurons in CA1 and CA3 regions of both young and old transgenic mice. In both age groups no pathologic silver positive staining or amyloid ThS positive staining could be observed. Stainings with the 15G7 antibody, which specifically recognizes the transgenic human αSyn, displayed the main difference between the healthy young transgenic mice and the impaired old transgenic mice. Only hippocampi of old transgenic animals displayed αSyn positive stainings in the synaptical region of CA1 and CA3. This αSyn was not phosphorylated and could also not be visualised with ThS stainings. It is known that presynaptic accumulation of αSyn has a negative effect on neuronal transmission (Kramer et al., 2007) and that hippocampal CA1 and CA3 regions are important for episodic memory (Langston et al., 2010), which itself is the basic for a functional long term memory. Furthermore it was shown that the hippocampal CA1 and the subiculum, which both were positive for pSer129 αSyn, are undergoing long term potentiation (O'Mara et al., 2000, Behr et al., 2009). Young transgenic animals displayed a similar pSer129 αSyn staining in the CA1 and subiculum but did not have the CA1/CA3-synaptical [A30P]αSyn. Assuming that the episodic memory is impaired in aged αSyn transgenic mice due to the CA1/CA3-synaptic [A30P]αSyn, it would explain why the contextual long term memory is impaired in these animals. However this finding may not have to be the only reason for the measured contextual impairment. The amygdala pathology identified in affected old transgenic animals might also contribute to this measured effect (Tsoory et al., 2008). Nevertheless this observation shows again the neuronal and brain region specific answer to the stress induced by αSyn overexpression.

3.3.2 Motoric system neuropathology and disfunction

Prior to the development of the MB and BS synucleinopathy related endstage (Neumann et al., 2002), the animals used in this work display motorical impairment measurable on the rotarod (Freichel et al., 2007) at an age of 16 months – 22 months. Only the BS and the MB of aged endstage animals displayed pSer129 αSyn positive somal inclusions, neuritic profiles and spheroids (Kahle et al., 2001, Neumann et al., 2002, Schell et al., 2009). Furthermore amyloidosis and silver staining positive neuropathology could be confirmed with ThS and Gallyas silver staining. Interestingly, although ThS positive Lewy neurites were detected in neuronal branches, the majority of ThS signals were localised in the soma. The majority of silver staining positive signals were localised into neurites. This finding stands in contrast to the finding in glomerular olfactory bulb, where both ThS positive staining and silver positive stainings were localised in the soma of glomerular cells. Interestingly cerebellar tissue, although displaying robust expression of the transgene (Freichel et al., 2007), did not show the severe synucleinopathy observed in the MB and BS of aged transgenic mice. Other groups have also observed detergent insoluble αSyn in somatodendritic acumulations in mice overexpressing wt αSyn, [A30P]αSyn and [A53T]αSyn under control of the Thy1 (Kahle et al., 2000, van der Putten et al., 2000, Kahle et al., 2001, Rockenstein et al., 2002, Maskri et al., 2004). The (Thy1)-[A53T]αSyn animals employed by Van der Putten et al. died prematurely due to the development of a rapid motoric deterioration. This effect was ascribed to degeneration of neuromuscular junctions. Other lines of (Thy1) [wt]αSyn mice, displayed early and progressive sensorimotoric aberations in a beam walking test already at an age of 4 – 6 months (Fleming et al., 2004).

3.3.3 Olfactory system neuropathology and disfunction

The olfactory system is among the first neuronal systems affected by Lewy body pathology in humans (Braak et al., 2003, Kranick et al., 2008). Therefore in this work immunohistological and neuropathological stainings

were also performed with olfactory bulb tissue from young and old transgenic animals. Immunostainings of transgenic, overexpressed αSyn displayed strong signals in the cytoplasm of glomerular neurons of the olfactory bulb. Thereby the signal intensity increased in an age-dependent manner. Stainings with Pser129 αSyn specific antibodies displayed simmilar results. Investigation of amyloidosis with ThS displayed positive neurons in glomerular region only in aged transgenic mice. In contrast to the stainings observed in the BS and MB of old transgenic and motoricaly impaired mice, where the majority of the observed signals was present in neurite like structures, pathologic silverstaining of the olfactory bulb interestingly only stained neuronal somata and only in aged transgenic mice. In an other study a mouse model was used expressing the human wt αSyn under control of the Thy1 promoter (Fleming et al., 2008). Included animals displayed olfactory impairments in three different testing paradigms already at an age of 9 months. Furthermore proteinase K resistant inclusions were found throughout the olfactory bulb. Therefore it would be intersting to confirm a very probable impairment of olfaction also in the (Thy1)h[A30P]αSyn animals used in this work and to detect the age of onset of the olfaction deficite in correlation to the neuropathology.

3.4 Expression of c-Fos after fear conditioning induced activation of the amygdala in young and old [A30P]αSyn transgenic mice: Involvement of PLK2 and PLK3

Radulovic and colleagues used the induction of the immediate early gene Fos to demonstrate the involvement of the amydaloid central nucleus (Ce) in the classical fear conditioning (Radulovic et al., 1998). This method was employed in this work to investigate the effect of the observed synucleinopathy in the amygdala of old cognitively impaired αSyn transgenic mice. Old wild type as well as young and old αSyn transgenic animals were trained in the classical fear conditioning (FC), to test their abbility for hippocampal function dependent contextual and amygdala function

dependent emotional (cued) learning (Freichel et al., 2007, Schell et al., 2009). All mice displayed the ability of contextual and cued learning, however FC aged αSyn transgenic animals spent the shortest time freezing. This resulted in a significantly higher measured exploration activity of the group of aged transgenic αSyn mice in the cued test, when compared to the fear conditioned wild type and young αSyn transgenic mice. Histological investigation of the BLA and the Ce with c-Fos specific antibodies displayed a significant upregulation of Fos in all conditioned groups, with exception of the group of aged αSyn transgenic mice. Again the upregulation measured for the group of old transgenic mice displayed just a trend for a FC induced Fos upregulation in the BLA and Ce. Fos upregulation in the BLA of conditioned young αSyn mice was significant compared to the not conditioned control group, but intersetingly was also significantly lower when compared to the FC-conditioning dependent upregulation measured in old wild type mice. This observation points to an impairment of neuronal function in the BLA resulting from the observed nuclear pSer129 αSyn in neurons of the BLA of young and old transgenic αSyn mice. Since fear conditioned old transgenic αSyn mice displayed a much stronger pSer129 αSyn staining in nuclei of the BLA than young trangenic αSyn mice and the old αSyn mice obviously have the lowest activation of the BLA, a nuclear pSer129 αSyn dosage/age dependant effect impairing BLA function of αSyn transgenic animals is very probable. Furthermore measured activation of the Ce in conditioned young αSyn transgenic and conditioned wild type mice was similar. Conditioned aged αSyn mice on the other hand showed only a trend for an activation of the Ce. Histopathological pSer129 αSyn stainings displayed distrophic neurite and synaptic staining only in the Ce of aged αSyn mice. This synucleinopathy therefore could inhibit the Ce activation in the affected animals. Taken together it can be concluded that fear conditioning impairment in aged αSyn transgenic mice results from BLA misfunction induced by nuclear pSer129 αSyn and Ce misfunction induced by neuritic pSer129 αSyn. Young αSyn mice are only affected by nuclear

pSer129 αSyn pathology in the BLA and show significant cued learning. However old wt animals, which do not have any pSer129 αSyn in the BLA or the CE display significantly better cued learning than young αSyn transgenic mice.

Interestingly the context learning was not affected in young αSyn transgenic mice. This indicates that the observed pSer129 αSyn in hippocampal CA1, CA3 region and the subiculum of young transgenic mice has no negative effect on hippocampal function. Aged transgenic animals showed a worse performence in context learning and displayed a similar hippocampal staining pattern. However these mice additionally displayed synaptical αSyn staining of CA1 and CA3 neurons. This transgenic αSyn is neither Ser129 phosphorylated, nor ThS posititve and was the only clear, visible difference between young and old αSyn transgenic mice. It is indeed possible that the reduced abilitiy of context learning in old αSyn mice is not only caused by a reduced function of the Hip (McNish et al., 1997), but also the reduced function of the amygdala induced by the identified synucleinopathy in the amygdaloid Ce and the BLA may contribute to this impairment (Goosens et al., 2001, Scicli et al., 2004).

As it was shown that the Ser129 αSyn phosphorylating kinases PLK2 and PLK3 are expressed in response to synaptic activation and furthermore seem to have an effect on synaptic plasticity, remodelling and homeostasis (Kauselmann et al., 1999, Seeburg et al., 2005, Seeburg et al., 2008b), brain tissue from animals of all groups were included in histological stainings with antibodies specific for PLK2 and PLK3. Positive PLK3 staininigs were always diffusely scattered in the neurophil regardless of age or neuronal activation status. In contrast PLK2 stainings displayed a FC related functional relevance. Except of the conditioned group of old αSyn transgenic mice all other conditioned groups displayed an upregulation of PLK2 in the BLA and interestingly also in the Ce after fear conditioning. This observations stand in line with the findings that both the BLA (Amano et al., 2011,

Goosens et al., 2001) as well as the Ce (Duvarci et al., 2011, Samson et al., 2005), namely the medial part, are involved in synaptic plasticity. Interestingly the upregulation in the Ce of young transgenic and old wild type mice was comparable, whereas the PLK2 upregulation in the BLA of young transgenic mice was lower than in the wild type mice. This activation pattern could again be related to the observed synucleinopathy in the BLA of young transgenic mice and the missing neuritic pSer129 αSyn staining pattern in the Ce. This is an interesting aspect, as pSer129 αSyn and PLK2 stainings displayed similar nucelar staining patterns in neurons of the BLA. On the other hand the old conditioned αSyn transgenic mice displayed an unexpected opposite reaction. Here a tendency of a fear conditioning dependent down-regulation of PLK2 was observed in the BLA of these mice, and a significant downregulation of PLK2 in the Ce upon FC could be measured. The missing PLK2 upregulation in the conditioned old αSyn transgenic mice could result from the more severe synucleinopathy in the BLA and the presence of neuritic pSer129 αSyn in the Ce of these animals. This would implicate, that PLK2 levels are downregulated by the presence of phosphorylated proteins or pSer129 αSyn. Assuming that PLK2 is involved in synaptic plasticity and remodelling, it is not surprising that old αSyn transgenic mice, which do not display an upregulation of PLK2 after FC, display learning deficites. As a learning effect is still visible in the cognitively impaired mice, PLK2 is most likely not the only protein involved in synaptic plasticity and remodelling in the BLA. The finding that PLK2 is also FC dependent upregulated in the Ce of healthy wt mice, a region which does not underlie synaptic plasticity, points to possible other not defined functions of PLK2. Despite of its importance for synaptic plasticity, remodeling (Kauselmann et al., 1999, Seeburg et al., 2005, Seeburg et al., 2008b) and neuronal differentiation (Draghetti et al., 2009) PLK2 was shown to interact with the postsynaptic scaffolding protein 95 (PSD95), spine associated Rap guanosine triphosphatase activating protein (SPAR) and Cib, a Ca^{2+} and integrin binding protein (Pak et al., 2003). Furthermore it was shown that

induced PLK2 resulted in phosphorylation and degradation of PSD95 and SPAR by the ubiquitin-proteasome system. This led to a loss of synapses and mature dendrite spines in cell lines and primary neuron cultures (Seeburg et al., 2008b). Whether pSer129 αSyn directly interacts with PLK2 or is influencing PLK2 homeostasis via one of the described pathways, can not be stated from the described findings. The link between the influence of synucleinopathy in the BLA and Ce and the regulation of PLK2 homeostasis and thereby neuroplasticity remains to be disentangled and is very important for the understanding of the intracellular processes induced by synucleinopathy. The understanding of this neurodegenerative pathways will facilitate the developing of proper therapeutics.

Taken together, PLK2 is upregulated in the BLA and Ce of fear conditioned healthy mice. This activation is important for learning (neuronal plasticity), as conditioned old αSyn mice with cognitive decline do not show a PLK2 upregulation in the amygdala after fear conditioning (Kauselmann et al., 1999, Pak et al., 2003, Seeburg et al., 2008a, Seeburg et al., 2008b). The neuropathologic pathway leading to an absent PLK2 upregulation and furthermore to downregulation in aged fear conditioned cognitively impaired mice is not known.

4 Outlook

In this work a mouse model for α-Synucleinopathy that develops the disease in several neuronal systems, including the motoric system and the emotional and context learning system, was used to closer investigate the synucleinopathy in the emotional learning circuit. Furthermore the impact of the disease on neuronal function in the respective affected brain regions was investigated. Proteinbiochemical and histopathological investigation of BS and MB tissue displayed pSer129 positive LBs and LNs. Furthermore the affected tissue was affected by amyloidosis, displayed positive silver staining and contained all different types or aggregated αSyn that could be isolated by sequential extraction. Weiss and colleagues demonstrated a method to separate high molecular protein species via electrophoresis in agarose gels (Weiss et al., 2008). This method could be used as a tool to further separate and further characterise isolated high-molecular weight αSyn aggregates.

Histopathological investigation of amygdala and Hip displayed nuclear pSer129 αSyn, with an increasing age-dependent staining intensity in the basolateral amygdala (BLA) and the Cx. The necessary biochemical investigation for the nuclear pSer129 αSyn observed in the BLA, hippocampal CA1 and CA3 and in the Cx, was performed only with cortical tissue up to now. Unfortunately cytoplasmatic-nuclear fractionations of cortical lysates did not reveal any Cx specific signal. Solubility assays with tissue from Cx and other brain regions without nuclear pSer129 αSyn, displayed only in the enriched sarcosyl fraction from cortices isolated from aged cognitively impaired mice a signal corresponding to monomeric αSyn. The phosphorylation of this αSyn at the Ser129 residue remains to be confirmed. Furthermore it would be interesting to perform solubility assays of already separated cytoplasmatic and nuclear fractions, to better specify the nature of nuclear and cytoplasmatic αSyn species in neurons affected by synucleinopathy. It would be interesting to develop sensitive proteomic tools

to analyze nuclear pSer129 αSyn positive tissue isolated from the hippocampal CA1 and the BLA via laser-microdissection.

Neuronal activation of the emotional and context learning circuit via fear conditioning and the following readout by quantification of Fos positive neurons, demonstrated a nuclear pSer129 αSyn dosage dependent inhibition of BLA-neuronal activation in the αSyn transgenic mice. PLK2 was found to be upregulated in the same manner after the fear conditioning dependant upregulation of the BLA. Histological investigation with pSer129 αSyn specific antibodies displayed a positive neuritic staininig pattern mainly in the medial amygdaloid central nucleus (CeM) of aged αSyn transgenic mice (Fig. 1.8, page 20). An upregulation of Fos in the Ce of old transgenic mice could not be measured, very likely due to the detected pSer129 αSyn. Furthermore an upregulation of PLK2 was completely missing in the aged cognitively impaired αSyn mice. Here it would be important to include the amygdaloid intercalated regions, which connect the LA with the Ce and the BA with the Ce, into these investigations (Ehrlich et al 2009).

Impairment of context learning of the aged αSyn animal group was adressed to the presence of transgenic non-phosphorylated αSyn, in the synaptic region of the CA1 and CA3 layer in the Hip. Furthermore the CA1, CA3 layer and especially the subiculum are positive for the kinase PLK2 that phosphorylates αSyn at the Ser129 residue. Additionally this kinase was shown to be upreglated after neuronal activation in hippocampal neurons (Seeburg et al., 2008b) and it was shown that PLK2 is required for homeostatic plasticity in hippocampal neurons (Pak et al., 2003, Seeburg et al., 2008a). As investigation of Fos and PLK2 upregulation after fear conditioning was only performed in the amygdala, it would be interesting to extend this type of analyses also to the Hip to find out if information process faces a dead end in the Hip and when, which part it may be. Assuming that CA1 and CA3 neurons are activated during the fear conditioning training, despite of the presence of nuclear pSer129 αSyn in the granular layer, and

that the transgenic, not phosphorylated αSyn in the synaptical region of CA1 and CA3 has a negative effect on neuronal transmission (Kramer et al., 2007), the neurons in the subiculum, which connects the Hip with the Cx, should show a reduced activation in old [A30P]αSyn mice. This would explain the poorer performance of old transgenic mice in the context test. Under the same circumstances it would be possible to investigate the activation of PLK2 in the Hip, as it was observed that the CA1 - subiculum connections underlie synaptical plasticity after activation of the Hip (O'Mara et al 2000, Behr et al 2009). Since PLK2 is upregulated after FC, it would be also interesting to estimate if pSer129 αSyn levels are upregulated in the transgenic mice involved. Thereby one would expect to observe an upregulation only in young αSyn transgenic mice.

As for the nuclear pSer129 αSyn in cortical neurons it would be intersting to investigate if the synapses of these neurons also contain transgenic not phosphorylated αSyn, like the neurons in the hippocampal CA1 and CA3 layer. For this purpose the regions, which receive projections from the Cx, i.e. the corpus calosum, the striatum, putamen, nucleus caudate (dorsolateral and ventromedial), ventral striatum, or the subthalamic nucleus, would be examined.

Another region that should be investigated for anomalies would be the nucleus accumbens (NAc). This region is known to be involved in emotions related to reward, and it receives into its core region (NAc core) upon others projections from the basolateral amygdala and the parahippocampal Cx (Kelley et al 1982, Heimer er al 1995, Robbins and Everitt 1996, Setlow 1997). The shell region of the NAc (NAc shell) receives projections upon others from the subiculum, the hippocmpal CA1 region and also from the BLA (Groenewegen and Trimble, 2007).

Concerning the effect of high αSyn or pSer129 αSyn levels on neuronal function, several well-established possibilities are at hand for further investigation. One possibility would comprise the recording of how potential

information transmission deteriorates with age in αSyn transgenic animals compared to wild type animals. To do so one would have transgenic and wild type animals with electrode array implants, already at young age, i.e. in the barrel cortex, a well characterised brain region receiving projections from the whiskers (Petersen, 2007, Alloway, 2008, Sehara and Kawasaki, 2011), and which is affected by α-Synucleinopathy in the transgenic mice. This preparation would allow an extraction how the cortex of transgenic and wt animals is dealing with stimulation to the whiskers. Furthermore it would be interesting to see how the performence of the cortices affected in high age by severe synucleinopathy compared to the performance of cortical tissue in "healthy" wild type mice. As the same animals are measured during their whole life, the construction of a "deterioration curve" would be possible and i.e. estimate if a possible deterioration is accelerated in age dependant manner. An other possibility would be the performing of patch clamp in hippocampal subiculum or CA1 layer directly after fear conditioning to estimate the effect of synucleinopathy on neuroplasticity in these brain regions, although this intention would be rather difficult, as performing of patch clamp in tissue of aged animals is known to be a challenge.

Very important would be to perform the work done in this study and also the described experiments above with mice, which are transgenic for αSyn but also deficient for PLK2 and / or PLK3. These investigations are important to understand the interplay between PLKs and pSer129 αSyn in neurons affected by synucleinopathy. Furthermore this research would point out the role of PLKs in the development of Synucleinopathy and also on the learning related neuroplasticity in the emotional learning system.

All this studies would be interesting to perform also with other double transgenic mice; these would be animals with transgenes or knockouts for PD related proteins and crossbred with the αSyn transgenic animals used in this work. This knowledge will forward the understanding of the biogenesis and neurotoxicity of α-Synucleinopathy related disorders.

5 Material and Methods

5.1 Materials – Chemicals

1,4-Dithiothreitol (DTT)	Roth
2-propanol	Merck
40% Acrylamid/Bis solution 19:1	Biorad
ABC Antibody-Kit (rabbit / rat)	Vector Laboratories
Acetic acid (glacial) 100%	Merck
Adenine hemisulphate	Sigma
Agar	Fluka
Alpha-Synuclein, recombinant, human	Centic Biotech
Aluminiumsulfate - 18-hydrate ($Al_2(SO_4)_3$ * $18H_2O$	Merck
All Trans-Retinoic Acid	Sigma
Amonium nitrate	Roth
Ammonium persulfate (APS)	Sigma
Ampicillin	Sigma
BCA Protein Assay Kit	Pierce
BDNF, human	Peprotech
Bicine	Roth
Bis-Tris	Roth
Blasticidin S (selection antibiotic)	InvivoGen
Bovine Serum Albumin (BSA)	Roth
Bradford Protein Assay Kit	Bio-Rad
Bromphenol blue sodium salt (BPB)	Merck
Catwalk	Noldus
CIP -phosphatse, alkaline from calf intestine-grade 1	AppliChem
Complete, protease inhibitor cocktail	Roche
Coomassie brilliant blue R-250	AppliChem
Coverslip (round shape, ϕ12mm)	Roth
Coverslips, SuperFrost Plus	Fisher Scientific
DABCO	Roth
Dimethylsulfoxide (DMSO)	Sigma
DMEM (Dulbecco's minimal essential medium)	PAA
DMEM/HAM's F12	PAA
DNA 1 kb ladder	NEB/Fermentas
DNA 100 bp ladder	NEB/Fermentas
DNA T4 Ligase (1U/µl), DNA T4 Ligase buffer (10x)	Fermentas
DNeasy -Blood and tissue kit	Quiagen
EDTA	Sigma
EGTA	Roth
Ethanol	Merck
Ethidium bromide (1% in water)	Merck
Fetal bovine serum gold (FBS)	PAA Laboratories
FBS (tetracycline free)	PAA Laboratories
Fear Conditioning System	TSE
Formaldehyde	Roth
Fluorescence mounting medium	Dako
FuGENE 6 transfection reagent	Roche
G418 (selection antibiotic)	InvivoGen
Gold chloride	Roth
Glycerol	AppliChem

Glycine	Roth
GoTaq Polymerase Kit	Promega
GTP-sepharose	Jena Biosciences
GRK5-FLAG tag vector (G protein–coupled receptor kinase 5)	Dr. Takeo Kato *
H_2O_2 30%	Roth
Hepes	Sigma
Hoechst33342	Molecular Probes
Hydrochloric acid (HCl)	Merck
Hybond-P polyvinyllidene difluoride, (PVDF) membrane	Millipore
Hyperfilm ECL, high performance chemiluminiscence	GE Healthcare
Hygromycine (selection antibiotic)	Roth
Kanamycin	Sigma
kinase buffer 10x	Cell Signaling
Kongored	Sigma
LightCycler I (32 samples)	Roche
Magnesium Chloride (MgCl)	Roth
Mowiol	Roth
Methanol	Merck
Miniprep Kit	Qiagen
N,N,N',N'-Tetramethylethylendiamine (TEMED)	Merck
Non fat milk powder Sucofin	(Edeka)
Nuclear fast red	Fluka
Nucleotides (ATP, CTP, GTP, GDP, GTPγS)	Sigma
NuPAGE Novex Bis-Tris 4-12% Gel (Tricine Gels)	Invitrogen
Optimem	Gibco
Peroxidase substrat kit	Vector SG
Perjodic acid	Roth
Pertex	Merck
PLK2, recombinant, human	Calbiochem
PLK3, recombinant, HIS Tag	Calbiochem
Poly-D-lysine (PDL)	Sigma
Polyethylene glycol (PEG)	Sigma
Ponceau S Staining Solution	Sigma
Potassium chloride (KCl)	Merck
Potassium dihydrogen phosphate (KH2PO4)	Merck
Potasium iodid	Roth
Precision Plus Protein Standard, prestained	Biorad/Fermentas
Protein Standard for Bis-Tris Gel: SeeBlue Plus2	Invitrogen
Protease inhibitor (Complete)	Roche
Protein G-agarose	Roche/Upstate
QIAprep spin MiniPrep Kit	Qiagen
QIAquick gel extraction kit	Qiagen
Restriction endonucleases and buffers	Roche/Fermentas
Restriction enzymes	Fermentas
RotaRod	TSE
Shrimp alkaline phosphatase (SAP)	Roche
Shrink alkaline phosphatase (SAP), SAP buffer (10x)	Fermentas
Silver Nitrate	Roth
SNCA, C-terminal peptide	Mybiosource
Sodium azide (NaN3)	Sigma
Sodium carbonate	Roth
Sodium chloride (NaCl)	Merck
Sodium dodecyl sulfate (SDS)	Sigma
Sodium hydroxide (NaOH)	Merck
Sodium phosphate dibasic heptahydrate (Na2HPO4-7 H2O)	Merck
Sodium pyrophosphate tetrabasic decahydrate (NaPP)	Sigma

Sodium thiosulfate	Roth
Sucrose	Roth
Sudan Black	Sigma
Super pap pen	Daido Sangyo
Surgical equipment	FST
CYBR Green I (mini kit)	Roche
T4 DNA ligase kit	Fermentas
Taq DNA polymerase (+ 10x buffer, dNTPs)	Qiagen
Thioflavine-S	Sigma
To-Pro-3	Molecular Probes
Tungstosilicic acid	Roth
Trichloroacetic acid solution, 6.1 N (TCA)	Sigma
Triton X-100	AppliChem
TRIZMA Base (Tris base)	Roth
Trypsin-EDTA (10x)	Gibco
Tryptone/Peptone	Roth
Tween 20	Merck
Urea	Sigma
Vectastain ABC kit	Vectorlabs
Western Blocking Reagent	Roche
Zeocin (selection antibiotic)	MP Biomedicals
Xylene	Roth
β-Mercaptoethanol	Roth

* Yamagata University, Yamagata, Japan

5.2 Companies

Abcam	Cambridge, UK
Alabama Research and Developement	Munford, Alabama, USA
American National Can Company	Norwalk, CT, USA
Amersham Biosciences Europe GmbH	München, Germany
Analyticon Biotechnologies AG	Lichtenfels, Germany
Ansell	München, Germany
Applied Biosystems/Ambio	Austin, TX, USA
ATCC, American Type Culture Collection	Manassas, Virginia, USA
BD Biosciences	San Jose, CA, USA
Beckman Coulter GmbH	Krefeld, Germany
Berna Biotech AG	Bern, Switzerland
Binder	Tuttlingen, Germany
Biochrom AG	Berlin, Germany
Bio-Rad Laboratories GmbH	München, Germany
BioVex Inc.	Woburn, Massachusetts, USA
BioWhittaker, Lonza Verviers, S.p.r.l.	Verviers, Belgium
Biozym Scientific GmbH	Hessisch Oldendorf, Germany
Bitplane AG	Zürich, Switzerland
Braun Melsungen AG	Melsungen, Germany
Cambrex	East Rutherford, New Jersey, USA
Carl Zeiss MicroImaging GmbH	Jena, Germany
Charles-River	Sulzfeld, Germany
Corning Costar	Lowell, Massachusetts, USA
Dako	Hamburg, Germany
Daido Sangyo Co., Ltd.	Tokyo, Japan
Dr. Köhler Chemie	Bensheim, Germany
Dr. Schumacher GmbH	Melsungen, Germany
ECACC, European Collection of Cell Cultures	Porton Village, UK

Ecolab	Düsseldorf, Germany
Eppendorf AG	Wesseling-Berzdorf, Germany
Eurofins MWG Operon	Ebersberg, Germany
Fermentas GmbH	St. Leon-Rot, Germany
Fischar GmbH & Co. KG	Saarbrücken, Germany
GATC Biotech AG	Konstanz, Germany
Gibco, Invitrogen GmbH	Darmstadt, Germany
GraphPad Software, Inc	Ja Jolla, Kaliformien, USA
Greiner Bio-One GmbH	Frickenhausen, Germany
Hareaus	Buckinghamshire, UK
Hartmann	Neuhausen, Switzerland
Ika Werke GmbH & Co. KG	Staufen, Germany
InforMax Inc.	Bethesda, Maryland, USA
Invitrogen GmbH	Karlsruhe, Germany
Invivogen	Ja Jolla, Kalifornien, USA
Kimberley Clark Professional	Mainz, Germany
Kitasato	Kitamoto-shi, Saitama, Japan
Leica Microsystems	Nussloch, Germany
Macherey-Nagel GmbH & Co. KG	Düren, Germany
MBI Fermentas	St. Leon-Rot, Germany
Merck KGaA	Darmstadt, Germany
Microsoft Germany GmbH	Unterschleißheim, Germany
Millipore GmbH	Schwalbach, Germany
Miltenyi	Bergisch Gladbach, Germany
Molecular Probes, Invivogen	Karlsruhe, Germany
Molecular Bio Products	San Diego, CA, USA
MWG-BIOTECH AG	Ebersberg, Germany
Nalgene	Roskilde, Denmark
New England Biolabs GmbH (NEB)	Frankfurt, Germany
Novo Nordisk Pharma GmbH	Mainz, Germany
Nunc GmbH & Co. KG	Langenselbold, Germany
Olympus Germany GmbH	Hamburg, Germany
Oncolytics Biotech	Calgary, Alberta, Kanada
PAA Laboratories GmbH	Pasching, Österreich
Peqlab	Erlangen, Germany
Personna Medical	Cedar Knolls, New Jersey, USA
Pfizer Germany GmbH	Berlin, Germany
Promega	Mannheim, Germany
Qiagen GmbH	Hilden, Germany
Roche Applied Science	Grenzach-Wyhlen, Germany
Roth, Carl Roth GmbH & Co. KG	Karlsruhe, Germany
Sanofi Pasteur MSD GmbH	Leimen, Germany
Sanyo	Bad Nenndorf, Germany
Sarstedt	Nümbrecht, Germany
Sartorius Stedim biotech	Aubagne, France
Schülke & Mayr GmbH	Norderstedt, Germany
Sigma-Aldrich Chemie GmbH	München, Germany
Soft Imaging System GmbH	Münster, Germany
Süd-Laborbedarf GmbH	Gauting, Germany
Stratagene	Amsterdam, The Netherlands
Systec GmbH	Wettenberg, Germany
Tecan Group Ltd.	Männedorf, Switzerland
TSE Systems	Bad Homburg, Germany
Vector Laboratories, Inc.	Burlingame, CA, USA
Wilhelm Ulbrich GdbR (WU)	Mainz, Germany

5.3 Molecular biology

5.3.1 Solution and buffers

Ampicillin stock solution
100 mg/ml in H_2O bidest. Aliquots were stored at –20°C.

Kanamycin stock solution
30 mg/ml in H_2O bidest. Aliquots were stored at –20°C.

LB medium
10 g Tryptone, 5 g Bacto-Yeast extract, and 8 g NaCl were dissolved in 1000 ml H_2O and sterilized by autoclaving. Ampicillin (100 µg/ml) or Kanamycin (30 µg/ml) was added after cooling down to approximately 50°C. LB containing antibiotic was stored at 4°C.

LB agar plates
10 g Bacto-Tryptone, 5 g Yeast extract, 8 g NaCl, and 16 g Bacto-Agar were dissolved in 1 l H_2O and sterilized by autoclaving. Ampicillin (100 µg/ml) or Kanamycin (30 µg/ml) was added after cooling down to approximately 50°C. Plateswere stored at 4°C.

10x DNA gel loading buffer
250 mg bromphenol blue, 33 ml 150 mM Tris base (pH 7.6), 60 ml glycerol, 7 ml H_2O bidest. Stored at 4°C.

Tris-borate buffer (TBE) 10x
108 g Tris, 55 g Boric acid in 900 ml H_2O bidest. 40 ml 0.5 M Na_2EDTA (pH 8.0) was added and volume adjusted to 1 liter with H_2O bidest.

1% (w/v) Agarose gel
1 g agarose was dissolved in 100 ml 1x TBE by microwave heating. 2.0 µl of ethidium bromide (1% in water solution) were added after cooling to ~50°C.

Minipreparation buffer I
0.9% Glucose, 10 mM EDTA, 25 mM Tris, 100 µg/ml RNAse A

Minipreparation buffer II
200 mM NaOH, 1% SDS

Minipreparation buffer III
3 M Potassium acetate (pH 5.0), 11.5% acetic acid

5.3.2 Methods

5.3.2.1 Genotyping qPCR

Isolation of mouse DNA was performed using DNeasy-Blood and tissue kit.

Mastermix for 5 samples:

buffer – Promega (5x)	10 µl
H_2O	27 µl
dNTPs (10 mM)	1 µl
primer-r (10 pmol)	1 µl
primer-f (10 pmol)	1 µl
Taq – Biomol	0.25 µl

→ 8 µl of this mastermix + 2µl DNA for PCR are used for one reaction

Program:

5′	94°C	
30″	94°C	} 35 cycles
30″	58°C	
30″	72°C	
5′	72°C	
forever	12°C	

Genotyping Primers

Mouse β-actin primer (61°C)
F: 5'-TAT TGG CAA CGA GCG G-3'
R: 5'-CGG ATG TCA ACG TCA C-3'
Human SNCA (60°C):
F: 5′-TGTAGGCTCCAAAACCAAGG-3′
R: 5′-TGTCAGGATCCACAGGCATA-3′
Human LRRK2 (58°C):
F: 5′-ATTGACCGGAAACGATTAT-3′
R: 5′-TGCCCTTAGGGTGTTTTG-3′

5.3.2.2 Light-Cycler-PCR

Program:
A LightCycler I and CybrGreen (both provided by Roche) was used for the PCR. The amount of produced PCR product was detectable with CybrGreen which intercalates in the DNA. A standard curve was made for a house-keeping gene (i.e. Mouse β-actin) and for the gene of interest (h*SNCA* or h*LRRK2*) of a homozygot animal. The results of the PCR with unknown samples were compared with the standard curve. In each run a negative control and a positive control (DNA of a homozygot animal) was included. The result of the positive control was set to 1. The results of the PCR with unknown samples were matched to the result of the positive control

(homozygote mouse = 1). Values between 0.8 and 1 stand for homozygot animals and between 0.2 to 0.5 for heterozygot animals.

5.3.2.3 Transformation of competent bacteria

1. thaw chemocompetent bacterien on ice
2. add 2 µl DNA to the bacteria aliquot and incubate 20 min on ice
3. heatshock, 2 min 42°C
4. incubate 2 min on ice
5. add 250-500 µl LB- / Shock– Medium (without antibiotics)
6. incubate for 1 h at 37°C under continuous shaking (300 RPM)
7. plate 50 µl LB/bacteria mixture on plates with respective antibiotics
8. incubate over night at 37°C
9. select 1 colony → incubate in 1 ml LB with antibiotics
10. incubate 1 day at 37°C under continuous shaking (300 RPM)
11. add 100 µl bacteria to 100 ml LB (with antibiotics) (1:1000)
12. incubate over night at 37°C under continuous shaking (300 RPM)
13. isolate Plasmids via Midi Preparation (Qiagen Midiprep Kit)

5.4 Protein biochemistry

5.4.1 Solution and buffers

1x Transfer buffer
3.03 g Tris base, 14.5 g glycine, 200 ml methanol; ad 1 liter H_2O bidest.

1x TBS-T - Tris buffered saline/0.1% Tween 20
Dissolving of 1.0 ml Tween-20 in 1 liter 1x TBS.

4x SDS-PAGE sample buffer (4x Laemmli buffer)
2.5 ml 1 M Tris base (pH 6.8), 2.0 ml 20% SDS, 4.0 ml glycerol, 1.0 ml ß-mercaptoethanol, 250 mg bromphenol blue, adjusted to 10 ml volume with H_2O bidest. Aliquots were stored at –20°C.

5x Ripa
250 mM Tris (pH7.4), 750 mM NaCl, 5% NP40, 0.5% (w/v) SDS, 2.5% desoxycholate, $_{dd}H_2O$, add 1x EDTA-free complete prior to use.

10x SDS-PAGE running buffer
30.3 g Tris base, 145 g glycine, 10 g SDS in 1 liter H_2O bidest.

10x TBS - Tris buffered saline
Dissolve 302.85 g Tris, 438.3 g NaCl in 4 liter H_2O. Adjust pH to 7.5 with 1 M HCl and add H_2O volume to 5 liter. Stable at 4°C for three months.

10% Blocking solution
Dissolve 50 g of non fat milk powder in 500 ml 1x TBS-T.

Coomassie staining solution
Add 0.5 g Commassie blue R250, 92 ml acetic acid (glacial), 454 ml methanol to 454 ml H_20 bidest (total volume 1000 ml).

Coomassie destaining solution
50 ml acetic acid (glacial), 250 ml methanol are added to 700 ml H_20 bidest (total volume 1000 ml).

HEPES lysis buffer
50 mM HEPES (pH 7.5), 10 mM KCl, 50 mM NaCl, 1 mM EDTA, 0.5 mM EGTA, 1.5 mM $MgCl_2$, 10% Glycerol, 0.2% Nonidet P-40, 10 mM NaPPi, 2 mM PMSF, 0.1 mM NEM, 2 mM Sodium orthovanadate, 100 mM NaF.

NP-40 lysis buffer
150 mM Tris/HCl (pH 7.6), 50 mM NaCl, 10 mM NaPPi, 0.5% Nonidet P-40, 2 mM PMSF, 0.1 mM NEM, 2 mM Sodium orthovanadate, 100 mM NaF.

Primary antibody solution
5% Western Blocking Reagent, 0.02% Sodiumazide in TBS-T

SDS-PAGE stacking gel buffer
0.5 M Tris base, pH 6.8 and 0.4% SDS

SDS-PAGE resolving gel buffer
1.5 M Tris base, pH 8.8 and 0.4% SDS

SDS lysis buffer
150 mM Tris/HCl (pH 7.6), 50 mM NaCl, 1% SDS

Secondary antibody solution
5% non-fat dried milk powder in TBS-T

Western Blot stripping solution
62,5 mM Tris pH 7.6
2% SDS
100 mM Mercaptoethanol
1l:
7,57g Tris-Base pH 7.6
20g SDS
7,813g Mercaptoethanol (6,98ml ß-ME)
ad 1l H_2O_{dd}

Urea lysis buffer
10 mM Tris (pH 8.0), 100 mM NaH2PO4, 8 M Urea, 10 mM Imidazole

5.4.2 Methods

5.4.2.1 Western Blot

SDS-polyacrylamide-gel electrophoresis (SDS-PAGE)
This method is used to separate proteins by size. Thereby SDS, which has a negative charging, binds to all proteins and converts the indivual charging of each protein to a negative charge. The separation of proteins then only depends on their molecular weight. Composition of separation and stacking gels is described in the tables below. 25 µg or 50 µg protein was directly loaded on the gel after adding 6x laemmli buffer (Laemmli, 1970) to a final contration of 1x. As a standard, 10 µl marker were loaded. Electrophoresis was started with 110 V, after 30 min voltage was increased to 140 V.

Transfer
After the SDS-PAGE proteins were transfered on a polyvinylidenfluorid (PVDF) membrane. Therefore PVDF membrane was activated for 1 min in 100% methanol and equilibrated in transfer buffer together with the gel, blotting-papers (whatman paper) and the blotting sponges. The blotting sandwich was assambled as followed:

cathode
sponge
plotting paper
gel
PVDF membrane
blotting paper
sponge
anode

Transfer was performed in a cooling room (5°C) for 2 h at 100 V or over night at 25 V. Then, membrane was incubated in blocking solution for 1 h at room temperature on a shaker. After a short washing with TBST (to get rid of the milk contained in the blocking solution) membrane was incubated with the first antibody over night at 4°C. Washing was done 3 x 15 min with TBST on a shaker at room temperature. Membrane was than incubated in secondary antibody for 1 h at room temperature followed by additional 3 x 15 min washing steps with TBST. Detection was done with a chemiluminescent HRP substrate. Signals were recorded on ECL high performance chemiluminescent hyperfilms (Amersham).

Composition of polyacrylamide gels

Stacking gel	4%
stacking gel buffer	0.69 ml
Acryl amide 40% (19:1)	0.31 ml
ddH2O	1.7 ml
10% APS	0.028 ml
TEMED	0.003 ml

Separating gel	7.5%	10%	12.5%
separation gel buffer	2.75 ml	2.75 ml	2.75 ml
Acryl amide 40% (19:1)	2.1 ml	2.8 ml	3.4ml
ddH2O	6.1 ml	5.4 ml	4.7ml
10% APS	0.11 ml	0.11 ml	0.11 ml
TEMED	0.011 ml	0.011 ml	0.011 ml

5.4.2.2 **Coomassie staining**

1. cover acrylamide-gel directly after blotting with coomasie staining solution
2. incubate for 30 min, RT on the shaker
3. poor coomasie staining solution back in the original bottle (reusable)
4. cover stained acrylamide-gel with destaining solution
5. Destain by incubating on shaker with a small piece of a paper towel (absorbs coomasie reagent), ON, RT. Use a lid or foil to cover the gel.
6. Coomasie destaining solution can be reused after carbon filtration.

5.4.2.3 **Drying of acrylamide gels**

1. cover coomasie or silver-stained gels with 20% EtOH, 10% Glycerol and incubate for 30 min at RT
2. cover 2 cellophane foils with H_2O and let stand for 1-2 min (take care to keep the borders flat)
3. place 1 foil on the backplate of the drieing frame (remove air bubles)
4. place gel on the foil and cover with 1-2ml EtOH/Glycerol-buffer
5. place second cellophane foil on the gel and seal frame
6. let dry in horizontal position at room temperature over night
7. after drieing carefully remove sealed gel from the plate

5.4.2.4 **Stripping of PVDF membranes**

1. cover membrane with stripping solution and seal container
2. incubate in a shaking water bath at 56°C for 30 min
3. wash with TBST until ß-mercaptoethanol smell is gone

5.4.2.5 Isolation of insoluble αSyn aggregates from brain tissue

To isolate αSyn aggregates from brain tissue, tissue sample of 0.2-1.0 g were used.

buffer A
EGTA 1 mM
DTT 1 mM
Tris 50 mM (pH 7.5)
1 tablet of protease inhibitor (Complete)

buffer A + 1% Tx-100

buffer A + 0.5M NaCl + 10% Sucrose

buffer A + 0.5M NaCl + 10% Sucrose + 1% Sarcosyl

Sarcosylbuffer 3 x (only for proteinase-k digestion)
EGTA 3 mM
Tris 150 mM (pH 7.5)
DTT 3 mM
NaCl 1.5 M
Sucrose 30%
Sarcosyl 3%

1. Prepare buffer A
2. add 10 volumes buffer A to tissue (e.g. 0.5 g: 5 ml buffer)
3. homogenise with electric potter (level 5-10)
4. cetrifugate 10 min 1000 x g (2400 rpm) at 4°C in FALCON-tube
5. discard pellet (P1)
6. supernatant: centrifugate again 20 min 350,000 x g at 4°C
    a. supernatant: *S2 (buffer-soluble)* → proteinase-k digestion
7. homogenise pellet (P2) (~150 mg) in 3-4 ml buffer A + 1% Tx-100
    a. use a glaspiston and start with low volume
    b. fill slowly up to end volume and avoid foaming
    c. centrifugate again for 20 min at 350,000 x g 4°C
8. supernatant*: S3 (Tritonsoluble)*
    a. take care to completly remove white layer from pellet (P3)
    b. pellet (P3): (~100 mg) pestle in 2-3 ml buffer A + 0.5 M NaCl, 10% Sucrose
    c. centrifugate again for 20 min at 350,000 x g 4°C
9. supernatant: *S4 (high salt soluble)*
10. pellet (P5) (~90 mg)
    a. homogenise in 1 ml Puffer A + 0.5 M NaCl, 10% Sucrose, 1% Sarcosyl
11. incubate 1 h at 37°C
12. centrifuge for 20 min at 27,000 x g
13. supernatant: *S5 (Sarcosyl soluble)* → Proteinase-K digestion

14. Pellet: *P5 (Sarcosyl insoluble)*
    a. resuspend in Sarcosylpuffer for protein assay + control gel
15. add 600 µl Sarcosylpuffer
16. incubate 30 min at 37°C (shaking 300 rpm in thermocycler)
17. centrifuge for 30 min at 350,000 x g 4°C
18. supernatant*: S6*
    a. Pellets*: P6* (clear, sometimes detached)
19. if necessary repeat centrifugation 30 min at 350,000 x g 4°C
20. add Loading-Buffer with 6 M UREA
21. load on acrylamide Gel
22. if no pellets are forming continue extraction with formic acid
    a. + 100 µl FA (formic acid)
23. incubate 30 min at room temperature
24. dry sampled inspeedvac (to remove formic acid) – or centrifugate for 30 min at 350,000 x g
    a. then: + LB with UREA (8M-9M) → Gel

Example: human brain BCA-Protein assay
S_2 1.8 mg/ml → Proteinase-k digestion
S_3 1.2 mg/ml
S_4 1.1 mg/ml
S_5 1.7 mg/ml → Proteinase-k digestion of 0.1-1 mg in 250-500 µl
P_5 1.5 mg/ml
S_6 1.0 mg/ml
P_6 Pellet after proteinase-k digestion = *proteinase-K-resistence* → Gel

5.4.2.6 **Sequential detergent extraction protocol**

Hypotonic lysis buffer (HOB)

Tris-HCl (pH 7.4)	10 mM
Sucrose	0.1 M
NaCl	10 mM
DTT	1 mM
complete protease inhibitor	1 x

1x RIPA

Tris-HCl (pH 7.4)	50 mM
NaCl	150 mM
NP-40%	1%
Deoxycholate	0.5%
25x EDTA- complete	1x

1% triton X-100 / PBS

8 M urea / 5% SDS

1. resuspend cells/tissue in hypotonic lysis buffer (HOB) (> 100 µl/3.5 cm dish or 0.5 g tissue in 10 volumes HOB)
2. centrifuge cells at 12,000xg for 20 min
3. supernatant: buffer soluble fraction (Sup1)
4. resuspend pellet in 1% Triton X-100 / PBS
5. centrifuge cells at 12,000 x g for 20 min
6. supernatant: detergent soluble fraction (Sup2)
7. resuspend pellet in RIPA buffer
8. centrifuge cells at 12,000 x g for 20 min
9. supernatant: detergent insoluble fraction (Sup3)
10. resuspend pellet in 8 M urea / 5% SDS
11. centrifuge cells at 12,000 x g for 20 min
12. supernatant: urea soluble fraction (Sup4)
13. add 6 x sample buffer and load to SDS-PAGE

5.4.2.7 **Nucleus / Cytoplasm fractionation**

Buffer A

HEPES / KOH (pH 7.6)	10 mM
$MgCl_2$	1.5 mM
KCl	10 mM
DTT	0.1 mM
25 x EDTA- complete	1 x

Buffer S1

Sucrose	0.25 M
$MgCl_2$	10 mM
25 x EDTA- complete	1 x

Buffer S3

Sucrose	0.88 M
$MgCl_2$	0.5 mM
25 x EDTA- complete	1x

5x RIPA

Tris-HCl (pH 7.4)	250 mM
NaCl	750 mM
NP40	5%
Deoxycholate	2.5%

1x RIPA

Tris-HCl (pH 7.4)	50 mM
NaCl	150 mM
NP-40	1%
Deoxycholate	0.5%
25 x EDTA- complete	1 x

1. harvest cells (0.5-2.5 x 10^7 or 0.5 g tissue) by trypsinization or PBS/EDTA
2. centrifuge at 228 g for 4 min at 4°C and wash once with ice cold PBS
3. resuspend pellet in 2 ml of ice cold buffer A and incubate for 5 min on ice
4. break cells to release nuclei
    a. use a pre-chilled dounce tissue homogenizer with a tight pestle (20 strokes)
5. centrifuge dounced tissue at 228g for 5min at 4°C
6. supernatant: cytoplasmic fraction
    a. transfer supernatant to a fresh polypropylene tube
7. resuspend the nuclear pellet in 1 ml pre-chilled S1 and carefully layer over a 1 ml cushion of cold S3.
8. centrifuge at 2,800 g for 10 min at 4°C

Preparation of cytoplasmic lysate
1. ad 400 µl of 5 x RIPA to 500 µl cytoplasmic fraction and mix well
2. centrifuge at 2, 800 g for 10 min at 4°C
3. supernatant: clean cytoplasmic lysate

Preparation of nuclear lysate
1. solubilize nuclear pellet in 1 ml RIPA buffer
2. sonicate on ice (50% output, 3x5sec)
3. centrifuge 10 min at 2,800 g, 4°C
4. Supernatant: clean nuclear lysate

5.5 Cell biology

5.5.1 Solution and buffers

10x PBS - Phosphate buffered saline
80 g NaCl, 2 g KCl, 26.8 g Na2HPO4-7 H_2O and 2.4 g KH_2PO_4 in 800 ml H_2O. pH was adjusted to 7.4 with HCl and ad H_2O to 1 liter.

Cell lysis buffer
150 mM NaCl, 1% TritonX-100, 50 mM Tris base (pH 7.4), 1 mM EDTA, and 10 mM Na-pyrrophosphate in H_2O bidest. 1x Complete protease inhibitor cocktail (Roche) was added freshly.
Culture medium for SHSY5Y cells
10% FCS in DMEM/HAM's F12

Culture medium for HEK293E cells
10% FCS in DMEM

Embedding Media (Mowiol/DABCO)
1. mix 6 g Glycerine with 2.4 g Mowiol on stirrer for 1 h at RT
2. add 6 ml H_2O_{dd}, stirr 1h at RT
3. add 12 ml 0.2 M Tris-HCl (pH 8.5), incubate 2 h at 50°C (stir every 20 minutes for 2 min on stirrer)
4. if Mowiol is still not dissolved completely centrifuge 15min at 5,000 x g, use supernatant
5. add DABCO at a final concentration of 25 mg/ml and stir till you receive a clear liquid
6. aliquot in 1.5 or 2 ml tubes
7. store at -20°C

For usage of the mounting medium, thaw Mowiol/DABCO solution and keep it on ice. Do not freeze it again. Store it at 4°C (approximately 2 weeks). Seal cover slips with nail polish. Store slides at 4°C.

Freezing medium for HEK 293E and SHSY5Y cells
40 ml DMEM medium, 40 ml fetal bovine serum and 20 ml DMSO were mixed, sterile filtrated using a 0.22 µm filter, and stored at 4°C .

Poly-D-lysine or collagen (100 µg/ml)
Dissolve 5 mg lyophilized poly-D-lysine or collagen into 50 mL DDW. This solution can be stored at 4 ^{o}C

5.5.2 Methods

5.5.2.1 Coating coverslips with poly-D-lysine or collagen

I. Cleaning of coverslips to remove residual oil/grease

Coating cover slips is highly critical to prepare a good condition culture and subsequent immunostaining. Above all, initial cleaning step is most important for successful coating.
1. spread coverslips onto glass petri dish
2. add 1N NaOH and let it stand for 1h
3. after removing NaOH, add 1N HCl and let it stand for 1h
4. remove HCl and wash with DDW for three times
5. dry up in the clean bench

II. Autoclave coverslips

III. Coating coverslips with poly-D-lysine or collagen
1. put the coverslips onto sterirised petri dish. Pour 100 mg/ml Poly-D-Lysine or collagen on each coverslips and let it stand for 5 min
2. aspirate poly-D-lysine/collagen solution and wash with DDW for two times
3. completely dry up in the clean bench

5.5.2.2 Differentiation of SHSY5Y cells

1. prepare 24 Well plates with poly-D-lysine coated coverslips
2. seed $1x10^4$ cels / well
    a. incubate 1-2 days untill cell leyer has a densitiy of 70%-80%
3. replace normal culture media with culture media containing 10 µM retinoic acid and incubate for 5 days
    a. Starvation of the cell cycle in G1-phase and induction of expresion of TrkB receptor (TrkB receptor = receptor for BDNF)
4. carefully wash cells with 1x PBS
    a. make sure to completely remove FCS containing culture media
5. replace old media with serumfree culture media with BDNF (50 ng/ml) and incubate for 5 days

SHSY5Y-Cells in culture:

1 day after retinoic acid treatement

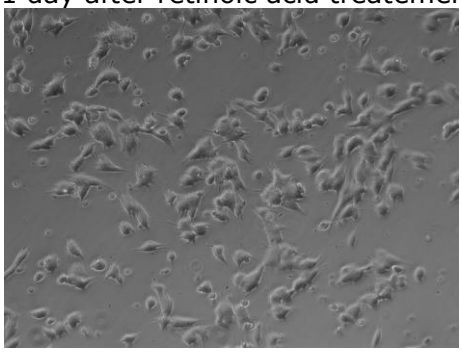

1 day after BDNF treatment

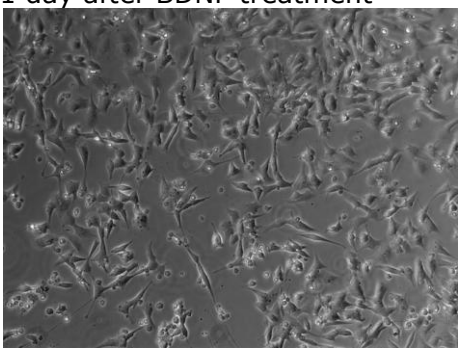

2 days after retinoic acid treatement

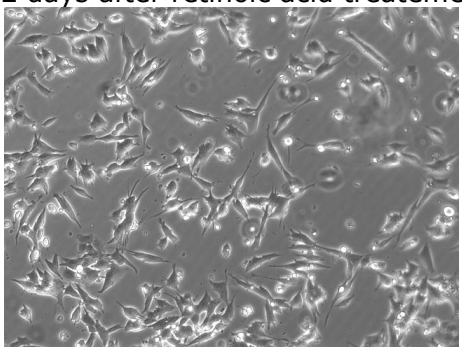

2 days after BDNF treatment

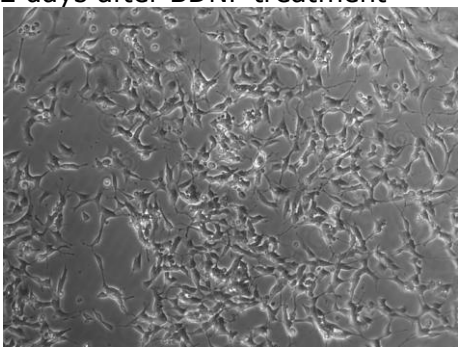

5 days after retinoic acid treatement

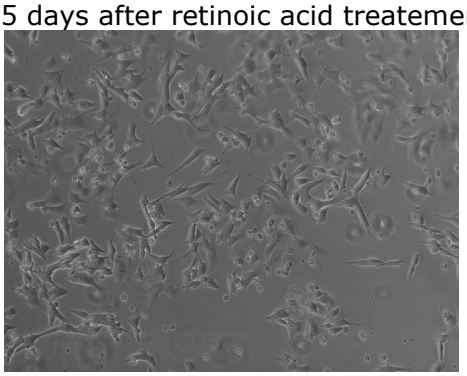

5 days after BDNF treatment

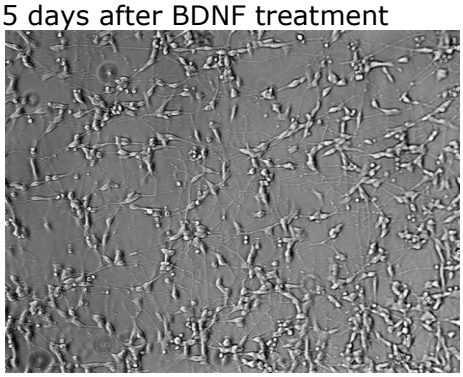

5.5.2.3 **Immunocytochemistry**

I. Fixation and permeabilization

1. culture cells on poly-D-Lysine-coated coverslips
2. aspirate medium and wash once with 1 X PBS at RT
3. fix cells with 4% PFA/PBS for 20 min. Wash once with 1 x PBS
4. permeabilize cells with 0.5% Triton X-100/PBS for 10 min. Wash once with 1 x PBS
5. for αSyn Ser129 residue dephosphorylation, some sections were treated with 10% calf intestinal phosphatase over night in a humified 37°C incubator

II. Blocking

1. blocking is performed with 3% NGS/PBS for 30 min

III. Antibody reaction

1. cells are incubated with diluted 1st Ab (200µl per coverslip) for 2-3 hr at RT (or overnight at 4 ^{o}C).
2. wash twice with 1 x PBS
3. cells are incubated with diluted 2nd Ab (1:2000 dil. for AlexaFluor-conjugated 2nd Ab) for 1 hr under light protection
4. if counterstaining for nucleus is required, add TO-PRO-3 (1:1000 dil.) into 2nd Ab solution
5. Wash twice with 1 X PBS

IV. Embedding

1. cells are embedded on slide glass using aqueous mounting medium (protection from light, specimens can be stored at 4^{o}C for several months)

V. Observation under fluorescent/confocal microscope

1. wavelength settings of excitation/emission for confocal LSM are as follows:

	Laser	Excitation	Emission
AlexaFluor 488 (Green)	Ar	488nm	519nm
AlexaFluor 568 (Red)	HeNe-G	543nm	603nm
TO-PRO-3 (Cherry red)*	HeNe-R	633nm	661nm

(*for triple-color staining, TO-PRO-3 can be visualized by blue-pseudocolor)

5.5.2.4 **Thioflavine-S staining of cultured cells**

1. dissolve 1% ThS in TBS or PBS
2. put 1% ThS on cells, incubate 5 min, RT
3. all following working steps should be proceeded under light protection
4. wash with 70% EtOH on a shaker for 2 min, RT, twice

5. EtOH should stay clear after the last washing step (if necessary repeat washing, otherwise the background of the staining will be too high)
6. wash with TBS or PBS for 3 min, RT, twice
7. mounting (in aqueous mounting medium)
    a. Moviol/DABCO storage at 4°C
    b. Vectashield storage at 4°C
8. protect ThS slides from light
9. ThS positive stainings can be observed with a fluorescent microscope (488 nm)
10. unspecific background (lipofuscin, blood vessels, etc.) are visible in all channels, but ThS just with 488 nm

5.5.2.5 **Preparation of lysates from HEK293E and SHSY5Y cells**

1. detach cells and wash 3x with PBS (1100 RPM, 4°C, 5 min)
2. add proteinase inhibitor (1x), NaF (100 mM) and NaV_2O_4 (10 mM) to the lysis buffer
3. add 100-150 µl lysis buffer / well or tube
4. inubate ½ h, 4°C
5. centrifuge 15 min, 18,000 rpm, 4°C
6. supernatant contains proteins

5.5.2.6 **Transient transfection with FuGene 6**

1. plate the cells in 6 well Plate in medium without antibiotics (number should be chosen so that they reach only a confluency of 50-80% till next day)
    a. For most adherent cells : 100 000 – 300 000 cells/2 ml in one well of a 6well plate
2. let the FuGene reagent warm to room temperature
3. warm serum-free DMEM (no additives) or Optimem to room temperature
4. prepare reagent for 6 Wells:
    a. 94 µl Med / 6 µl Fugene / 1 µg DNA
5. Mix the FuGene (vortex 1 sec), add it carefully (directly into medium)
    a. Avoid a Fugene Reagent layer on top of the serum-free medium
6. immediately tap, flick or vortex 1sec
7. incubate for 5 min at RT
8. add DNA to each tube
9. vortex 1 sec
10. 20-30 min RT
11. add 100 µl of complex drop-wise to its designated well, swirl the plate
12. incubate cells 1-3 days prior to measuring gene expression

5.5.2.7 Histology

Citrate Buffer:
Solution A: 21.01 g citric acid ($C_6H_8O_7$-H_2O) in 1000 ml $_{dd}H_2O$
Solution B: 29.41 g sodium citrate ($C_6H_5Na_3O_7$-H_2O) in 1000 ml $_{dd}H_2O$ 18 ml

Solution A + 82 ml Solution B + 900 ml $_{dd}H_2O$ > pH 6.0

EtOH (75 %)
75 ml 100% EtOH + 25 ml $_{dd}H_2O$

EtOH (95 %)
95 ml 100% EtOH + 5 ml $_{dd}H_2O$

H_2O_2 solution
1ml 30% H_2O_2 + 9 ml TBS/PBS

Nuclear fast red (NFR) staining solution 1%
1 g NFR, heat to boil in 1000 ml 5% $AlSO_4$, allow to cool, filter once and add a grain of thymol as apreservative

Nuclear fast red (NFR) counterstaining
1. after histological staining incubate slides for 5 min in NFR-solution
2. wash slides with tap water
3. dehydration and embedding

Sudan Black B (SBB) (0.3%) preparation and usage
(reduces fluorescent unspecific background staining)
1. stir 0.3% SBB in 70% EtOH at RT for 2h under light protection
2. filtrate
3. use before immunolabeling by incubating 30min at RT

Thioflavine-S (0.5 %)
0.5 g Thioflavine-S in 100 ml $_{dd}H_2O$, vortex, let stand for 5 min, filter or be careful not to take precipitate (always prepare fresh, directly before use)

5.5.2.8 Gallyas silver staining

5% periodic acid

Alkaline silver iodid
4.0 g NaOH in 50 ml $_{dd}H_2O$
add 10 g potassium iodid, mix thoroughly
add 3.5 ml 1% silver nitrate drop by drop
stir and add $_{dd}H_2O$ up to 100 ml

0.5 % acetic acid

0.1 % gold chloride

1 % sodium thiosulfate

Developer

Stock Solution A:	5% sodium carbonate
Stock Solution B:	For 100 ml: 0.2 g ammonium nitrate 0.2 g silver nitrate 1 g tungstosilicic acid
Stock Solution C:	50 ml solution B + 0.345 ml 37% formaldehyde

1. deparaffinise sections
2. incubate 5 min 5% periodic acid
3. wash 2 x 5 min $_{dd}H_2O$
4. incubate 1 min alkaline silver iodid with constant gentle agitation
5. incubate 10 min in 0.5 % acetic acid
6. 5-30 min developer:
    a. Prepare fresh:
       B:A:C = 3:10:7
       Solution B (7.5 ml) + Solution A (25 ml), mix
       add Solution C (17,5 ml), stir until solution becomes clear
7. incubate 3 min 0.5 % acetic acid
8. incubate 5 min H_2O
9. incubate 5 min 0.1 % gold chloride
10. rinse in H_2O
11. incubate 5 min 1 % sodium thiosulfate
12. rinse in H_2O
13. counterstain with Nuclear Fast Red
14. ascending ethanol series, cover slip

5.5.2.9 **Thioflavine-S staining of paraffin-embeded brain sections**

Because thin cuts (4 µm) are used, there is no need for a permeabilisation and deparaffination can start immediately:

1.	Xylene	5 min
2.	Xylene (fresh)	5 min
3.	100% EtOH	3 min
4.	100% EtOH	3 min
5.	95% EtOH	3 min
6.	95% EtOH	3 min
7.	75% EtOH	3 min
8.	75% EtOH	3 min
9.	TBS/PBS	3 min
10.	TBS/PBS	3 min

11. use TBS if a staining against phosphorylated proteins is proceeded after ThS staining
12. dissolve 1% ThS in TBS or PBS
13. put 1% ThS on tissue, incubate for 5 min at RT

14. all following working steps should be proceeded under light protection
15. wash samples with 70% EtOH on a shaker for 2 min at RT
16. wash samples with 70% EtOH on a shaker for 2 min at RT
    a. EtOH should stay clear after the last washing step. If necessary repeat washing, otherwise the background of the staining will be too high
17. wash samples with TBS or PBS for 3 min at RT
18. wash samples with TBS or PBS for 3 min at RT
19. mounting in aqueous mounting medium)
    a. Moviol/DABCO storage at 4°C
    b. Vectashield storage at 4°C
    c. protect ThS slides from light
20. ThS positive stainings can be observed with a fluorescent microscope (488 nm) unspecific background (lipofuscin, blood vessels) are visible in all channels, but ThS just with 488nm

5.5.2.10 **Immunostaining of paraffin-embedded tissue**

1. put isolated brains in 4% PFA in TBS for at least 48h (fixation)
2. rinse brains for 1h in TBS
3. paraffin embedding
4. cut brain in 4 µM thick sections
5. let sections dry (30°C in oven or at RT, overnight or for at least 4 h)
6. heat sections embedded in paraffin in a glass rack overnight at 58°C, clean Paraffin on the side with a paper towel. Be sure not to damage the tissue.
7. de-paraffinise and dehydrate sections
    a. Xylene 5 min
    b. Xylene 5 min (fresh)
    c. 100% EtOH 3 min (2x), 95% EtOH 3 min (2x), 75% EtOH 3 min (2x), PBS/TBS 3 min (2x)
8. H_2O_2 inhibition: 0.3% H_2O_2 in TBS for 30 min (mix before use)
    a. inhibition of background staining of blood and vessels
9. wash 3 x 5 min in TBS (until there are no bubbles)
10. heat in citrate buffer at 90°C for 35 min (antigen retrieval; allow to cool at room temperature in buffer afterward 30-45 min)
11. wash 3 x 5 min in TBS
12. for αSyn Ser129 residue dephosphorylation, some sections were treated with 10% calf intestinal phosphatase over night in a humified 37°C incubator
13. blocking
    a. 5% antiserum in TBS for 30 min:
    b. 1st Ab made in rabbit → goat serum
    c. 1st Ab made in mouse → horse antiserum
    d. 1st Ab made in rat → rabbit antiserum

TBS/PBS	antiserum
1 ml	50 µl
5 ml	250 µl
10 ml	500 µl

14. incubate 1st Ab over night at 4°C
    a. 2% antiserum 10 µl
    b. TBS/PBS 490 µl
    c. Ab 1 µl (if 1:500 dilution)
15. wash 3 x 5 min in TBS
16. incubate 2nd Ab (biotynilated) RT for 1h
    a. prepare 15-20 min prior use
    b. 3% antiserum
    c. 1:200 2nd Ab in TBS/PBS
17. wash 3 x 5 min in TBS
18. ABC complex (Avidin rxn), incubate for 1 h at RT
    a. PBS
    b. 0.8% Reactant A mix
    c. 0.8% Reactant B mix
    d. mix 20min before use and keep at 4°C (or RT)

TBS/PBS	reactant A	reactant B
1ml	8µl	8µl
3ml	24µl	24µl
10ml	80µl	80µl

19. wash 3 x 5 min
20. prepare developing reaction
    a. peroxidase substrate kit
    b. 5 ml PBS
    c. 3 drops SG blue, mix
    d. 3 drops H_2O_2, mix
    e. take care of each slide individually
21. wash thoroughly in TBS/PBS
22. counterstain for 5 min in nuclear fast red
23. processing slides
    a. 3 min 70% EtOH (too much time may diminish staining)
    b. 5 min 95% EtOH
    c. 5 min 100% EtOH
    d. 2 x 5 min Xylene
24. coverslip using Pertex /mounting medium and allow to dry (over night)

5.5.2.11 **Preparation of parafin-embeded tissue for quantification of neuronal activation**

After paraffin embedding, whole brains were cut into 4 µm coronal sections. During this process a row of 3 serial sections was isloated on one objectiv. Between each row 4 sections were discarded. Cutting process was started from the cerebellum to the olfactory bulb. After observation of the lateral ventricles 4 coronary sections were rejected, 3 serial sections were kept and directly transferred onto SuperFrost Plus coverslips (Fisher Scientific). This procedure was hold, until the unification of the lateral ventricles with the medial ventricle could be observed. Out of this block 7 coverslips with tissue containing basal amygdala, lateral amygdala and the amygdaloid central nucleus were chosen for histological staining with rabbit polyclonal antibody against FOS and rabbit polyclonal antibody against PLK2.

5.5.2.12 **Antibodies**

Primary antibodies

1° antibody	(source)	-dilution-	Use	-manufacturer-
anti αSyn	(rb)	-1:1000-	WB	-Affiniti-
anti αSyn	(rb)	-1:1000-	WB	-ChemiconInternational-
anti αSyn(15G7)	(r)	-1:5/1:10-	ICC/IHC/WB	-*-
anti αSyn	(m)	-1:500/1:1000-	ICC/WB	-Zymed-
anti γSyn	(m)	-1:500/1:1000-	ICC/WB	-**-
anti β-actin ***	(m)	-1:5000-	WB	-Sigma-
anti CK2****	(rb)	-1:250/1:1000-	IHC/WB	-Biomol-
anti c-FOS	(rb)	-1:100/1:250-	IHC	-Santa Cruz-
anti Histone-3	(rb)	-1:2000-	WB	-Cell Signaling-
anti HSP90	(m)	-1:1000-	WB	-Stressgen-
anti P38 MAPK	(rb)	-1:1000-	WB	-Cell Signaling-
anti pSer129 αSyn	(rb)	-1:500/1:1000-	ICC/IHC/WB	-Abcam-
anti pSer129 αSyn	(rb)	-1:500/1:1000-	IHC/WB	-Acris-
anti pSer129 αSyn	(rb)	-1:500/1:1000-	IHC	-Assaybiotech-
anti pSer129 αSyn	(rb)	-1:500/1:5000-	IHC/WB	-Epitomics-
anti pSer129 αSyn	(m)	-1:250/1:500-	IHC	-Wako-
anti pSer133 CREB	(rb)	-1:50/1:100-	IHC	-Millipore-
anti pSer133 CREB	(rb)	-1:50/1:100-	IHC	-Santa Cruz-
anti Fnk (PLK3)	(g)	-1:100/1:250-	IHC/WB	-Santa Cruz-
anti Fnk (PLK3)	(rb)	-1:250/1:500-	IHC/WB	-BETHYL Laboratories-
anti Snk (PLK2)	(rb)	-1:250/1:500-	IHC/WB	-BETHYL Laboratories-
anti TH*****	(rb)	-1:100-	WB	-Cell Signaling-

ICC Immunocytochemistry
IHC Immunohistochemistry
WB Western Blot
rb rabbit
m mouse
r rat
g goat

* Dr. Elisabeth Kremmer, Institut für Molekulare Immunologie, Helmholtz Zentrum München
** BD Transduction Laboratories
*** clone AC-15
**** Anti casein kinase 2, beta subunit
***** Tyrosine Hyfroxylase

Secondary antibodies

2° antibody	(source)	-dilution-	manufacturer
anti-rat-HRP	(rabbit)	-1:5.000-	DakoCytomation
anti-mouse-HRP	(sheep)	-1:10.000 – 1:20.000-	GE healthcare
anti-rabbit-HRP	(donkey)	-1:10.000 – 1:20.000-	GE healthcare
anti-mouse-HRP	(goat)	-1:10.000 – 1:20.000-	Jackson Laboratories
anti-rabbit-HRP	(goat)	-1:10.000 – 1:20.000-	Jackson Laboratories
anti-mouse/rabbit Alexa Fluor 488	(goat)	-1:1000-	Invitrogen
anti-mouse/rabbit Alexa Fluor 568	(goat)	-1:1000-	Invitrogen
anti-mouse/rabbit Alexa Fluor 647	(goat)	-1:1000-	Invitrogen

5.6 *In vivo* Experiments

5.6.1 Transgenic mice

The local animal welfare and ethics committee of the country commission Tübingen approved all experiments and procedures. Number of animals used and their suffering was kept to a minimum. Test cohorts comprised homozygote line 31 [A30P]αSyn transgenic male mice of C57BL/6 background and aged matched wild-type controls. 18-22 months animals were defined as aged mice, 4-6 months animals were defined as young mice. The transgenic mice expressed the human [A30P]αSyn under control of the CNS neuron specific Thy1 promotor (Kahle et al., 2000; Neumann et al., 2002; Freichel et al., 2007), resulting in a two- to threefold increase of the total αSyn protein load (Kahle et al., 2001).

5.6.2 Fear conditioning

Day1:

1. start computer, run FC-program, turn control-unit on, prepare experiment
2. bring mice into room (acclimatisation for 30-60min)
3. place mice into FC-Box
4. after 30 sec start FC Program on the computer
    a. 2 min 30 sec pause
    b. 20 sec light
    c. tone (2.9 kHz) / shock (2x 0.6mA)

d. 30 sec pause
e. 20 sec light
f. tone (2.9 kHz) / shock (0.05mA)
g. 30 sec pause
h. repeat e-g 5times
i. 24 h incubation in home cage

Point 3: FC-chamber black (optical cue), bedding material paper (smell)

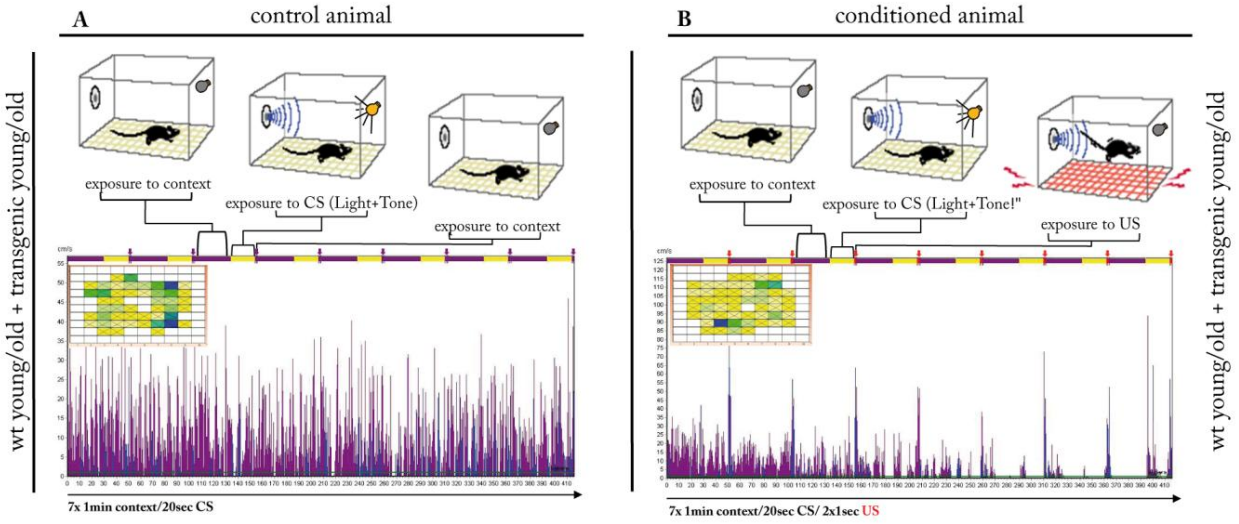

Day2:

1. place mice into FC-Box (same setup like day 1)
2. 3 min incubation in absence of CS and US
3. mice are put back to home cage

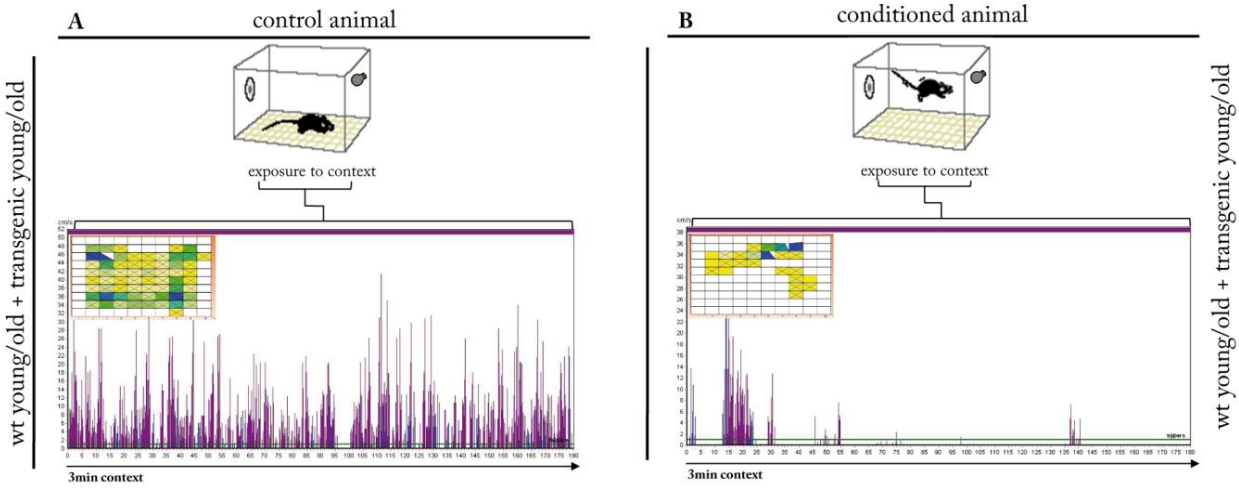

4. 6 h later cued learning in novel test chamber

5. start computer, run FC-program, prepare setup.
6. bring mice into room (30-60min acclimatisation)
7. place mice into FC-box
8. after 30 sec start FC-program on the computer
    a. 1 min pause
    b. 3 min light/tone cue
    c. freezing time

Point 7: FC-chamber clear, bedding material wood

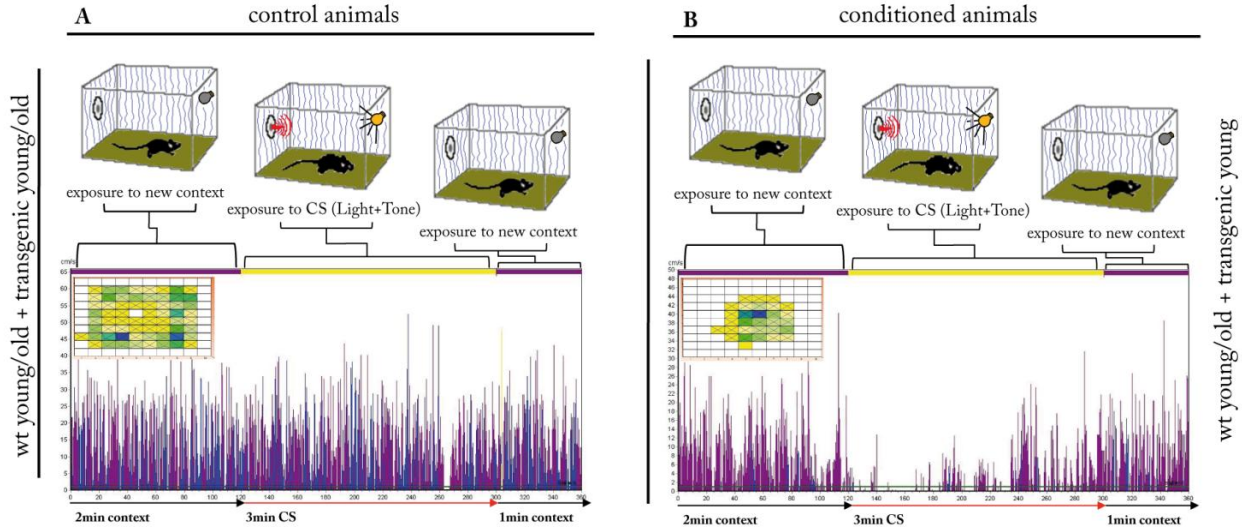

For quantification the test chamber was represented as virtual field consisting of 256 elements. The percentage of visited fields out of the whole area was determined. Significance was checked with the unpaired t-test.

6 References

Abeliovich A, Schmitz Y, Farinas I, Choi-Lundberg D, Ho WH, Castillo PE, Shinsky N, Verdugo JM, Armanini M, Ryan A, Hynes M, Phillips H, Sulzer D, Rosenthal A (2000) Mice lacking alpha-synuclein display functional deficits in the nigrostriatal dopamine system. Neuron 25:239-252.

Anderson JP, Walker DE, Goldstein JM, de Laat R, Banducci K, Caccavello RJ, Barbour R, Huang J, Kling K, Lee M, Diep L, Keim PS, Shen X, Chataway T, Schlossmacher MG, Seubert P, Schenk D, Sinha S, Gai WP, Chilcote TJ (2006) Phosphorylation of Ser-129 is the dominant pathological modification of alpha-synuclein in familial and sporadic Lewy body disease. J Biol Chem 281:29739-29752.

Arai K, Kato N, Kashiwado K, Hattori T (2000) Pure autonomic failure in association with human alpha-synucleinopathy. Neurosci Lett 296:171-173.

Arawaka S, Saito Y, Murayama S, Mori H (1998) Lewy body in neurodegeneration with brain iron accumulation type 1 is immunoreactive for alpha-synuclein. Neurology 51:887-889.

Arawaka S, Wada M, Goto S, Karube H, Sakamoto M, Ren CH, Koyama S, Nagasawa H, Kimura H, Kawanami T, Kurita K, Tajima K, Daimon M, Baba M, Kido T, Saino S, Goto K, Asao H, Kitanaka C, Takashita E, Hongo S, Nakamura T, Kayama T, Suzuki Y, Kobayashi K, Katagiri T, Kurokawa K, Kurimura M, Toyoshima I, Niizato K, Tsuchiya K, Iwatsubo T, Muramatsu M, Matsumine H, Kato T (2006) The role of G-protein-coupled receptor kinase 5 in pathogenesis of sporadic Parkinson's disease. J Neurosci 26:9227-9238.

Archambault V, Glover DM (2009) Polo-like kinases: conservation and divergence in their functions and regulation. Nat Rev Mol Cell Biol 10:265-275.

Arima K, Ueda K, Sunohara N, Arakawa K, Hirai S, Nakamura M, Tonozuka-Uehara H, Kawai M (1998) NACP/alpha-synuclein immunoreactivity in fibrillary components of neuronal and oligodendroglial cytoplasmic inclusions in the pontine nuclei in multiple system atrophy. Acta Neuropathol 96:439-444.

Barr FA, Sillje HH, Nigg EA (2004) Polo-like kinases and the orchestration of cell division. Nat Rev Mol Cell Biol 5:429-440.

Behr J, Wozny C, Fidzinski P, Schmitz D (2009) Synaptic plasticity in the subiculum. Prog Neurobiol 89:334-342.

Braak H, Braak E, Yilmazer D, de Vos RA, Jansen EN, Bohl J, Jellinger K (1994) Amygdala pathology in Parkinson's disease. Acta Neuropathol 88:493-500.

Braak H, Del Tredici K, Rub U, de Vos RA, Jansen Steur EN, Braak E (2003) Staging of brain pathology related to sporadic Parkinson's disease. Neurobiol Aging 24:197-211.

Braak H, Ghebremedhin E, Rub U, Bratzke H, Del Tredici K (2004) Stages in the development of Parkinson's disease-related pathology. Cell Tissue Res 318:121-134.

Buter TC, van den Hout A, Matthews FE, Larsen JP, Brayne C, Aarsland D (2008) Dementia and survival in Parkinson disease: a 12-year population study. Neurology 70:1017-1022.

Calne DB, Stoessl AJ (1986) Early parkinsonism. Clin Neuropharmacol 9 Suppl 2:S3-8.

Chartier-Harlin MC, Kachergus J, Roumier C, Mouroux V, Douay X, Lincoln S, Levecque C, Larvor L, Andrieux J, Hulihan M, Waucquier N, Defebvre L, Amouyel P, Farrer M,

Destee A (2004) Alpha-synuclein locus duplication as a cause of familial Parkinson's disease. Lancet 364:1167-1169.

Clayton DF, George JM (1999) Synucleins in synaptic plasticity and neurodegenerative disorders. J Neurosci Res 58:120-129.

Critchley M (1957) Medical aspects of boxing, particularly from a neurological standpoint. Br Med J 1:357-362.

Crowther RA, Jakes R, Spillantini MG, Goedert M (1998) Synthetic filaments assembled from C-terminally truncated alpha-synuclein. FEBS Lett 436:309-312.

Dai W (2005) Polo-like kinases, an introduction. Oncogene 24:214-216.

Dauer W, Kholodilov N, Vila M, Trillat AC, Goodchild R, Larsen KE, Staal R, Tieu K, Schmitz Y, Yuan CA, Rocha M, Jackson-Lewis V, Hersch S, Sulzer D, Przedborski S, Burke R, Hen R (2002) Resistance of alpha -synuclein null mice to the parkinsonian neurotoxin MPTP. Proc Natl Acad Sci U S A 99:14524-14529.

Dauer W, Przedborski S (2003) Parkinson's disease: mechanisms and models. Neuron 39:889-909.

Davidson WS, Jonas A, Clayton DF, George JM (1998) Stabilization of alpha-synuclein secondary structure upon binding to synthetic membranes. J Biol Chem 273:9443-9449.

de Lau LM, Breteler MM (2006) Epidemiology of Parkinson's disease. Lancet Neurol 5:525-535.

Dev KK, Hofele K, Barbieri S, Buchman VL, van der Putten H (2003) Part II: alpha-synuclein and its molecular pathophysiological role in neurodegenerative disease. Neuropharmacology 45:14-44.

Di Rosa G, Puzzo D, Sant'Angelo A, Trinchese F, Arancio O (2003) Alpha-synuclein: between synaptic function and dysfunction. Histol Histopathol 18:1257-1266.

Draghetti C, Salvat C, Zanoguera F, Curchod ML, Vignaud C, Peixoto H, Di Cara A, Fischer D, Dhanabal M, Andreas G, Abderrahim H, Rommel C, Camps M (2009) Functional whole-genome analysis identifies Polo-like kinase 2 and poliovirus receptor as essential for neuronal differentiation upstream of the negative regulator alphaB-crystallin. J Biol Chem 284:32053-32065.

Duda JE (2004) Pathology and neurotransmitter abnormalities of dementia with Lewy bodies. Dement Geriatr Cogn Disord 17 Suppl 1:3-14.

el-Agnaf OM, Irvine GB (2002) Aggregation and neurotoxicity of alpha-synuclein and related peptides. Biochem Soc Trans 30:559-565.

Eliezer D, Kutluay E, Bussell R, Jr., Browne G (2001) Conformational properties of alpha-synuclein in its free and lipid-associated states. J Mol Biol 307:1061-1073.

Feany MB, Bender WW (2000) A Drosophila model of Parkinson's disease. Nature 404:394-398.

Findley LJ, Gresty MA (1981) Tremor. Br J Hosp Med 26:16-32.

Fleming SM, Salcedo J, Fernagut PO, Rockenstein E, Masliah E, Levine MS, Chesselet MF (2004) Early and progressive sensorimotor anomalies in mice overexpressing wild-type human alpha-synuclein. J Neurosci 24:9434-9440.

Fleming SM, Tetreault NA, Mulligan CK, Hutson CB, Masliah E, Chesselet MF (2008) Olfactory deficits in mice overexpressing human wildtype alpha-synuclein. Eur J Neurosci 28:247-256.

Franco R, Li S, Rodriguez-Rocha H, Burns M, Panayiotidis MI (2010) Molecular mechanisms of pesticide-induced neurotoxicity: Relevance to Parkinson's disease. Chem Biol Interact 188:289-300.

Freichel C, Neumann M, Ballard T, Muller V, Woolley M, Ozmen L, Borroni E, Kretzschmar HA, Haass C, Spooren W, Kahle PJ (2007) Age-dependent cognitive decline and amygdala pathology in alpha-synuclein transgenic mice. Neurobiol Aging 28:1421-1435.

Fujiwara H, Hasegawa M, Dohmae N, Kawashima A, Masliah E, Goldberg MS, Shen J, Takio K, Iwatsubo T (2002) alpha-Synuclein is phosphorylated in synucleinopathy lesions. Nat Cell Biol 4:160-164.

Galasko D, Kwo-on-Yuen PF, Klauber MR, Thal LJ (1990) Neurological findings in Alzheimer's disease and normal aging. Arch Neurol 47:625-627.

George JM (2002) The synucleins. Genome Biol 3:REVIEWS3002.

Giasson BI, Duda JE, Quinn SM, Zhang B, Trojanowski JQ, Lee VM (2002) Neuronal alpha-Synucleinopathy with severe movement disorder in mice expressing A53T human alpha-synuclein. Neuron 34:521-533.

Giasson BI, Forman MS, Higuchi M, Golbe LI, Graves CL, Kotzbauer PT, Trojanowski JQ, Lee VM (2003) Initiation and synergistic fibrillization of tau and alpha-synuclein. Science 300:636-640.

Giasson BI, Murray IV, Trojanowski JQ, Lee VM (2001) A hydrophobic stretch of 12 amino acid residues in the middle of alpha-synuclein is essential for filament assembly. J Biol Chem 276:2380-2386.

Gispert S, Del Turco D, Garrett L, Chen A, Bernard DJ, Hamm-Clement J, Korf HW, Deller T, Braak H, Auburger G, Nussbaum RL (2003) Transgenic mice expressing mutant A53T human alpha-synuclein show neuronal dysfunction in the absence of aggregate formation. Mol Cell Neurosci 24:419-429.

Goers J, Manning-Bog AB, McCormack AL, Millett IS, Doniach S, Di Monte DA, Uversky VN, Fink AL (2003) Nuclear localization of alpha-synuclein and its interaction with histones. Biochemistry 42:8465-8471.

Goosens KA, Maren S (2001) Contextual and auditory fear conditioning are mediated by the lateral, basal, and central amygdaloid nuclei in rats. Learn Mem 8:148-155.

Graham JG, Oppenheimer DR (1969) Orthostatic hypotension and nicotine sensitivity in a case of multiple system atrophy. J Neurol Neurosurg Psychiatry 32:28-34.

Greffard S, Verny M, Bonnet AM, Seilhean D, Hauw JJ, Duyckaerts C (2010) A stable proportion of Lewy body bearing neurons in the substantia nigra suggests a model in which the Lewy body causes neuronal death. Neurobiol Aging 31:99-103.

Hamilton RL (2000) Lewy bodies in Alzheimer's disease: a neuropathological review of 145 cases using alpha-synuclein immunohistochemistry. Brain Pathol 10:378-384.

Hanson JC, Lippa CF (2009) Lewy body dementia. Int Rev Neurobiol 84:215-228.

Harding AJ, Halliday GM (2001) Cortical Lewy body pathology in the diagnosis of dementia. Acta Neuropathol 102:355-363.

Harding AJ, Stimson E, Henderson JM, Halliday GM (2002) Clinical correlates of selective pathology in the amygdala of patients with Parkinson's disease. Brain 125:2431-2445.

Hely MA, Reid WG, Adena MA, Halliday GM, Morris JG (2008) The Sydney multicenter study of Parkinson's disease: the inevitability of dementia at 20 years. Mov Disord 23:837-844.

Ho L, Qin W, Pompl PN, Xiang Z, Wang J, Zhao Z, Peng Y, Cambareri G, Rocher A, Mobbs CV, Hof PR, Pasinetti GM (2004) Diet-induced insulin resistance promotes amyloidosis in a transgenic mouse model of Alzheimer's disease. Faseb J 18:902-904.

Holahan MR, White NM (2004) Amygdala inactivation blocks expression of conditioned memory modulation and the promotion of avoidance and freezing. Behav Neurosci 118:24-35.

Hornykiewicz O (2002) L-DOPA: from a biologically inactive amino acid to a successful therapeutic agent. Amino Acids 23:65-70.

Hoyer W, Cherny D, Subramaniam V, Jovin TM (2004) Impact of the acidic C-terminal region comprising amino acids 109-140 on alpha-synuclein aggregation *in vitro*. Biochemistry 43:16233-16242.

Ibanez P, Bonnet AM, Debarges B, Lohmann E, Tison F, Pollak P, Agid Y, Durr A, Brice A (2004) Causal relation between alpha-synuclein gene duplication and familial Parkinson's disease. Lancet 364:1169-1171.

Inglis KJ, Chereau D, Brigham EF, Chiou SS, Schobel S, Frigon NL, Yu M, Caccavello RJ, Nelson S, Motter R, Wright S, Chian D, Santiago P, Soriano F, Ramos C, Powell K, Goldstein JM, Babcock M, Yednock T, Bard F, Basi GS, Sham H, Chilcote TJ, McConlogue L, Griswold-Prenner I, Anderson JP (2009) Polo-like kinase 2 (PLK2) phosphorylates alpha-synuclein at serine 129 in central nervous system. J Biol Chem 284:2598-2602.

Iseki E, Marui W, Yamamoto R, Togo T, Katsuse O, Kato M, Iwatsubo T, Kosaka K, Arai H (2005) The nigro-striatal and nigro-amygdaloid pathways undergo different degeneration processes in brains of dementia with Lewy bodies. Neurosci Lett 380:161-165.

Ishii A, Nonaka T, Taniguchi S, Saito T, Arai T, Mann D, Iwatsubo T, Hisanaga S, Goedert M, Hasegawa M (2007) Casein kinase 2 is the major enzyme in brain that phosphorylates Ser129 of human alpha-synuclein: Implication for alpha-synucleinopathys. FEBS Lett 581:4711-4717.

Iwai A, Masliah E, Yoshimoto M, Ge N, Flanagan L, de Silva HA, Kittel A, Saitoh T (1995) The precursor protein of non-A beta component of Alzheimer's disease amyloid is a presynaptic protein of the central nervous system. Neuron 14:467-475.

Jankovic J (2008) Parkinson's disease: clinical features and diagnosis. J Neurol Neurosurg Psychiatry 79:368-376.

Jellinger KA (2009) Formation and development of Lewy pathology: a critical update. J Neurol 256 Suppl 3:270-279.

Jenkyn LR, Reeves AG, Warren T, Whiting RK, Clayton RJ, Moore WW, Rizzo A, Tuzun IM, Bonnett JC, Culpepper BW (1985) Neurologic signs in senescence. Arch Neurol 42:1154-1157.

Kahle PJ (2008) alphα-Synucleinopathy models and human neuropathology: similarities and differences. Acta Neuropathol 115:87-95.

Kahle PJ, Haass C, Kretzschmar HA, Neumann M (2002a) Structure/function of alpha-synuclein in health and disease: rational development of animal models for Parkinson's and related diseases. J Neurochem 82:449-457.

Kahle PJ, Neumann M, Ozmen L, Muller V, Jacobsen H, Schindzielorz A, Okochi M, Leimer U, van Der Putten H, Probst A, Kremmer E, Kretzschmar HA, Haass C (2000) Subcellular localization of wild-type and Parkinson's disease-associated mutant alpha -synuclein in human and transgenic mouse brain. J Neurosci 20:6365-6373.

Kahle PJ, Neumann M, Ozmen L, Muller V, Jacobsen H, Spooren W, Fuss B, Mallon B, Macklin WB, Fujiwara H, Hasegawa M, Iwatsubo T, Kretzschmar HA, Haass C (2002b) Hyperphosphorylation and insolubility of alpha-synuclein in transgenic mouse oligodendrocytes. EMBO Rep 3:583-588.

Kahle PJ, Neumann M, Ozmen L, Muller V, Odoy S, Okamoto N, Jacobsen H, Iwatsubo T, Trojanowski JQ, Takahashi H, Wakabayashi K, Bogdanovic N, Riederer P, Kretzschmar HA, Haass C (2001) Selective insolubility of alpha-synuclein in human Lewy body diseases is recapitulated in a transgenic mouse model. Am J Pathol 159:2215-2225.

Kalmijn S, Launer LJ, Ott A, Witteman JC, Hofman A, Breteler MM (1997) Dietary fat intake and the risk of incident dementia in the Rotterdam Study. Ann Neurol 42:776-782.

Kauselmann G, Weiler M, Wulff P, Jessberger S, Konietzko U, Scafidi J, Staubli U, Bereiter-Hahn J, Strebhardt K, Kuhl D (1999) The polo-like protein kinases Fnk and Snk associate with a Ca(2+)- and integrin-binding protein and are regulated dynamically with synaptic plasticity. Embo J 18:5528-5539.

Killcross S, Robbins TW, Everitt BJ (1997) Different types of fear-conditioned behaviour mediated by separate nuclei within amygdala. Nature 388:377-380.

Klucken J, Ingelsson M, Shin Y, Irizarry MC, Hedley-Whyte ET, Frosch M, Growdon J, McLean P, Hyman BT (2006) Clinical and biochemical correlates of insoluble alpha-synuclein in dementia with Lewy bodies. Acta Neuropathol 111:101-108.

Kontopoulos E, Parvin JD, Feany MB (2006) Alpha-synuclein acts in the nucleus to inhibit histone acetylation and promote neurotoxicity. Hum Mol Genet 15:3012-3023.

Kramer ML, Schulz-Schaeffer WJ (2007) Presynaptic alpha-synuclein aggregates, not Lewy bodies, cause neurodegeneration in dementia with Lewy bodies. J Neurosci 27:1405-1410.

Kranick SM, Duda JE (2008) Olfactory dysfunction in Parkinson's disease. Neurosignals 16:35-40.

Kruger R, Kuhn W, Muller T, Woitalla D, Graeber M, Kosel S, Przuntek H, Epplen JT, Schols L, Riess O (1998) Ala30Pro mutation in the gene encoding alpha-synuclein in Parkinson's disease. Nat Genet 18:106-108.

Kurata T, Kametaka S, Ohta Y, Morimoto N, Deguchi S, Deguchi K, Ikeda Y, Takao Y, Ohta T, Manabe Y, Sato S, Abe K (2011) PSP as Distinguished from CBD, MSA-P and PD by Clinical and Imaging Differences at an Early Stage. Intern Med 50:2775-2781.

Lakso M, Vartiainen S, Moilanen AM, Sirvio J, Thomas JH, Nass R, Blakely RD, Wong G (2003) Dopaminergic neuronal loss and motor deficits in Caenorhabditis elegans overexpressing human alpha-synuclein. J Neurochem 86:165-172.

Langston RF, Stevenson CH, Wilson CL, Saunders I, Wood ER (2010) The role of hippocampal subregions in memory for stimulus associations. Behav Brain Res 215:275-291.

Lavedan C (1998) The synuclein family. Genome Res 8:871-880.

LeDoux JE (2000) Emotion circuits in the brain. Annu Rev Neurosci 23:155-184.

LeDoux JE, Iwata J, Cicchetti P, Reis DJ (1988) Different projections of the central amygdaloid nucleus mediate autonomic and behavioral correlates of conditioned fear. J Neurosci 8:2517-2529.

Lee MK, Stirling W, Xu Y, Xu X, Qui D, Mandir AS, Dawson TM, Copeland NG, Jenkins NA, Price DL (2002) Human alpha-synuclein-harboring familial Parkinson's disease-linked Ala-53 --> Thr mutation causes neurodegenerative disease with alpha-synuclein aggregation in transgenic mice. Proc Natl Acad Sci U S A 99:8968-8973.

Lesage S, Brice A (2009) Parkinson's disease: from monogenic forms to genetic susceptibility factors. Hum Mol Genet 18:R48-59.

Li J, Uversky VN, Fink AL (2001) Effect of familial Parkinson's disease point mutations A30P and A53T on the structural properties, aggregation, and fibrillation of human alpha-synuclein. Biochemistry 40:11604-11613.

Lindersson E, Beedholm R, Hojrup P, Moos T, Gai W, Hendil KB, Jensen PH (2004) Proteasomal inhibition by alpha-synuclein filaments and oligomers. J Biol Chem 279:12924-12934.

Lowe J, Blanchard A, Morrell K, Lennox G, Reynolds L, Billett M, Landon M, Mayer RJ (1988) Ubiquitin is a common factor in intermediate filament inclusion bodies of diverse type in man, including those of Parkinson's disease, Pick's disease, and Alzheimer's disease, as well as Rosenthal fibres in cerebellar astrocytomas, cytoplasmic bodies in muscle, and mallory bodies in alcoholic liver disease. J Pathol 155:9-15.

Ma S, Charron J, Erikson RL (2003) Role of Plk2 (Snk) in mouse development and cell proliferation. Mol Cell Biol 23:6936-6943.

Maren S (1999) Long-term potentiation in the amygdala: a mechanism for emotional learning and memory. Trends Neurosci 22:561-567.

Maren S (2001) Neurobiology of Pavlovian fear conditioning. Annu Rev Neurosci 24:897-931.

Maroteaux L, Campanelli JT, Scheller RH (1988) Synuclein: a neuron-specific protein localized to the nucleus and presynaptic nerve terminal. J Neurosci 8:2804-2815.

Marui W, Iseki E, Nakai T, Miura S, Kato M, Ueda K, Kosaka K (2002) Progression and staging of Lewy pathology in brains from patients with dementia with Lewy bodies. J Neurol Sci 195:153-159.

Maskri L, Zhu X, Fritzen S, Kuhn K, Ullmer C, Engels P, Andriske M, Stichel CC, Lubbert H (2004) Influence of different promoters on the expression pattern of mutated human alpha-synuclein in transgenic mice. Neurodegener Dis 1:255-265.

Masliah E, Rockenstein E, Veinbergs I, Mallory M, Hashimoto M, Takeda A, Sagara Y, Sisk A, Mucke L (2000) Dopaminergic loss and inclusion body formation in alpha-synuclein mice: implications for neurodegenerative disorders. Science 287:1265-1269.

Matsuoka Y, Vila M, Lincoln S, McCormack A, Picciano M, LaFrancois J, Yu X, Dickson D, Langston WJ, McGowan E, Farrer M, Hardy J, Duff K, Przedborski S, Di Monte DA (2001) Lack of nigral pathology in transgenic mice expressing human alpha-synuclein driven by the tyrosine hydroxylase promoter. Neurobiol Dis 8:535-539.

Mbefo MK, Paleologou KE, Boucharaba A, Oueslati A, Schell H, Fournier M, Olschewski D, Yin G, Zweckstetter M, Masliah E, Kahle PJ, Hirling H, Lashuel HA (2010) Phosphorylation of synucleins by members of the Polo-like kinase family. J Biol Chem 285:2807-2822.

McLean PJ, Hyman BT (2002) An alternatively spliced form of rodent alpha-synuclein forms intracellular inclusions *in vitro*: role of the carboxy-terminus in alpha-synuclein aggregation. Neurosci Lett 323:219-223.

McNaught KS, Shashidharan P, Perl DP, Jenner P, Olanow CW (2002) Aggresome-related biogenesis of Lewy bodies. Eur J Neurosci 16:2136-2148.

McNish KA, Gewirtz JC, Davis M (1997) Evidence of contextual fear after lesions of the hippocampus: a disruption of freezing but not fear-potentiated startle. J Neurosci 17:9353-9360.

Mikolaenko I, Pletnikova O, Kawas CH, O'Brien R, Resnick SM, Crain B, Troncoso JC (2005) Alpha-synuclein lesions in normal aging, Parkinson disease, and Alzheimer disease:

evidence from the Baltimore Longitudinal Study of Aging (BLSA). J Neuropathol Exp Neurol 64:156-162.

Mizumori SJ, Ragozzino KE, Cooper BG, Leutgeb S (1999) Hippocampal representational organization and spatial context. Hippocampus 9:444-451.

Morris MC, Evans DA, Bienias JL, Tangney CC, Bennett DA, Aggarwal N, Schneider J, Wilson RS (2003) Dietary fats and the risk of incident Alzheimer disease. Arch Neurol 60:194-200.

Morris RG (2006) Elements of a neurobiological theory of hippocampal function: the role of synaptic plasticity, synaptic tagging and schemas. Eur J Neurosci 23:2829-2846.

Murray IV, Giasson BI, Quinn SM, Koppaka V, Axelsen PH, Ischiropoulos H, Trojanowski JQ, Lee VM (2003) Role of alpha-synuclein carboxy-terminus on fibril formation *in vitro*. Biochemistry 42:8530-8540.

Negro A, Brunati AM, Donella-Deana A, Massimino ML, Pinna LA (2002) Multiple phosphorylation of alpha-synuclein by protein tyrosine kinase Syk prevents eosin-induced aggregation. Faseb J 16:210-212.

Neumann M, Kahle PJ, Giasson BI, Ozmen L, Borroni E, Spooren W, Muller V, Odoy S, Fujiwara H, Hasegawa M, Iwatsubo T, Trojanowski JQ, Kretzschmar HA, Haass C (2002) Misfolded proteinase K-resistant hyperphosphorylated alpha-synuclein in aged transgenic mice with locomotor deterioration and in human alpha-synucleinopathys. J Clin Invest 110:1429-1439.

O'Mara SM, Commins S, Anderson M (2000) Synaptic plasticity in the hippocampal area CA1-subiculum projection: implications for theories of memory. Hippocampus 10:447-456.

Okochi M, Walter J, Koyama A, Nakajo S, Baba M, Iwatsubo T, Meijer L, Kahle PJ, Haass C (2000) Constitutive phosphorylation of the Parkinson's disease associated alpha-synuclein. J Biol Chem 275:390-397.

Olanow CW, Perl DP, DeMartino GN, McNaught KS (2004) Lewy-body formation is an aggresome-related process: a hypothesis. Lancet Neurol 3:496-503.

Pak DT, Sheng M (2003) Targeted protein degradation and synapse remodeling by an inducible protein kinase. Science 302:1368-1373.

Parkinson J (1817) An Essay on the Shaking Palsy. In Sherwood, N, and Jones, (ed), London.

Payan CA, Viallet F, Landwehrmeyer BG, Bonnet AM, Borg M, Durif F, Lacomblez L, Bloch F, Verny M, Fermanian J, Agid Y, Ludolph AC, Leigh PN, Bensimon G (2011) Disease severity and progression in progressive supranuclear palsy and multiple system atrophy: validation of the NNIPPS--Parkinson Plus Scale. PLoS One 6:e22293.

Poirier LJ, Sourkes TL (1965) Influence of the Substantia Nigra on the Catecholamine Content of the Striatum. Brain 88:181-192.

Polymeropoulos MH, Lavedan C, Leroy E, Ide SE, Dehejia A, Dutra A, Pike B, Root H, Rubenstein J, Boyer R, Stenroos ES, Chandrasekharappa S, Athanassiadou A, Papapetropoulos T, Johnson WG, Lazzarini AM, Duvoisin RC, Di Iorio G, Golbe LI, Nussbaum RL (1997) Mutation in the alpha-synuclein gene identified in families with Parkinson's disease. Science 276:2045-2047.

Pronin AN, Morris AJ, Surguchov A, Benovic JL (2000) Synucleins are a novel class of substrates for G protein-coupled receptor kinases. J Biol Chem 275:26515-26522.

Radulovic J, Kammermeier J, Spiess J (1998) Relationship between fos production and classical fear conditioning: effects of novelty, latent inhibition, and unconditioned stimulus preexposure. J Neurosci 18:7452-7461.

Rathke-Hartlieb S, Kahle PJ, Neumann M, Ozmen L, Haid S, Okochi M, Haass C, Schulz JB (2001) Sensitivity to MPTP is not increased in Parkinson's disease-associated mutant alpha-synuclein transgenic mice. J Neurochem 77:1181-1184.

Recchia A, Debetto P, Negro A, Guidolin D, Skaper SD, Giusti P (2004) Alpha-synuclein and Parkinson's disease. Faseb J 18:617-626.

Richfield EK, Thiruchelvam MJ, Cory-Slechta DA, Wuertzer C, Gainetdinov RR, Caron MG, Di Monte DA, Federoff HJ (2002) Behavioral and neurochemical effects of wild-type and mutated human alpha-synuclein in transgenic mice. Exp Neurol 175:35-48.

Rieker C, Dev KK, Lehnhoff K, Barbieri S, Ksiazek I, Kauffmann S, Danner S, Schell H, Boden C, Ruegg MA, Kahle PJ, van der Putten H, Shimshek DR (2011) Neuropathology in mice expressing mouse alpha-synuclein. PLoS One 6:e24834.

Rizvi TA, Ennis M, Behbehani MM, Shipley MT (1991) Connections between the central nucleus of the amygdala and the midbrain periaqueductal gray: topography and reciprocity. J Comp Neurol 303:121-131.

Rochet JC, Conway KA, Lansbury PT, Jr. (2000) Inhibition of fibrillization and accumulation of prefibrillar oligomers in mixtures of human and mouse alpha-synuclein. Biochemistry 39:10619-10626.

Rockenstein E, Mallory M, Hashimoto M, Song D, Shults CW, Lang I, Masliah E (2002) Differential neuropathological alterations in transgenic mice expressing alpha-synuclein from the platelet-derived growth factor and Thy-1 promoters. J Neurosci Res 68:568-578.

Rockenstein E, Schwach G, Ingolic E, Adame A, Crews L, Mante M, Pfragner R, Schreiner E, Windisch M, Masliah E (2005) Lysosomal pathology associated with alpha-synuclein accumulation in transgenic models using an eGFP fusion protein. J Neurosci Res 80:247-259.

Saito Y, Kawashima A, Ruberu NN, Fujiwara H, Koyama S, Sawabe M, Arai T, Nagura H, Yamanouchi H, Hasegawa M, Iwatsubo T, Murayama S (2003) Accumulation of phosphorylated alpha-synuclein in aging human brain. J Neuropathol Exp Neurol 62:644-654.

Schell H, Hasegawa T, Neumann M, Kahle PJ (2009) Nuclear and neuritic distribution of serine-129 phosphorylated alpha-synuclein in transgenic mice. Neuroscience 160:796-804.

Scicli AP, Petrovich GD, Swanson LW, Thompson RF (2004) Contextual fear conditioning is associated with lateralized expression of the immediate early gene c-fos in the central and basolateral amygdalar nuclei. Behav Neurosci 118:5-14.

Seeburg DP, Feliu-Mojer M, Gaiottino J, Pak DT, Sheng M (2008a) Critical role of CDK5 and Polo-like kinase 2 in homeostatic synaptic plasticity during elevated activity. Neuron 58:571-583.

Seeburg DP, Pak D, Sheng M (2005) Polo-like kinases in the nervous system. Oncogene 24:292-298.

Seeburg DP, Sheng M (2008b) Activity-induced Polo-like kinase 2 is required for homeostatic plasticity of hippocampal neurons during epileptiform activity. J Neurosci 28:6583-6591.

Shie FS, Jin LW, Cook DG, Leverenz JB, LeBoeuf RC (2002) Diet-induced hypercholesterolemia enhances brain A beta accumulation in transgenic mice. Neuroreport 13:455-459.

Shults CW, Rockenstein E, Crews L, Adame A, Mante M, Larrea G, Hashimoto M, Song D, Iwatsubo T, Tsuboi K, Masliah E (2005) Neurological and neurodegenerative

alterations in a transgenic mouse model expressing human alpha-synuclein under oligodendrocyte promoter: implications for multiple system atrophy. J Neurosci 25:10689-10699.

Sidhu A, Wersinger C, Vernier P (2004) Does alpha-synuclein modulate dopaminergic synaptic content and tone at the synapse? Faseb J 18:637-647.

Singleton AB, Farrer M, Johnson J, Singleton A, Hague S, Kachergus J, Hulihan M, Peuralinna T, Dutra A, Nussbaum R, Lincoln S, Crawley A, Hanson M, Maraganore D, Adler C, Cookson MR, Muenter M, Baptista M, Miller D, Blancato J, Hardy J, Gwinn-Hardy K (2003) alpha-Synuclein locus triplication causes Parkinson's disease. Science 302:841.

Snyder H, Mensah K, Theisler C, Lee J, Matouschek A, Wolozin B (2003) Aggregated and monomeric alpha-synuclein bind to the S6' proteasomal protein and inhibit proteasomal function. J Biol Chem 278:11753-11759.

Souza JM, Giasson BI, Chen Q, Lee VM, Ischiropoulos H (2000) Dityrosine cross-linking promotes formation of stable alpha -synuclein polymers. Implication of nitrative and oxidative stress in the pathogenesis of neurodegenerative synucleinopathys. J Biol Chem 275:18344-18349.

Spillantini MG, Crowther RA, Jakes R, Cairns NJ, Lantos PL, Goedert M (1998) Filamentous alpha-synuclein inclusions link multiple system atrophy with Parkinson's disease and dementia with Lewy bodies. Neurosci Lett 251:205-208.

Spillantini MG, Schmidt ML, Lee VM, Trojanowski JQ, Jakes R, Goedert M (1997) Alpha-synuclein in Lewy bodies. Nature 388:839-840.

Stefanova N, Reindl M, Neumann M, Haass C, Poewe W, Kahle PJ, Wenning GK (2005) Oxidative stress in transgenic mice with oligodendroglial alpha-synuclein overexpression replicates the characteristic neuropathology of multiple system atrophy. Am J Pathol 166:869-876.

Stefanova N, Reindl M, Neumann M, Kahle PJ, Poewe W, Wenning GK (2007) Microglial activation mediates neurodegeneration related to oligodendroglial alpha-synucleinopathy: implications for multiple system atrophy. Mov Disord 22:2196-2203.

Takahashi T, Yamashita H, Nakamura T, Nagano Y, Nakamura S (2002) Tyrosine 125 of alpha-synuclein plays a critical role for dimerization following nitrative stress. Brain Res 938:73-80.

Takeda A, Mallory M, Sundsmo M, Honer W, Hansen L, Masliah E (1998) Abnormal accumulation of NACP/alpha-synuclein in neurodegenerative disorders. Am J Pathol 152:367-372.

Tanaka M, Kim YM, Lee G, Junn E, Iwatsubo T, Mouradian MM (2004) Aggresomes formed by alpha-synuclein and synphilin-1 are cytoprotective. J Biol Chem 279:4625-4631.

Thiruchelvam MJ, Powers JM, Cory-Slechta DA, Richfield EK (2004) Risk factors for dopaminergic neuron loss in human alpha-synuclein transgenic mice. Eur J Neurosci 19:845-854.

Tofaris GK, Garcia Reitbock P, Humby T, Lambourne SL, O'Connell M, Ghetti B, Gossage H, Emson PC, Wilkinson LS, Goedert M, Spillantini MG (2006) Pathological changes in dopaminergic nerve cells of the substantia nigra and olfactory bulb in mice transgenic for truncated human alpha-synuclein(1-120): implications for Lewy body disorders. J Neurosci 26:3942-3950.

Touchman JW, Dehejia A, Chiba-Falek O, Cabin DE, Schwartz JR, Orrison BM, Polymeropoulos MH, Nussbaum RL (2001) Human and mouse alpha-synuclein genes:

comparative genomic sequence analysis and identification of a novel gene regulatory element. Genome Res 11:78-86.

Trenkwalder C, Schwarz J, Gebhard J, Ruland D, Trenkwalder P, Hense HW, Oertel WH (1995) Starnberg trial on epidemiology of Parkinsonism and hypertension in the elderly. Prevalence of Parkinson's disease and related disorders assessed by a door-to-door survey of inhabitants older than 65 years. Arch Neurol 52:1017-1022.

Tsoory MM, Vouimba RM, Akirav I, Kavushansky A, Avital A, Richter-Levin G (2008) Amygdala modulation of memory-related processes in the hippocampus: potential relevance to PTSD. Prog Brain Res 167:35-51.

Ueda K, Fukushima H, Masliah E, Xia Y, Iwai A, Yoshimoto M, Otero DA, Kondo J, Ihara Y, Saitoh T (1993) Molecular cloning of cDNA encoding an unrecognized component of amyloid in Alzheimer disease. Proc Natl Acad Sci U S A 90:11282-11286.

van de Weerdt BC, Medema RH (2006) Polo-like kinases: a team in control of the division. Cell Cycle 5:853-864.

van der Putten H, Wiederhold KH, Probst A, Barbieri S, Mistl C, Danner S, Kauffmann S, Hofele K, Spooren WP, Ruegg MA, Lin S, Caroni P, Sommer B, Tolnay M, Bilbe G (2000) Neuropathology in mice expressing human alpha-synuclein. J Neurosci 20:6021-6029.

Wakabayashi K, Hayashi S, Kakita A, Yamada M, Toyoshima Y, Yoshimoto M, Takahashi H (1998) Accumulation of alpha-synuclein/NACP is a cytopathological feature common to Lewy body disease and multiple system atrophy. Acta Neuropathol 96:445-452.

Wakamatsu M, Ishii A, Iwata S, Sakagami J, Ukai Y, Ono M, Kanbe D, Muramatsu S, Kobayashi K, Iwatsubo T, Yoshimoto M (2008) Selective loss of nigral dopamine neurons induced by overexpression of truncated human alpha-synuclein in mice. Neurobiol Aging 29:574-585.

Wakamatsu M, Ishii A, Ukai Y, Sakagami J, Iwata S, Ono M, Matsumoto K, Nakamura A, Tada N, Kobayashi K, Iwatsubo T, Yoshimoto M (2007) Accumulation of phosphorylated alpha-synuclein in dopaminergic neurons of transgenic mice that express human alpha-synuclein. J Neurosci Res 85:1819-1825.

Waxman EA, Giasson BI (2008) Specificity and regulation of casein kinase-mediated phosphorylation of alpha-synuclein. J Neuropathol Exp Neurol 67:402-416.

Weiss A, Klein C, Woodman B, Sathasivam K, Bibel M, Regulier E, Bates GP, Paganetti P (2008) Sensitive biochemical aggregate detection reveals aggregation onset before symptom development in cellular and murine models of Huntington's disease. J Neurochem 104:846-858.

Winkles JA, Alberts GF (2005) Differential regulation of polo-like kinase 1, 2, 3, and 4 gene expression in mammalian cells and tissues. Oncogene 24:260-266.

Winner B, Lie DC, Rockenstein E, Aigner R, Aigner L, Masliah E, Kuhn HG, Winkler J (2004) Human wild-type alpha-synuclein impairs neurogenesis. J Neuropathol Exp Neurol 63:1155-1166.

Winner B, Rockenstein E, Lie DC, Aigner R, Mante M, Bogdahn U, Couillard-Despres S, Masliah E, Winkler J (2008) Mutant alpha-synuclein exacerbates age-related decrease of neurogenesis. Neurobiol Aging 29:913-925.

Xie S, Xie B, Lee MY, Dai W (2005) Regulation of cell cycle checkpoints by polo-like kinases. Oncogene 24:277-286.

Xu J, Kao SY, Lee FJ, Song W, Jin LW, Yankner BA (2002) Dopamine-dependent neurotoxicity of alpha-synuclein: a mechanism for selective neurodegeneration in Parkinson disease. Nat Med 8:600-606.

Yahr MD, Duvoisin RC, Schear MJ, Barrett RE, Hoehn MM (1969) Treatment of parkinsonism with levodopa. Arch Neurol 21:343-354.

Yamada M, Iwatsubo T, Mizuno Y, Mochizuki H (2004) Overexpression of alpha-synuclein in rat substantia nigra results in loss of dopaminergic neurons, phosphorylation of alpha-synuclein and activation of caspase-9: resemblance to pathogenetic changes in Parkinson's disease. J Neurochem 91:451-461.

Yazawa I, Giasson BI, Sasaki R, Zhang B, Joyce S, Uryu K, Trojanowski JQ, Lee VM (2005) Mouse model of multiple system atrophy alpha-synuclein expression in oligodendrocytes causes glial and neuronal degeneration. Neuron 45:847-859.

Zaccai J, Brayne C, McKeith I, Matthews F, Ince PG (2008) Patterns and stages of alpha-synucleinopathy: Relevance in a population-based cohort. Neurology 70:1042-1048.

Zarranz JJ, Alegre J, Gomez-Esteban JC, Lezcano E, Ros R, Ampuero I, Vidal L, Hoenicka J, Rodriguez O, Atares B, Llorens V, Gomez Tortosa E, del Ser T, Munoz DG, de Yebenes JG (2004) The new mutation, E46K, of alpha-synuclein causes Parkinson and Lewy body dementia. Ann Neurol 55:164-173.